Design of an Underwater Object Detection and Location System using Wide-Beam SONAR

by

Renaldo Murray du Pisani

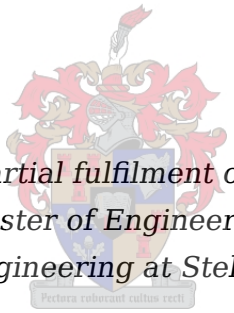

Thesis presented in partial fulfilment of the requirements for
the degree Master of Engineering (Research)
in the Faculty of Engineering at Stellenbosch University

Supervisor:

Mr J Treurnicht

Department of Electrical and Electronic Engineering

April 2014

Declaration

By submitting this thesis electronically, I declare that the entirety of the work contained therein is my own, original work, that I am the sole author thereof (save to the extent explicitly otherwise stated), that reproduction and publication thereof by Stellenbosch University will not infringe any third party rights and that I have not previously in its entirety or in part submitted it for obtaining any qualification.

April 2014

Renaldo Murray du Pisani

Abstract

This thesis describes the second project relating to the development of a SONAR (**SO**und **N**avigation **A**nd **R**anging) object detection and collision avoidance system for use on an AUV (**A**utonomous **U**nderwater **V**ehicle) at Stellenbosch University. The main goal is to develop and test techniques that make use of the existing SONAR laboratory platform and wide-beam SONAR transducers to detect and locate objects and their limits/bounds under water in the horizontal plane. The results of the work done show that it is possible to use wide-beam transducers to locate the centroid and edges of a flat target with an error that is significantly smaller than the beam-width. The techniques developed will enable the development of a cost-effective SONAR system that can be implemented on an AUV.

Uitreksel

Hierdie tesis beskryf the tweede projek rakende die ontwikkeling van ’n SONAR voorwerp opsporings en botsingvermydingstelsel vir gebruik op ’n OOV (**O**utonome **O**nderwater **V**oertuig) aan die Universiteit van Stellenbosch. Die hoofdoel is om tegnieke te ontwikkel en te toets wat gebruik maak van die bestaande SONAR laboratorium opstelling en wye-straal SONAR opnemers om die posisie van voorwerpe onder water te bepaal, sowel as die posisie van die voorwerp se rande in die horisontale vlak. Die resultate van die werk wat gedoen is wys dat dit moontlik is om wye-straal opnemers te gebruik om die posisie van die sentroïde en rande van ’n plat voorwerp te vind met ’n fout wat aansienlik kleiner is as die straal-wydte. Die tegnieke wat ontwikkel is sal ons in staat stel om ’n koste-effektiewe SONAR stelsel te ontwikkel wat op ’n OOV geïmplenteer kan word.

Contents

List of Figures

List of Tables

Nomenclature

Abbreviations and Acronyms

SONAR: Sound Navigation and Ranging

RADAR: Radio Navigation and Ranging

AUV: Autonomous Underwater Vehicle

UAV: Unmanned Aerial Vehicle

ESL: Electronic Systems Laboratory

FMCW: Frequency Modulated Continuous Wave

CW: Constant Wave

LFM: Linear Frequency Modulated

PL: Propagation Loss

SL: Source Level

TS: Target Strength

DI: Directivity Index

RL: Reverberation Level

SNR: Signal to Noise Ratio

MF: Matched Filter

IF: Inverse Filter

PRN: Pseudo-Random Number

DDS: Direct Digital Synthesiser

FIFO: First In First Out

DAC: Digital to Analogue Converter

ADC: Analogue to Digital Converter

PIR: Phase Increment Register

LPF: Low Pass Filter

SPI: Serial I/O Port Interface

LNA: Ultralow Noise Amplifier

VGA: Variable Gain Amplifier

CU: Control Unit

M&M: University of Stellenbosch Mechanical & Mechatronic Engineering

EMC: Electro Magnetic Coupling

2D: Two-Dimensional

3D: Three-Dimensional

DWT: Discrete Wavelet Transform

Acknowledgements

I would like to express my gratitude to the following people and institutions:

- IMT for giving me the opportunity for a challenging Masters.
- Mr. J. Treurnicht as my study leader.
- My amazing fiancée, Sandra, for her love and support and for being happy when I was happy and angry when I was angry.
- My parents for all of their support, encouragement, advice and financial support during my university career. Also, thanks dad for proofreading my thesis.
- Franci and Craig for letting us invite ourselves over for dinner all the time.
- Mr. Cobus Zietsman for the use of the Mechanical dept. towing tank as well as his patience with me.
- Du Toit, my friend and office buddy who was a great lab partner for 3 years and a good friend during my masters.

Chapter 1

Introduction

1.1 Overview

This project forms part of the work done by the Electronics Systems Laboratory at the Faculty of Electrical and Electronic Engineering of the University of Stellenbosch on **A**utonomous **U**nderwater **V**ehicles (AUV's). An AUV is, as the name suggests, a small underwater vehicle that can move around and navigate autonomously.

AUV's are of great importance in many different spheres of society. An underwater vehicle that can detect and classify objects or form images of its surroundings can be of great use in the commercial sector, and is specifically of great interest to the military. For example, in the commercial sector, AUV's can be used to scan the sea floor to see whether there are any objects of interest, or to see whether an underwater area is suitable for the construction of a pipeline or another engineering application. Another use of AUV's is to study underwater wreckages of ships and aeroplanes. After an Air France aircraft crashed into the ocean off the Brazilian coast in May 2009, authorities wanted to find the wreckage in order to study the accident and find out what had caused it. The Remus 6000 AUV was used to find the wreckage [1]. A picture of the Remus 6000 is shown below in Figure 1.1.

Figure 1.1 – The Remus 6000 used to find the Air France Aircraft wreckage.

In the military sector AUV's have a wide range of uses, including finding the location of undersea

mines or submarines. Another possibility is the scanning of the hull of a ship or submarine for damage and defects.

In order for an AUV to be designed and built, there are many different areas of expertise that need to be brought together. This project focuses solely on the SONAR (**SO**und **N**avigation **A**nd **R**anging) sensor used on the AUV. For any autonomous vehicle to be autonomous it needs to be able to navigate without human input. In order to navigate successfully, it must be able to "see" objects that are in its path so that it can plan a path around those objects.

Since an AUV finds itself under water, it needs to "see" objects under water, and the universal way to do so is to make use of SONAR, since sound/acoustic waves do not experience a large amount of attenuation in water. A more detailed explanation of how SONAR functions can be found in the literature study (Chapter 2). There are other options such as optical cameras or RADAR (**RA**dio **D**etection **A**nd **R**anging) [2], but RADAR waves and light waves are absorbed to a much greater extent than sound waves in water. Thus none of the other options can compete with SONAR when it comes to range and object detection under water. The reason for this is clearly stated in *Handbook of Underwater Acoustic Engineering* by Heinz G. Urban:

"Sound waves are mechanical vibrations. Compared to all other kinds of waveforms they travel easily through the ocean. Sound waves represent pressure changes in the medium and constitute wave fields in space and time. Wave fields of different frequency and intensity can superimpose in the medium." [3]

It is therefore logical to make use of SONAR on the AUV.

This project is a continuation of a previous project [4], in which the hardware and software needed for a simple SONAR system was developed. It could detect objects under water and achieved range resolution of 14mm. The platform was designed to make use of linear frequency modulated (LFM) waves as well as constant frequency (CF) waves of frequencies in the 230 kHz - 330 kHz band.

1.2 Scope of the Thesis

The use of SONAR for the purposes of collision detection/avoidance for an AUV is not a new concept. As mentioned, there are AUV's that make use of active SONAR as their primary collision detection sensor. The area in front of the AUV needs to be scanned for objects while taking the size, the speed and dynamics of the AUV into consideration. Figure 4.1 illustrates the area that needs to be scanned.

During the AUV design process it is important to consider the weight, physical size, and power consumption of components that are to be mounted on it. A typical AUV is a small craft [5], as can be seen in Figure 4.1, and therefore the components need to be light, small, and use little power because of the physical limitations of the AUV. There are SONAR systems that meet these requirements, but they are extremely expensive [6].

For an AUV to navigate successfully, it has to scan the area in front of it, as shown in Figure 4.1. The bounds of this area are defined by the maximum range that the AUV needs to scan, as well as the angle of the sector that needs to be scanned. This area needs to be scanned with a high level of accuracy, and to do so, SONAR transducers that have a narrow beam-width (typically <

2°) need to be used. To achieve a narrow beam-width, round transducers need to be either large in diameter (> 0.1m) or operate at a very high frequency (> 1 MHz). High frequency waves are absorbed to a greater extent, reducing the range at which the system can detect targets.

A narrow beam-width also increases the time taken by the scanning process of a SONAR system. A narrow beam divides the area that needs to be scanned into many narrow sections. Sound propagates at a speed of close to 1470 m/s in water (depending on depth, salinity, etc). For each of these narrow sections, a sound wave needs to be transmitted, and then the system has to wait for reflections from potential targets before the next section can be checked for targets. This process can take very long due to the speed of sound in water and the mechanical aspect of scanning, reducing the velocity at which the AUV can move.

SONAR transducers with a relatively wide beam (6°) were available for this project. These transducers are cheaper, smaller (4.4cm) and operate at lower frequencies (330 kHz). Due to the wider beam-width, the scanning process will be significantly faster therefore allowing the AUV to travel at higher speeds.

Any sound beam can be seen as wide if the target is far away from the source of the sound. For example, a beam angle of 2° may seem quite narrow, but at a range of 30m, the beam will be 1.05m wide. Thus, the methods and techniques developed are applicable to any SONAR transducer. The aim is to determine whether objects and details smaller than the width of the beam can be identified.

In order to do path planning and navigation it is important to know where an object is and where the bounds/edges of the object are so that the best path can be planned around it.

For these reasons the primary goal has been defined as follows:

The primary goal of this project is to develop and successfully test methods and techniques that make use of the existing SONAR laboratory platform and existing wide-beam SONAR transducers to detect and locate objects, their edges and the range to the objects in water in the horizontal plane. These methods should be of such a standard that they can be applied to any transducers to improve the quality of the results delivered.

In order to achieve the above goal, several assumptions concerning the environment will need to be made. Throughout the duration of this project, the following assumptions will be made:

- The AUV is moving at a slow speed and the SONAR scanning process takes a very short time. It will be assumed that the AUV is not moving during the SONAR scanning process.
- It will be assumed that the depth of the vehicle under water is between 1m and 2m due to the limitations of the water tank at the testing facility (this will be discussed further at a later stage).
- The water temperature is $20\,^\circ$C.
- The water salinity is 0.005 ppm.

This project deals with detecting and locating targets, not with how that information is used for collision detection/avoidance. The final product of this project will not be mounted on the AUV.

It's purpose is to discover whether it is possible to design and build a system that utilises wide-beam SONAR technology to locate objects under water and find where their edges lie, as well as how far away they are.

Finding the velocity of objects using Doppler techniques in SONAR was discussed in great depth in the previous project [4]. It has been decided to leave the velocity of objects discovered out of the scope of the thesis, since the main focus is the detection of objects and their edges.

Chapter 2

Literature Study

2.1 Overview

This project extends the work done by Konrad Jens Friedrich (Development of an active SONAR platform for AUV applications in a closed environment) [4], and thus the basics of active SONAR will not be discussed in such great depth again in this thesis as it has been covered in great depth in that document and will be referred to as needed.

Additional background information, such as research concerning sound wave interference, the use of SONAR for object detection and location, and the discrete wavelet transform, is also discussed to assist with the analysis.

2.2 Discussion of Existing Literature

A basic summary of the work in Konrad Friedrich's thesis is listed here [4]:

- In-depth research about the basics of active SONAR (Section 2.2.1).
- Research about signal design and processing techniques (Section 2.2.2 and Section 2.2.3).
- Simulation of the chosen signal design and processing techniques (Section 2.2.4).
- Design and construction of the SONAR laboratory platform (Section 2.2.6).
- Results of testing and simulations (Section 2.2.5).

Each of these areas of work is now discussed in varying levels of detail, depending on how applicable it is to this project.

2.2.1 Active SONAR Basics

Active SONAR involves the transmission of a sound/acoustic pulse in a specific direction in to a water volume that contains potential targets, and then waits for the return of possible reflections from the potential targets in the insonified volume of water [7]. The acoustic pulses are created using piezoelectric transducers, which convert the electric pulse applied to them into mechanical pressure waves [8]. There is usually a transmitting transducer that transmits the pulses using this principle, and a receiving transducer that then converts the reflected sound pulses back into

an electrical signal using the same (but inverse) mechanism. One transducer can also be used as both the transmitting and receiving transducer. Figure 2.1 illustrates the basic operation of active SONAR, where T_X is the transmitting transducer, and R_X is the receiving transducer.

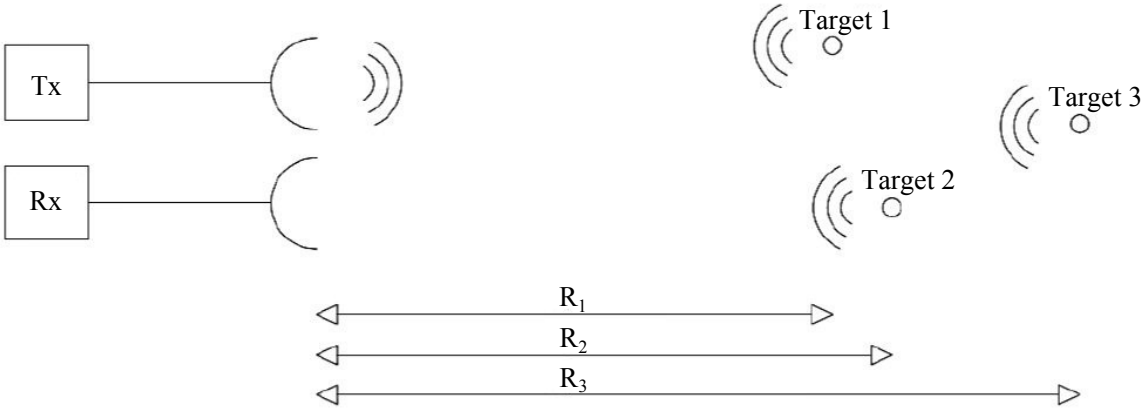

Figure 2.1 – Simple illustration of active SONAR [4].

2.2.1.1 Sound Velocity

The speed at which sound travels through water is very important for a SONAR system. It is needed in range calculations, as discussed in Section 2.2.1.2, and also in Doppler calculations, which will not be discussed in this thesis.

The speed of sound in water can be determined using Equation 2.2.1 from L.E. Kinsler, *Fundamentals of Acoustics* [9].

$$c = 1448.6 + t(4.618 - 0.0523t) + 1.25(s - 35) + 0.017d, \tag{2.2.1}$$

where

- c = Velocity of sound (m/s),
- t = Temperature ($^\circ$C),
- s = Salinity (ppt), and
- d = Depth (m).

2.2.1.2 Range

The further an object is away from the source of the sound pulses, the longer the delay will be between when the wave is transmitted and when it is received. Thus each of the targets in Figure 2.1 will cause a different time delay of τ_i corresponding to the range R_i of the object. This time delay can then be used to calculate the range of each object, using Equation 2.2.2 [4].

$$R = \frac{c\tau}{2} \tag{2.2.2}$$

In Equation 2.2.2, c is the speed of the sound pulse in water, and the factor of $\frac{1}{2}$ compensates for the return path time delay of the signal travelling to the target and back to the transducer [4]. There are practical factors that need to be taken into account when using this formula, such as the type of filter that is used as a signal processing technique, but that is not discussed here.

2.2.1.3 Range Resolution

The range resolution of SONAR, usually denoted as ΔR, describes the minimum separation between two objects where the SONAR system can still identify them as separate objects. Figure 2.2 shows a simple example of an arbitrary SONAR pulse and the received decoded signal.

Figure 2.2 – Arbitrary transmitted signal and received decoded signal [10].

Figure 2.3 and Figure 2.4 show the difference between a SONAR system with a large range resolution and another that has a small range resolution. If ΔR is not smaller than the difference in range between the two objects, the system cannot identify them as two separate objects.

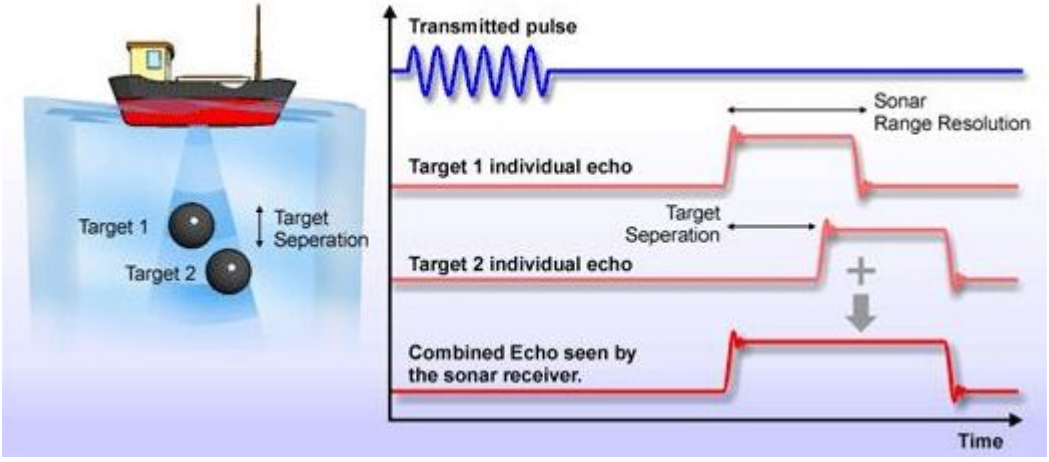

Figure 2.3 – SONAR range resolution: Target separation too small [10].

In Figure 2.4, ΔR is small enough for the SONAR system to be able to identify the two targets as separate.

The range resolution of a transmitted waveform with bandwidth B is calculated using Equation 2.2.3.

$$\frac{\Delta R}{\mathrm{m}} = \frac{c}{2B} \tag{2.2.3}$$

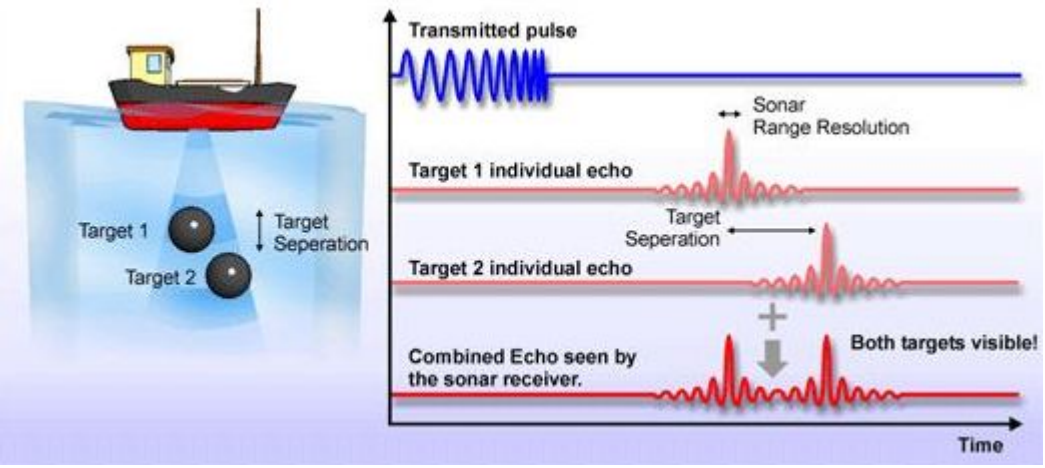

Figure 2.4 – SONAR range resolution: Target separation far enough [10].

2.2.1.4 Sound Propagation

Sound waves travel through water without too much attenuation [3], making the use of a SONAR system very effective under water. Unfortunately, the water in the ocean (where an AUV would usually find itself) is anything but homogeneous. It is filled with biological and non-biological material that reflects and refracts acoustic waves, and the ocean consists of different layers of water that have different temperatures (and therefore different densities) and salinities. If an acoustic wave enters a layer of water with a different density it will be refracted.

All of these issues are assumed to be negligible because of the controlled environment in which testing occurs (as is discussed in Section A). The controlled environment has negligible amounts of suspended particles that can reflect sound waves and it can be assumed that there are no layers that have different temperatures. The one big issue that needs to be addressed is reverberation. Reverberation occurs when a sound is produced in a environment with many reflective surfaces (especially in a closed environment), causing echoes to build up and then slowly decay as the sound is absorbed by the walls and the water. Since SONAR techniques make use of sound waves, it is quite applicable. For reverberation to occur, reflecting surfaces are needed to cause the echoes. In the ocean, the seabed and the water surface can both cause severe reverberation. In the closed environment of a harbour or even a testing tank, the man-made walls will result in high energy echoes.

Special precaution will have to be taken during this project to ensure that reverberation does not cause inaccurate readings and measurements. A more detailed discussion concerning reverberation can be found in Section 2.2.1.8.

2.2.1.5 Beam-Spread

Beam spread (also referred to as beam-width) in a SONAR system is of specific interest in this project. Knowing how wide the beam spread is will be important when it comes to finding the edges of located objects. Since the transducers used are circular in shape, the beam that is formed can be approached as conical in shape [11]. The beam spread angle is shown below in Figure 2.5, denoted as θ. The actual beam pattern is less ideal, with side lobes that insonify areas that are not intended to be insonified. A depiction this beam pattern with side lobes can be seen

in Figure 2.6.

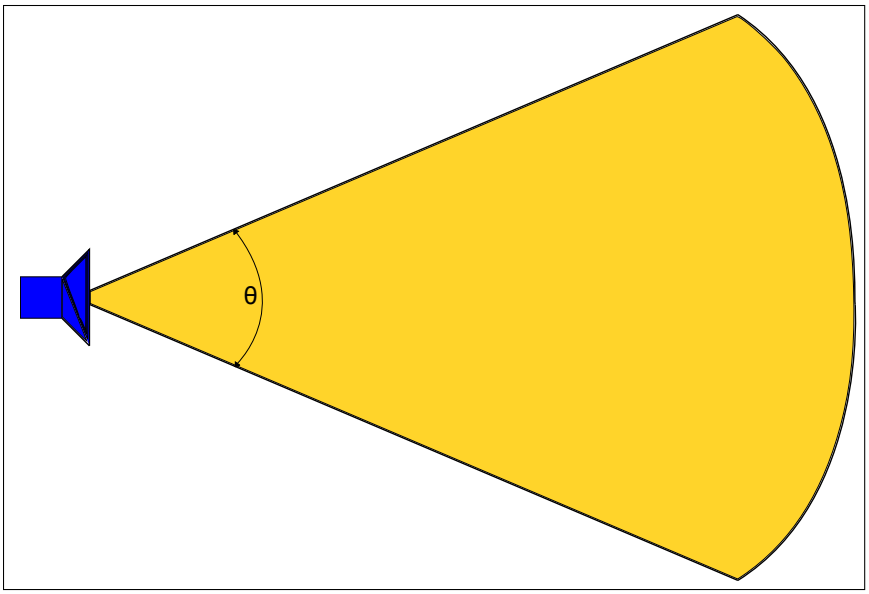

Figure 2.5 – Ideal (conical) SONAR beam-spread pattern for round transducers.

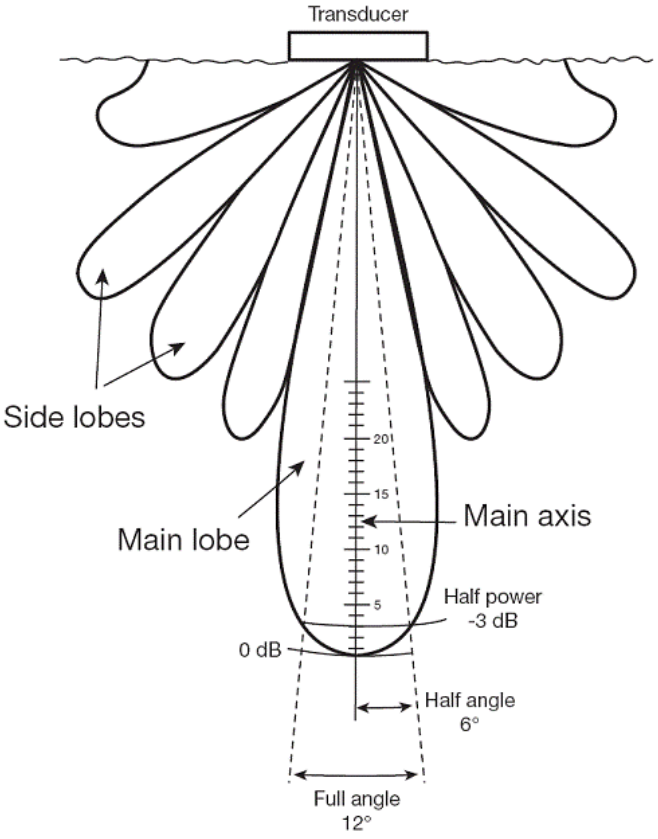

Figure 2.6 – An example of the theoretical SONAR beam-spread pattern for round transducers [12].

Naturally, the width of the beam increases as the distance from the transducers increases. Thus, even if the transducers have a very small beam-spread angle of 1° or 2°, at a certain distance from the transducer, the beam will very wide and thus less accurate.

Beam-spread is calculated using Equation 2.2.4 [13].

$$sin\theta = 1.2\frac{V}{DF}, \tag{2.2.4}$$

where

- θ = Beam-spread angle $(^\circ)$,
- V = Sound Velocity (m/s),
- D = Diameter of transducer (m), and
- F = Sound wave frequency (hz).

It is clear that the frequency of the sound wave and the diameter of the transducer both play an important role in determining the beam-spread. If a narrow beam-spread is required, the frequency and diameter will have to be increased.

2.2.1.6 Acoustical Reference Units

It is good practice to define reference units for sound pressure and sound intensity in underwater acoustics. According to *Handbook of Underwater Acoustics Engineering* [3] by Heinz G. Urban as well as *Sonar for Practising Engineers* [14] by A.D. Waite, the reference unit for sound pressure is defined as $\rho_0 = 1$ μPa. The reference for sound intensity, denoted as I_0, is calculated as shown in Equation 2.2.5. The calculations are done assuming the standard conditions for fresh water, thus $c = 1480$ m/s and $\rho_0 = 1000$ kg/m^3 [4].

$$I_0 = \frac{\rho_0^2}{\rho_0 c} = 0.67568 \times 10^{-18}\ \text{W/m}^2 \tag{2.2.5}$$

The formal definition of sound intensity is the energy per second crossing a unit area [15].

2.2.1.7 Source Level

The source level, or transmitted sound intensity [12], denoted as *SL*, is defined by Heinz G. Urban in his book, *Handbook of Underwater Acoustics Engineering* [3], as in Equation 2.2.6.

$$\frac{SL}{dB_{re1\mu Pa}} = 10log\left(\frac{\text{intensity of source at standard range}}{\text{reference intensity}}\right) = 10log\frac{I}{I_0} \tag{2.2.6}$$

The standard range, referred to in Equation 2.2.6, is defined as $r_0 = 1$m. The standard range is used to overcome difficulties in making practical measurements. If the source is assumed to be omni-directional, the surface area of the sound pulse can be described as that of a sphere, which is $4\pi r^2$. At the standard range the surface area is 12.6 m^2. Equation 2.2.6 can then be rewritten in logarithmic form as in Equation 2.2.7 by applying standard range r_0 and standard intensity I_0.

$$\frac{SL}{dB_{re1\mu Pa}} = 10logP + 170.7\,dB \quad [4] \tag{2.2.7}$$

P represents the total *acoustic* power radiated, which is a certain percentage of the *electrical* power applied to the transducer/projector, depending on the transducer efficiency.

Equation 2.2.7 is not entirely applicable because of the assumption of omnidirectional transmission. Most projectors are directional, thus the transmission Directivity Index, DI_t (gain) has to be incorporated into the equation, as done in Equation 2.2.8. Directivity is discussed further in Section 2.2.1.10.

$$\frac{SL}{dB_{re1\mu Pa}} = 10logP + 170.7\,dB + DI_t \quad [4] \tag{2.2.8}$$

2.2.1.8 Reverberation

A simple way of defining reverberation is "waves scattering in the sea" [16]. The sea contains inhomogeneities of many different kinds, ranging in size from tiny dust particles to large schools of fish and to mountains and hills on the seabed. These inhomogeneities intercept and reflect portions of the sound waves. This process is called scattering, and the sum of all the scattering that occurs is called reverberation [16]. Since reverberation can cause distortions and incorrect measurements in SONAR, steps have to be taken to ensure the limitations placed on a SONAR system by the effects of reverberation are minimised. To do so, the reverberation level has to be estimated.

Three different kinds of reverberation are usually encountered in the ocean:

- Volume reverberation,
- Sea surface reverberation, and
- Sea bottom reverberation.

Due to the fact that this project deals with collision avoidance and operates in shallow water, the AUV can be assumed to move mostly in the horizontal plane. Thus, sea surface and sea bottom reverberation are ignored for the purposes of this project and only volume reverberation is considered. Volume reverberation is caused by scattering due to in-homogeneities in the scanned water volume, such as suspended particles, changes in temperature or air bubbles in the water [4].

Reverberation calculations for SONAR are done similar to that of RADAR. The backscattering coefficient $S_{A,V}$ is defined as the ratio of the scattered intensity, referred to one meter from the acoustic centre, to the intensity of the incident plane wave. Unfortunately, $S_{A,V}$ is hard to predict. In Robert J. Urick's book *Principles of Underwater Sound for Engineers* [16], he states various values of $S_{A,V}$ for different environments. It can also be approximated using Equation 2.2.9.

$$\frac{S_{A,V}}{dB} = 10log\frac{I_{\text{scat}}}{I_{\text{incident}}} \tag{2.2.9}$$

Using this equation the reverberation level at the receiver caused by volume reverberation is expressed in *Principles of Underwater Sound for Engineers* [16], as:

$$\frac{RL}{dB} = SL - 40logr + S_V + 10logV, \tag{2.2.10}$$

where

- SL is the source level in dB,
- r is the range between the transmitter and the insonified volume in meters, and
- V is the insonified volume in m^3.

V also needs to be calculated as it is needed in Equation 2.2.10. For the case of the distance r being large in comparison to the cross-section of the insonified volume, which is true for this project, the following volume equality is true [4]:

$$V = \frac{cT}{2}\frac{\pi r^2 \theta_h \theta_v}{4}, \tag{2.2.11}$$

where

- c is the speed of sound in m/s,
- T is the pulse length of a CW pulse in seconds or the reciprocal bandwidth of a LFM pulse, and
- θ_h and θ_v are the respective horizontal and vertical beam-widths in radians. With the beam-spread being considered as conical, these angles are equal.

2.2.1.9 Propagation Losses

Propagation losses (PL) in SONAR also deserves a mention. It is the decrease in acoustic intensity between a source and a receiver, or the sum of spreading loss and absorption loss. In previous work [4], it is mentioned that the cylindrical spreading law, as discussed by A.D. Waite in his book *Sonar for Practicing Engineers* [14], is applicable to this project. Equation 2.2.12 is then derived [4].

$$\frac{PL}{dB} = 10log(r), \tag{2.2.12}$$

where r is the radius from the source.

2.2.1.10 Directivity

The directivity index, or DI, of SONAR transducers refers to the gain in SNR (signal to noise ratio) of the projector array due to the non-omni-directional beam pattern of the projectors/transducers. The transducers used in this project are round (piston) in shape, and since the projector face (40mm) is considerably greater in size than the wavelength of the transmitted wave ($\lambda \approx 4.5$ mm if $f = 330$ kHz), Equation 2.2.13 from *Principles of Underwater Sound for Engineers* [16] by Robert J. Urick, theoretically describes the DI of a circular source.

$$\frac{DI}{dB} = 10log\left(\frac{\pi D}{\lambda}\right)^2, \tag{2.2.13}$$

for $2D >> \lambda$.

2.2.1.11 Noise

One of the most noteworthy factors that limits the ability of SONAR to resolve targets is noise. A.D. Waite distinguishes between three main sources of noise in SONAR in his book *Sonar for Practising Engineers* [14]:

- Thermal noise,
- Ambient noise (noises from the ocean), and
- Vessel noise.

For the purposes of this project it is assumed that, of the three sources of noise mentioned, only thermal noise is significant. This is mainly because testing will be done in a water tank, which is a controlled environment free of ambient sound and water agitation. Also, the centre frequency of the SONAR platform is quite high (> 280 kHz). At high frequencies, thermal noise becomes dominant over other sources of noise [4].

Thermal noise is calculated for the environment used in this project and for a signal frequency of 330 kHz to be:

$$N_{\text{thermal}} = 35\ dB_{re\ 1\mu Pa}. \quad [4] \tag{2.2.14}$$

2.2.1.12 Target Strength

The Target Strength (*TS*) is the echo returned from an underwater target. According to *Sonar for Practicing Engineers* by A.D. Waite [14], the reflected acoustic intensity of a spherical object in water is as given in Equation 2.2.15.

$$I_r = \pi r_s^2 I_i, \tag{2.2.15}$$

where r_s is the radius of the spherical object and I_i is the intensity of the incident wave measured in $\frac{\text{W}}{\text{m}^2}$. It is worth noting that, in the previous work done [4], it was assumed that the targets are spherical.

If the sphere is at a range of 1m (this is done to keep with the standard notation established in previous sections), Equation 2.2.16 gives the target strength.

$$\frac{TS}{dB} = 10log\left(\frac{I_r}{I_s}\right) = 10log\left(\frac{r_s^2}{4}\right) \tag{2.2.16}$$

In the case where the target is not spherical, as with many of the tests done in this project, a different formula is used, as in Equation 2.2.17.

$$\frac{TS}{dB} = 10log\left(\frac{\sigma}{4\pi}\right), \quad [17] \tag{2.2.17}$$

where σ represents the backscattering cross-section. The backscattering cross section represents the degree to which sound is scattered off of a target.

In the specific case of a rectangular plate, the formula becomes:

$$\frac{TS}{dB} = 10log\left(\frac{ab}{\lambda}\right)^2, \quad [17] \tag{2.2.18}$$

where λ is the wavelength of the wave and a and b are the lengths of the sides of the target. This is only true if the incident angle of the sound wave is $0°$. This formula shows that a sphere with the same radius r_s will have a much lower target strength than a square surface with side length r_s.

2.2.1.13 Detection Threshold and Detection Index

The *Handbook of Underwater Acoustics* [3] defines detection threshold as follows: "The detection threshold is the signal-to-noise ratio at the input of the receiver that results in a signal-to-noise ratio at the output of the receiver, with defined probabilities of detection and false alarm". The detection threshold can be calculated as shown by Equation 2.2.19.

$$\frac{DT}{dB_{re1\mu Pa}} = 10log\left(\frac{S}{N_O}\right)_{in}, \tag{2.2.19}$$

where

- S is the signal power in the receiver input frequency band, and
- N_0 is the noise power in 1 Hz bandwidth.

Simply put, a pre-defined level of correctness is assigned to a required signal to noise ratio at the receiver input which leads to a signal to noise ratio at the output of the receiver. If the threshold is exceeded, a target is assumed to be detected. If the threshold is set too low, there might be many false alarms, and if it is set too high, only very strong targets will be detected.

The detection threshold has been covered in great depth previously [4], thus it will not be discussed further.

2.2.1.14 The SONAR Equation

The SONAR equation is of utmost importance when it comes to calculating the performance of different SONAR systems. It forms the basis for preliminary estimation. It is given in its simplest form by Heinz G. Urban in his book, *Handbook of Underwater Acoustics Engineering* [3]:

$$DT = SL - 2PL + TS - (NL + RL - DI), \tag{2.2.20}$$

where

- PL represents the propagation loss in dB,
- SL represents the projector source level in dB,
- TS represents the target strength in dB,
- DI represents the directivity index of the transducers in dB - calculated for transducers,
- NL represents the noise level in dB,
- RL represents the reverberation level in dB, and
- DT represents the detection threshold in dB.

The detection threshold may be thought of as the signal-to-noise ratio (SNR) at the receiver input, which ultimately indicates the effectiveness of a SONAR system design [4].

2.2.2 Signal Design

As mentioned in Section 2.2.1, the SONAR transducers convert an electric signal to mechanical (physical) waves by means of the piezoelectric effect. This electric signal has to be generated, and the specific waveform that is used as the electric signal needs to be chosen with great care. The selection of this signal wave form determines the ability of the SONAR system to resolve targets in range and velocity. Thus, the end goal of the SONAR platform determines the waveform. The environment in which the system is used also influences the choice of waveform. For example, if an environment causes high levels of reverberation, a signal waveform needs to be chosen that can negate the effects of reverberation.

There are three main categories of signal waveforms that are applicable for scanning the underwater environment:

- Constant Wave Pulses (CW),
- Frequency Modulated Pulses (FM), and
- Discrete Coded Waveforms.

All three of these categories were investigated for their suitability for the AUV in previous work [4], and the findings are summarised below.

2.2.2.1 Constant Wave Pulses

Constant wave pulses are the oldest and simplest waveforms used in SONAR. It is a pulse of constant frequency f and pulse length of T seconds, and is also referred to as a constant frequency (CF) pulse. Equation 2.2.21 shows an expression that describes a CW wave.

$$v(t) = \text{rect}\left(\frac{t}{T}\right) cos(2\pi f_0), \quad [4] \tag{2.2.21}$$

where

- rect$\left(\frac{t}{T}\right)$ defines the envelope of the pulse,
- T is the pulse length, and
- f_0 is the frequency of the pulse.

The effective bandwidth of a CW pulse shown in Equation 2.2.22, and the range resolution is given by Equation 2.2.23 [4].

$$\frac{B}{\text{Hz}} = \frac{1}{T} \tag{2.2.22}$$

$$\frac{\Delta R}{\text{m}} = \frac{c}{2B}, \tag{2.2.23}$$

where B is the bandwidth of the pulse in Hz, and f_0 is the frequency.

Figure 2.7 shows a time domain plot of a CW pulse.

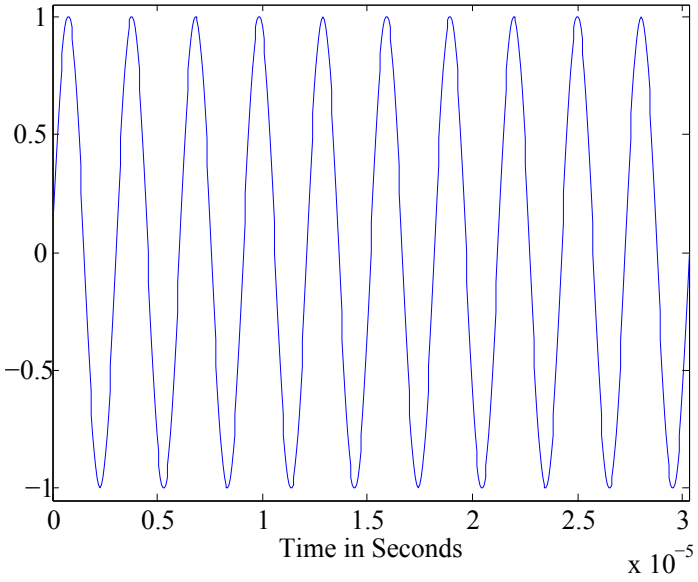

Figure 2.7 – CW pulse in the time domain.

The conclusion reached after discussing the properties of CW in depth [4], is that it is best used as a Doppler frequency resolving tool. Thus it is very applicable to situations where the velocity of the objects found under water is of importance. Since this project does not focus on finding the velocity of a target, CW is not used in this project.

2.2.2.2 Frequency Modulated Pulses

There are three prominent forms of frequency modulation: linear, sinusoidal and hyperbolic modulation. Of these three, linear frequency modulation (LFM) is selected for investigation in this project. According to previous work [4], it is the most widely used of the three and it may be implemented using low cost, off the shelf hardware. Using FM (Frequency Modulated) pulses increases the range resolution of the SONAR system, but it makes the system Doppler tolerant, which also means that Doppler frequency shifts cannot be determined accurately, if at all [4].

Another reason that LFM is chosen for investigation, is that LFM signals with sufficient bandwidth suppress interference very well, as energy is spread over a whole frequency band. This interference is classified as general background noise combined with reverberation. In fact, according to V. Pjachev [18], LFM has been found to provide the best reverberation suppression in many cases.

Equation 2.2.24 can be used to model an LFM pulse:

$$x(t) = \text{rect}\left(\frac{t}{T}\right) cos(2\pi \left[f_0 t + \frac{1}{2}kt^2\right]), \quad [4] \tag{2.2.24}$$

where

- $\text{rect}\left(\frac{t}{T}\right)$ defines the envelope of the pulse,
- T is the pulse length,
- f_0 is the centre frequency of the pulse, and
- k is the linear frequency sweep rate.

The sweep rate of an LFM pulse is defined by the bandwidth B and duration T, as done in Equation 2.2.25.

$$\frac{k}{\text{Hz/second}} = \frac{f_H - f_L}{T} = \frac{B}{T} \tag{2.2.25}$$

A time domain representation of an LFM pulse is shown in Figure 2.8. In this waveform, the frequency is swept from a lower frequency f_L to a higher frequency f_H over a period of time T, with a bandwidth B.

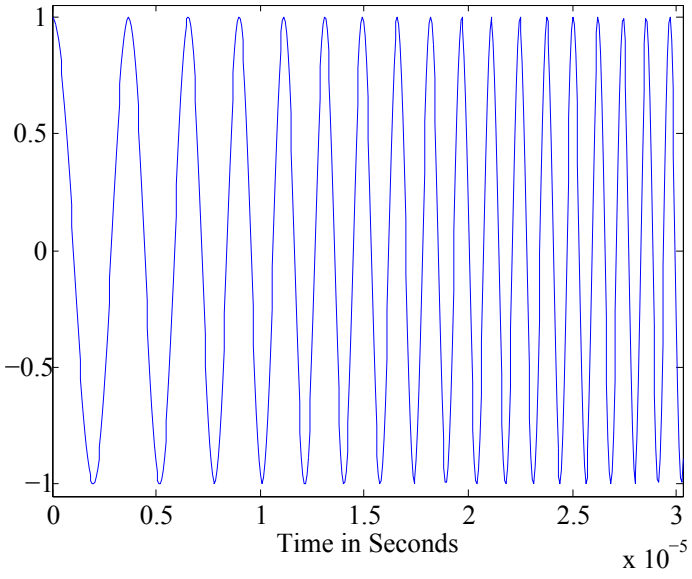

Figure 2.8 – LFM pulse in the time domain.

The bandwidth of a LFM signal is the frequency band the pulse is "chirped" in, which means that the bandwidth is not dependent on the pulse duration as in the case of CW, where $B = \frac{1}{T}$.

The range resolution of a LFM waveform is shown Equation 2.2.26. Since the bandwidth can be altered easily, the range resolution can theoretically be improved indefinitely.

$$\frac{\Delta R}{m} = \frac{c}{2B} = \frac{cT}{2} \tag{2.2.26}$$

The bandwidth product, or compression ratio of an LFM pulse is defined in Equation 2.2.27.

$$\xi = BT \tag{2.2.27}$$

The compression ratio gives an indication of how well range can be resolved compared to another waveform, such as a CW pulse. For example, a CW pulse of length $T = 0.1$ seconds has a range resolution $\Delta R = 73$m according to Equation 2.2.3. If a LFM signal of $T = 0.1$ seconds has a bandwidth of $B = 100000$ Hz, its compression ratio would be $\xi = 10000$. Thus the system's range resolution would be reduced, and thus improved, by a factor of $1/10000$ compared to the CW signal.

2.2.2.3 Discrete Waveforms

Generally CW and LFM waveforms, as already discussed, are analogue signals. Discrete coded waveforms have now evolved in both RADAR and SONAR applications due to the advance in digital technology. A discrete coded waveform commonly consists of a series of narrow-band pulses added together to form one pulse [4]. Discrete coded waveforms have been found to have potentially superior ability to resolve both range and Doppler. According to *Radar Signal Analysis and Processing using Matlab* by B.R. Mahafza [19], discrete coded waveforms are more effective when it comes to range than Doppler.

Another advantage of using discrete coded waveforms is that they are very difficult to detect and have inherent anti-jamming capability, which makes it of great interest for military applications. This aspect is, however, not pursued in this project.

Different forms of discrete coded waveforms have been discussed in great depth [4]. Unmodulated pulse train codes, phase modulated codes and frequency modulated codes are each discussed. After an investigation of all the different possibilities, it was decided that discrete coded pulses would not be used in his project. This is due to the fact that it is very difficult to achieve a compression ratio that can equal that of a LFM pulse using discrete coded pulses. If a competitive compression ratio is to be achieved, the minimum hardware requirements will be too expensive.

2.2.3 Range Processing Techniques

In order to extract range information from a signal received by the receiving transducer, the signal is usually correlated in a certain way against the transmitted signal. The two correlation techniques that are most widely used are matched filtering (MF) and inverse filtering (IF). Both of these techniques have advantages and disadvantages, and have been discussed thoroughly [4]. Thus the findings are only summarised here. The mathematics behind the workings of all the filters and techniques will not be discussed in great depth, and can be found in [4].

There is, however, another approach for obtaining range measurements called re-damping. It is discussed in Section 2.2.3.3.

2.2.3.1 Matched Filter

A matched filter is a correlator that compares two known signals to generate an output, indicating how well the two signals match [20]. An advantage of the MF, is that it is able to produce the maximum achievable signal to noise ratio (SNR). Maximum SNR means that the influence of the interference caused by noise is minimised.

From the research done, it is clear that SNR depends only on the energy of the signal and the input noise power. The signal waveform has no influence. Thus, it is optimised for the detection of a single dominant signal in noise. The MF does not fare very well when there are multiple closely spaced echoes.

2.2.3.2 Inverse Filter

The inverse filter can be used to improve upon the range resolution of the MF. The conclusion reached [4] is that the IF is designed to deliver optimal resolution, but struggles with regards to detection. It experiences even more problems with detection if the signal is submerged in noise.

N. Sharma sums the situation up quite well in his article *Trading detection for resolution in active sonar receivers* [21], when he says: "A matched filter cannot resolve some targets that it can detect, and an inverse filter cannot detect some targets that it can resolve". There will always be a trade-off between the MF and IF in SONAR.

2.2.3.3 Re-damping

Re-damping is a technique that is usually used in RADAR applications, and thus there is not much literature to be found concerning the use of re-damping in SONAR. This is mainly because it requires a continuous linear frequency-modulated pulse (FMCW) in order to work. It also requires a continuous signal to be transmitted, which may cause large amounts of noise in an environment where reverberation is a problem.

The basic idea behind re-damping is multiplying the transmitted and received signals to obtain two signals. The one signal has a frequency equal to the sum of w_T (transmitted signal frequency) and w_R (received signal frequency), and the other has a frequency equal to the difference between w_T and w_R.

This technique has been studied and found to be impractical for use in this project due to the fact that a continuous signal will cause too much reverberation.

2.2.3.4 The Ambiguity Function

The ambiguity function is a tool used to predict the performance of a chosen pulse waveform in range and Doppler frequency determination. It can be used in both SONAR and RADAR applications. It assumes that a matched filter is used in the processing of the signals. The mathematics behind the ambiguity function are not discussed in this thesis.

2.2.4 Design and Simulation of Signals and Processing Techniques

This section summarises the previous work done [4] concerning the choice of signal waveforms used in the project and the simulation of those waveforms to test their ability to detect targets.

2.2.4.1 Pulse Design Requirements

After the research was done for Section 2.2.2, it was decided that CW would be used to resolve Doppler frequency shifts and LFM would be used to determine range. Since Doppler frequency shifts fall outside the scope of this thesis, only LFM will be considered for this project. The following requirements for range were chosen [4]:

- Maximum range of 50 m.
- High accuracy in range resolution ΔR, ideally to the nearest 1 cm.
- Reverberation resistant.

2.2.4.2 LFM Pulse Design Requirements

As discussed previously, LFM pulses are very effective when it comes to combating the effects of reverberation, thus the design requirement regarding reverberation can be considered to be met. With that being the case, the only other design requirements that need to be addressed are the range and the range resolution. The maximum range theoretically depends solely on the energy of the pulse, not on the type of pulse [4]. In the case of an LFM pulse, the energy depends on the pulse length as well as the instantaneous power output level of the final amplification stage.

The formula used for the bandwidth calculation is Equation 2.2.26. It can be rewritten to calculate the bandwidth as done in Equation 2.2.28.

$$B = \frac{c}{2\Delta R} \tag{2.2.28}$$

If the design requirement of ΔR mentioned in Section 2.2.4.1 is to be reached, the bandwidth is calculated (with $c = 1476$ m/s) using Equation 2.2.28 to be $B = 73.8$ kHz. In order to compensate for signal loss due to noise and reverberation, the bandwidth is chosen as $B = 100$ kHz. This will give a theoretical range resolution of $\Delta R = 0.73$ cm [4]. It is thus over designed by a factor of 1.4.

2.2.4.3 Power Calculations

It is important to calculate how much energy needs to be transmitted to ensure target detection. If the amount of energy is too low, the signal to noise ratio of the signal captured by the receiving transducer will be too low. It is generally agreed upon that a signal to noise ratio should be more than 10 to achieve a positive and correct detection of a target [4].

The power requirements are the same for LFM and CW, and it was found that [4]:

$P_{acoustic} = 7.1W$
$P_{electrical} = 11W$

This is applicable if the following is true:

- Target sphere diameter $r_s = 1$ cm, and

- Range = 50 m.

The targets used during this project are not all spherical, as assumed for these power calculations. The targets used vary in size and shape, but all of them have a larger reflective surface than the 1cm sphere mentioned above. If these power requirements are used for the other targets, target detection will definitely occur due to the larger reflective surfaces.

2.2.4.4 Simulations

The LFM pulse designs are simulated using Matlab to verify the capacity of the pulse to resolve range [4].

Several different simulations were done to test the signal waveforms. The simulation results for CW waves will not be discussed here since CW is not used in this project.

For LFM, three targets at ranges of 9m, 26m and 50m were easily detected using Inverse Filter and Matched Filter techniques. The conclusion reached at the end of the simulations is that a range resolution of 1.5cm could be achieved using IF and MF techniques. This result can be seen in Figure 2.9 and Figure 2.10. The unit “dB re 1μPa” is "RMS acoustic pressure in micropascals".

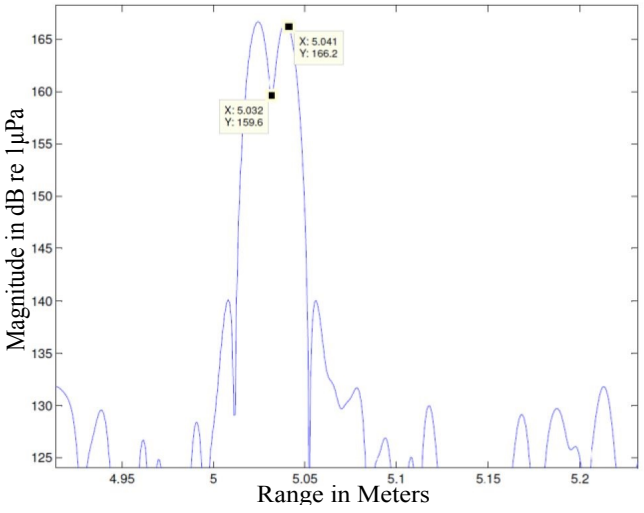

Figure 2.9 – MF output for two targets spaced 1.5cm apart [4].

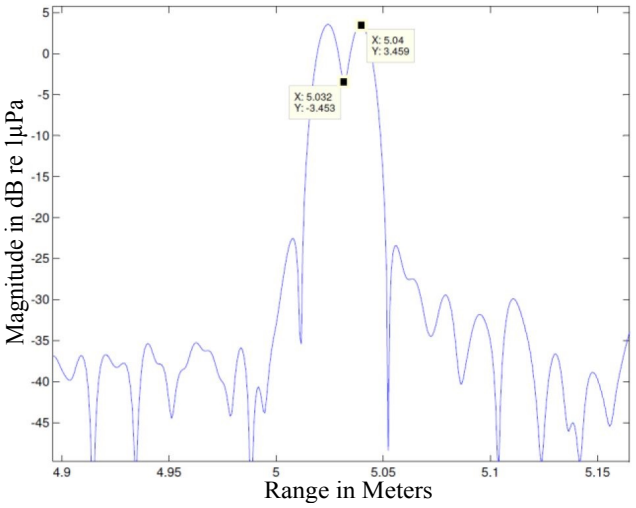

Figure 2.10 – IF output for two targets spaced 1.5cm apart [4].

2.2.5 Results of Previous Work Done

The results achieved are as follows [4]:

- Range resolution of 14mm using a LFM pulse and an inverse filtering technique,
- Targets could be located at a range of up to 51m, and
- Target velocity measurement resolution of less than 0.1m/s.

2.2.6 Laboratory Hardware Setup

2.2.6.1 Overview

The existing SONAR laboratory setup [4] is used in this project. It is a very flexible platform that allows for more freedom than what a ready-built SONAR system can offer. With this platform, the type of signal used, the frequency, the power and more can be changed at will (with some programming). It also gives the user the ability to measure and capture the signal at intermediate stages of the signal path. What is also significant is that most pre-built SONAR systems come with their own signal processing techniques, and rarely give the user access to the raw data. This system is thus ideal, because the user can study and process the raw SONAR data.

Figure 2.11 shows a simple flow-diagram of the hardware layout.

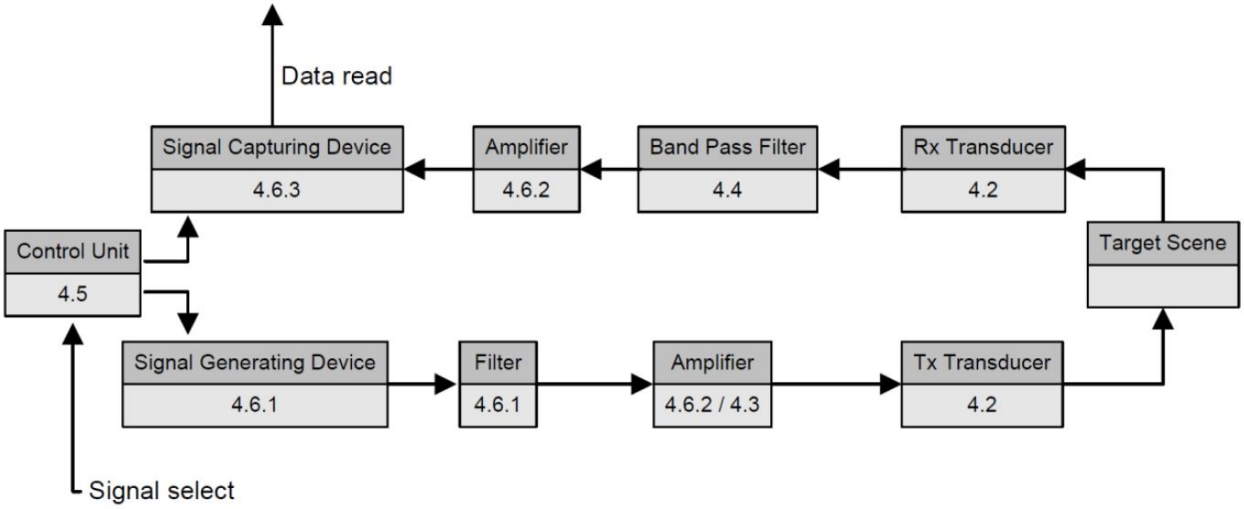

Figure 2.11 – Basic hardware layout [4].

The user selects a signal to be generated (this includes the signal type, length and frequency) using serial communication with the control unit. The signal generator (DDS or Direct Digital Synthesiser) then generates the signal, which is then filtered and amplified before it is sent out to the transmitting transducer. The transducer converts the electrical signal into a sound wave, which is transmitted into the water. Once the sound wave hits an object, it reflects back to the receiving transducer, which converts it back into an electrical signal, which is then filtered and amplified again before it is captured by the signal capturing device. Once captured, the data is sent to a computer where it can be processed and analysed using different techniques.

The entire hardware setup (as shown in Figure 2.11) has been left unchanged, and it has been discussed in great length [4]. Therefore it will only be discussed briefly here. New pieces of hardware that were built and used for this project are discussed in Chapter 3.

2.2.6.2 Transducers

Overview

The circular transducers used in this project are shown in Figure 2.12 below. As mentioned earlier, transducers make use of the piezoelectric principle to convert electrical signals to sound

waves and back again [22]. The transducers are 4.4 cm in diameter and have a maximum operating voltage of 100 V.

Figure 2.12 – Rx and Tx transducers.

Beam-Spread

The beam-spread of the transducers is discussed in more detail in Section 2.2.1.5, and is found to be as follows (using Equation 2.2.4):

$\alpha_{230kHz} = 7.9°$
$\alpha_{330kHz} = 6°$

Transducer Compensation

Circuits were also designed and built to match the impedance of the transducers and their cables with the impedance of the supplying and receiving components. This allows for maximum power transfer. The theory behind this has been discussed in great detail [4].

Using a Smith chart, the capacitive, resistive and and inductive values were found for the compensation circuits of both the Tx and Rx transducers [4].

Directivity

The average directivity gain per transducer was found to be [4]:

$DI = 24.4$ dB

This was found experimentally. There is a peak in the gain at approximately 350 kHz due to the transducers being resonant at that frequency, as can be seen in Figure 2.13. This figure also shows the calculated directivity using Equation 2.2.13 [4]. The most favourable frequency band is thus in the 230 kHz to 330 kHz range.

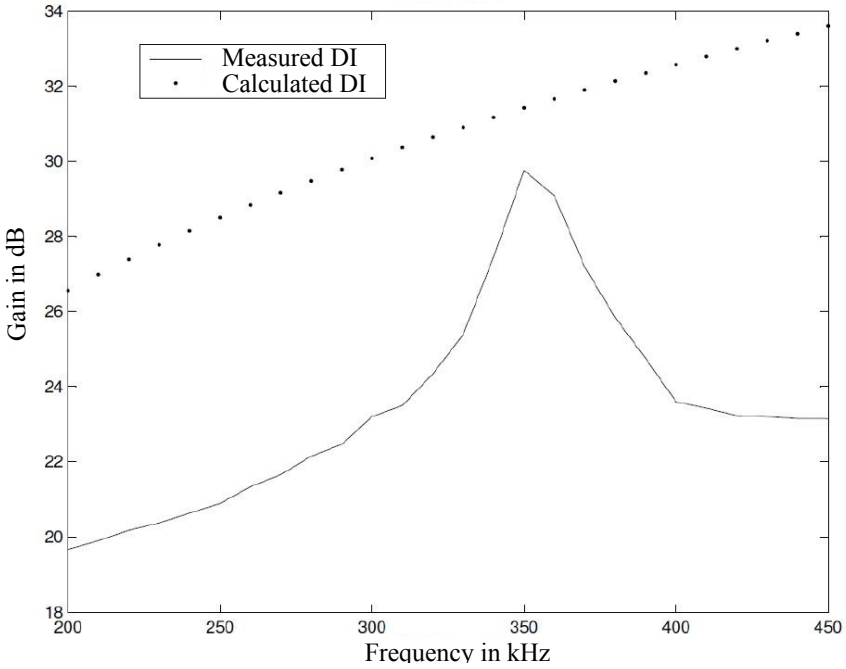

Figure 2.13 – Measured versus calculated DI gain of transducer [4].

2.2.6.3 Main Amplifier

The main amplifier that is used has been left unchanged for this project. The pre-amplifier that is used to amplify the signal from the DDS is discussed in more detail in Section 2.2.6.6. The main amplifier is a high power, fixed gain amplifier that drives the transmitting transducer, while the pre-amplifier is a low noise, variable gain amplifier.

The amplifier was built to cater for the characteristics of the transducers and thus has the following characteristics:

- Output Voltage up to 180 $V_{\text{peak to peak}}$.
- Voltage input of maximum 2 $V_{\text{peak to peak}}$.
- Slew Rate of 2500 $V/\mu s$.
- Rated RMS output current of $\pm$ 1.5 A.
- Peak output current of $\pm$ 5 A.

The amplifier, when combined with the transducers, was designed to have an almost constant gain over the desired frequency band.

Further details of the main amplifier, such as the circuit design, the PCB design, and the heat dissipation will not be discussed here as it is considered to be outside the scope of this thesis.

2.2.6.4 Band Pass Filter

The signal received from the receiving transducer is expected to be noisy, and thus a filter is used to filter out the worst of the noise. Due to the fact that the pass band is so large, one high pass

and one low pass filter were put in series, of which both are 6th order passive Butterworth filters to achieve sharp cut-offs. The high and low cut-off frequencies are as follows:

- $f_{low} = 180$ kHz
- $f_{high} = 380$ kHz

2.2.6.5 Power Supply

The hardware that has been discussed in this section thus far, as well as the development boards that will be discussed hereafter, all need numerous different voltages to operate. In order to simplify the process of giving power to the entire platform, a power supply PCB was built that supplies the correct voltages to each of the components.

2.2.6.6 Development Boards

The development boards used in the SONAR platform are as follows:

- Signal Generation - Direct Digital Synthesiser.
- Pre-Amplifier - Low-noise variable gain amplifier.
- Signal Capturing - ADC in conjunction with a First In First Out (FIFO) data capturing chip.
- Control Unit - ESL avionics board.

All of these boards needed to communicate with each other in such a way the the signal sending-and-receiving process is synchronised. To do this, a dsPIC (control unit) was used to facilitate communication between the development boards. The above-mentioned development boards and the dsPIC will now each be discussed briefly.

Direct Digital Synthesiser

The inner workings and finer details of the DDS will not be discussed here, but rather its functionality. It is a very versatile piece of hardware that can be programmed to produce a large variety of signals. It can be programmed via a USB connection using the appropriate proprietary software, but for the purposes of this SONAR platform, it was set up to be programmed by the dsPIC. The code that was written previously [4] has been rewritten during this project to give the user more freedom in signal choice. The user can now choose not only whether the signal should be a CW wave or an LFM wave, but also the length (T) and frequency (f) of the wave.

The DDS used for this project is mounted on the AD9959/PCB development board made by Analog Devices.

Pre-Amplifier

The AD8332-EVALZ board by Analog Devices is used for the SONAR platform. It features a variable gain, ultra-low noise pre-amplifier, and has a programmable input impedance, which is

set to 50 Ω to match the rest of the system's impedance. It is used on both the receiving and transmitting side of the platform. On the transmitting side, it acts as a buffer between the DDS and the main amplifier, to both boost the signal and protect the DDS in case the main amplifier fails.

On both sides the pre-amplifier acts as a gain controller, as its gain can be varied by the user. This pre-amplifier has a maximum output of $2\ V_{\text{peak to peak}}$, which is the maximum input for both the main amplifier and ADC.

ADC and FIFO

The ADC (analog to digital converter) board used is the AD9248 board. It is used in conjunction with the HSC-ADC-EVALB (First In First Out, or FIFO) evaluation board. Both are supplied by Analog Devices and feature dual signal processing capability. These boards are used to capture the received signal.

The only way to program the FIFO ADC board is via USB, using proprietary software. Data sampled by the ADC board is written to the FIFO board's memory chips until they are full. Once the process is complete, the data can be read from the FIFO board's memory via USB using the correct software.

The sampling rate was chosen to be $f_S = 1$ MHz. The highest frequency of the band pass signal is $f_{max} = 330$ kHz, so the selected sampling frequency is more than twice as fast, which satisfies Nyquist's criterion for the sampling rate [4].

Larger memory chips were installed in the FIFO board to allow for more data to be stored, because the standard memory size was not sufficient for the purposes of the project. With the new memory modules installed, the FIFO could store up to $t_{\text{pulse max}} = 188.25$ ms worth of data at the selected sampling rate, which is more than enough, since the tests done use pulses of 100ms in length and 67.75 ms is needed for a pulse to reflect back from a target at 50 m [4].

Control Unit

The control unit (CU) main component is a 30F5011 dsPIC, which has the following tasks:

- Program the DDS to output the desired pulse,
- Monitor the FIFO write enable, and
- Control the DDS.

The CU forms the synchronisation link between the DDS and FIFO board, but this is a challenge because the FIFO can only be controlled by using the evaluation software on a PC. Thus, the CU monitors the write enable pin of the FIFO board memory modules. As soon as the user requests data using the software, the on-board FPGA of the FIFO pulls the write-enable pin low. This is detected by the CU which then instructs the DDS to begin the signal transmission process. The CU controls the DDS by utilizing the SPI (Serial Peripheral Interface) communication protocol.

This entire sequence is explained in Figure 2.14.

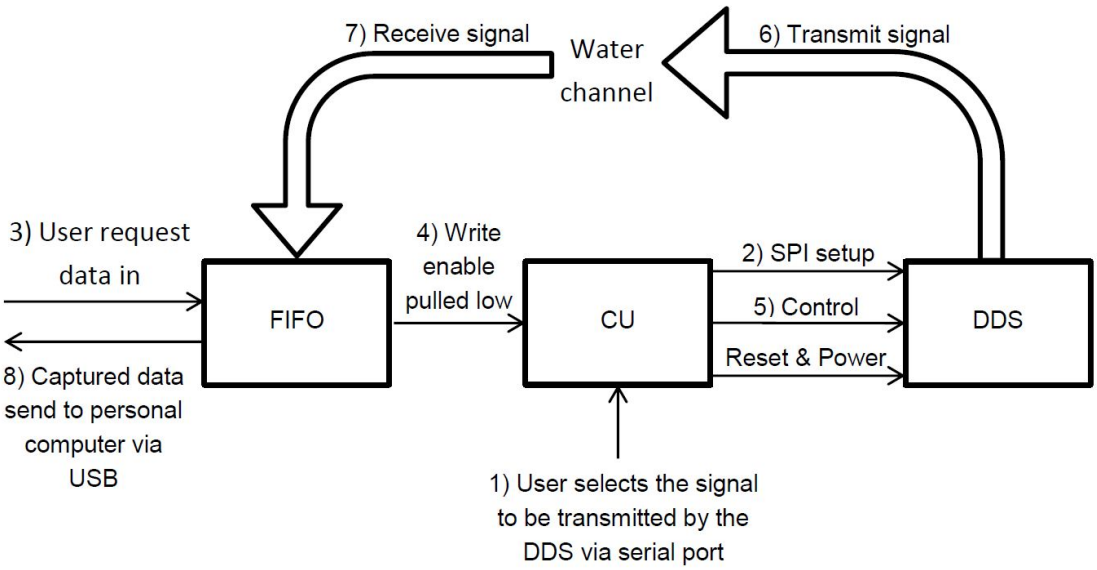

Figure 2.14 – SONAR platform operation [4].

General Remarks

The entire hardware setup can be seen in Figure 2.15, and it shows where each of the pieces of hardware discussed in this section are located in the setup. The control unit is on the same PCB as the power supply.

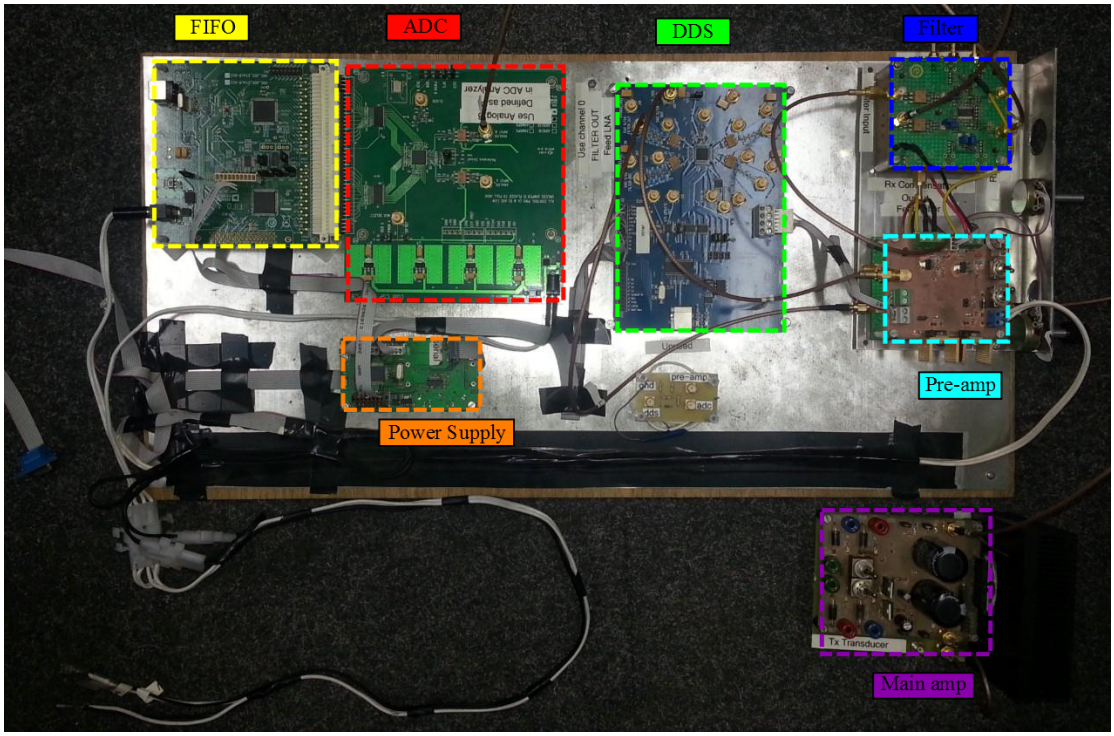

Figure 2.15 – The entire hardware setup.

2.3 Research Concerning Sound Wave Interference

2.3.1 Overview

During the course of this project, and specifically during the tests that were done, it became apparent that the physics of sound wave propagation is important for the interpretation of the test results. Wave interference was of particular importance.

2.3.2 Constructive and Destructive Interference

A sound wave will generally propagate as a sphere from a point source [23]. Since, for the purposes of this project, the targets and transducers are placed in one horizontal plane, the propagation of the transmitted sound waves could be likened to the propagation of a wave in water. This means that it forms crests and troughs in the plane in question. Thus, another wave in the same plane can cause destructive and constructive interference. Figure 2.16 below shows what constructive and destructive interference looks like for simple sine waves.

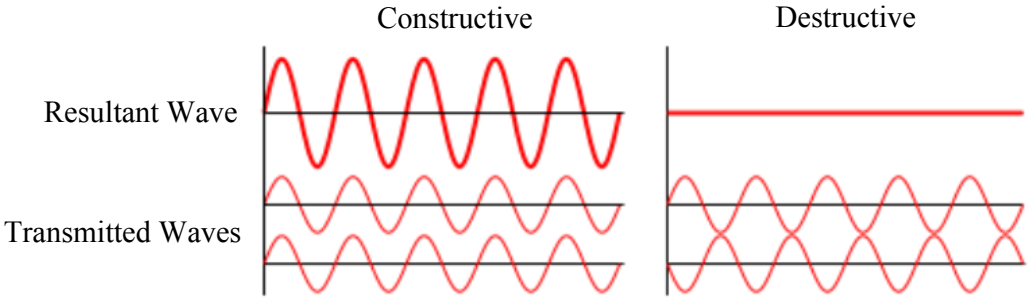

Figure 2.16 – Constructive and destructive sound wave interference.

If the waves are of the same frequency and are 1/2 period out of phase, destructive interference takes place, while constructive interference will take place if they are in phase [24].

If there are two waves of the same frequency, travelling in the same direction and plane, wave y_1 and wave y_2, the resultant wave, z, could be written as $z = y_1 + y_2$. The waves can be defined generically as follows:

$$y_1(x,t) = Asin(kx - \omega t)$$
$$y_2(x,t) = Asin(kx - \omega t + \phi)$$

Thus the resultant wave would be:

$$z(x,t) = 2Acos\left(\frac{\phi}{2}\right) sin\left(kx - \omega t + \frac{\phi}{2}\right) \quad [25], \tag{2.3.1}$$

where A is the amplitude and ϕ is the phase. Thus, when $\phi = 0°$ they interfere constructively, and when $\phi = 180°$ they interfere destructively. The variable k represents the wavenumber and is related to the angular frequency as shown in Equation 2.3.2 below.

$$k = \frac{w}{c} = \frac{2\pi f}{c} = \frac{2\pi}{\lambda} \tag{2.3.2}$$

In Equation 2.3.2, c represents the wave propagation speed.

2.3.3 Wave Reflection and Interference

2.3.3.1 Standing Waves

If a sound source is close to a reflective surface, waves will reflect off of the surface. The reflected waves can almost be seen as coming from a source that is on the opposite side of the reflective surface and is the same distance from the surface as the original source. The appearance of the interference pattern is determined by the distance between the source and the surface. If the distance is a multiple of the wavelength ($k\lambda$), a line of constructive interference will take place between the source and the surface. If the distance is a multiple of the wavelength plus half a wavelength ($k\lambda + \frac{\lambda}{2}$), a line of destructive interference will form. This concept is illustrated in Figure 2.17 and Figure 2.18, where the thick lines are crests and the thin lines are troughs. Where a crest and a crest or a trough and a trough meet, constructive interference takes place, while destructive interference takes place when a crest meets a trough.

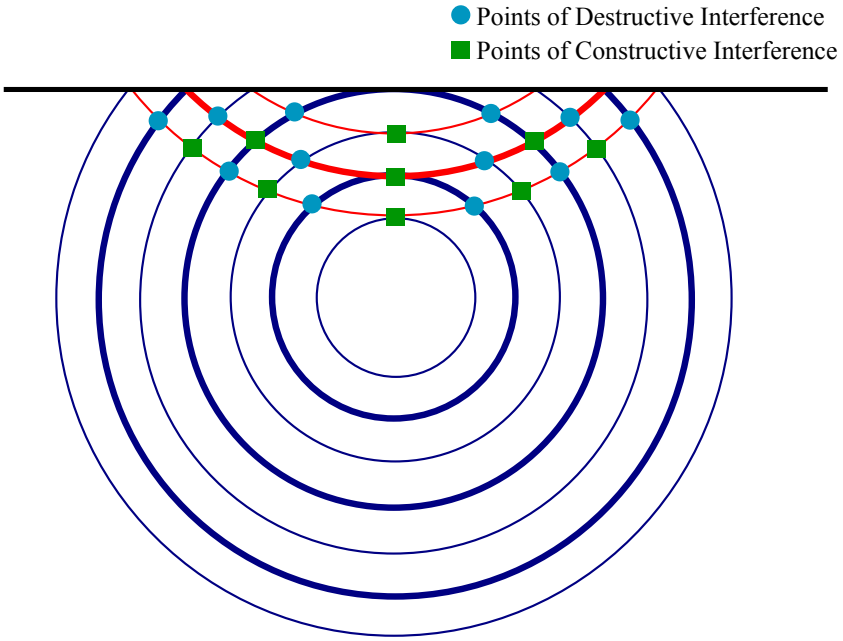

Figure 2.17 – Constructive Interference due to wave reflection.

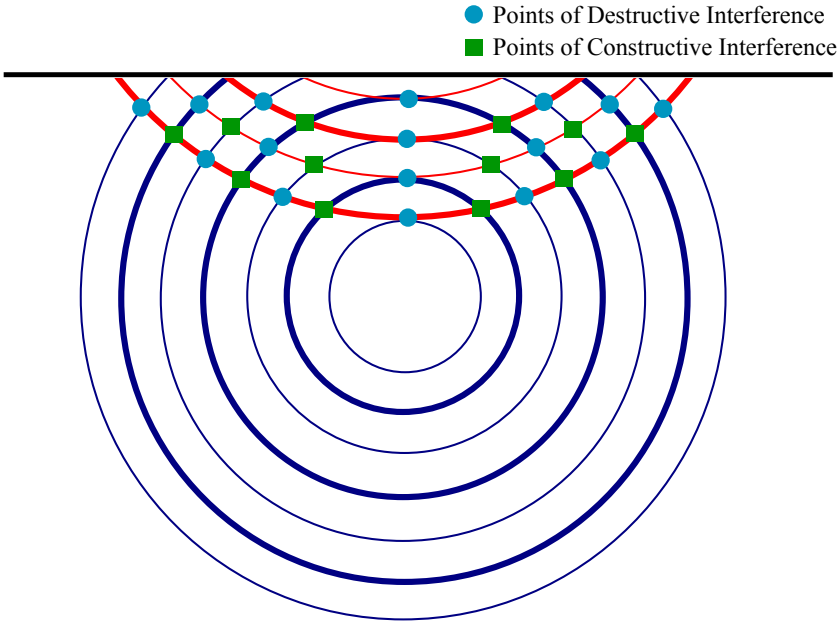

Figure 2.18 – Destructive Interference due to wave reflection.

Along this line of destructive or constructive interference, is formed what is known as a standing wave, which is only formed when waves move in opposite directions. Since the reflection and the original wave have the same frequency, they can be defined generically as follows:

$$y_1(x,t) = Asin(kx - \omega t)$$
$$y_2(x,t) = Asin(kx + \omega t)$$

Adding these two waves together results in the following:

$$z(x,t) = 2Asin(kx)cos(\omega t) \quad [25] \tag{2.3.3}$$

The wave is no longer a travelling wave, and can be seen as "standing", due to the fact that the position and time dependence have been separated. The wave appears to be just vibrating in one place.

2.4 Other SONAR Options for Object Detection and Location

2.4.1 Narrow Beam SONAR

SONAR technology has been used for many years, and thus the goal of this project has ultimately already been accomplished. There are many AUV's already in operation [26] using highly advanced SONAR systems. These SONAR systems however, make use of arrays of transducers that each have a very narrow beam-spread (pencil beam).

For example, in an article written by Y. Petillot, I. Ruiz and D. Lane called *Underwater Vehicle Obstacle Avoidance and Path Planning Using a Multi-Beam Forward Looking Sonar* [27], an array with 120 separate beams is used. Each beam is $1°$ in width, making the area scanned $120°$ in the horizontal axis, as seen in Figure 2.19.

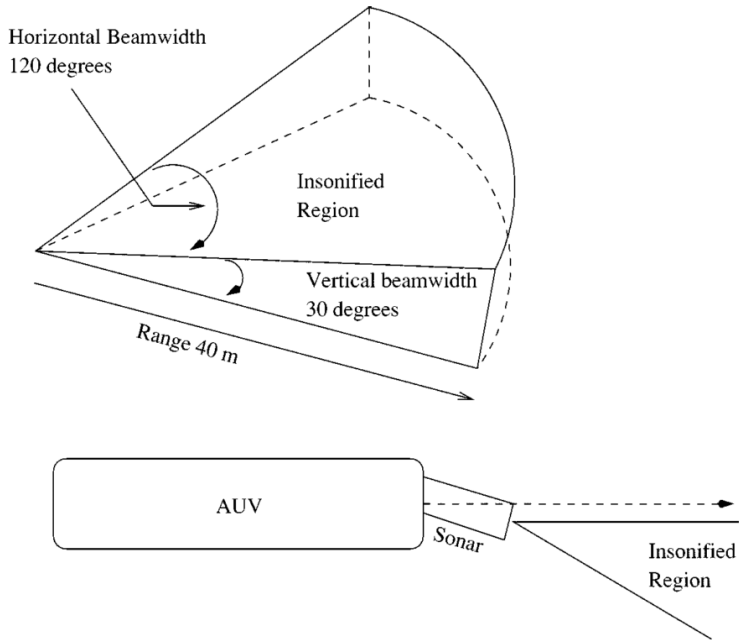

Figure 2.19 – SONAR setup with 120 separate beams, each with $1°$ beam-spread [27].

This makes it fairly easy to detect the location and dimensions of a target in the horizontal axis (in the insonified region). Since the beams are so narrow, it has an inherent high resolution, which allows for accurate location and edge detection. Another point worth noting about SONAR arrays, such as the one mentioned above, is that they are usually bought as a package bundled with software that is specifically written for the SONAR system.

This setup might sound ideal, but it does come with a fair amount of problems. It is very expensive and quite large. The large number of transducers also poses a serious problem. If they were to transmit and receive at the same time, each transducer and its receiver will have to use a different frequency from the rest, so that other reflections can be filtered out.

2.4.2 Multibeam SONAR: Beamforming

Using a multibeam SONAR system for beamforming applications is also an option. It involves using more than one source of sound (transmitting transducer) to form a *projector array* where

the waves from the different sources interfere constructively and destructively with each other resulting in beamforming [28]. The locations of each of the projectors relative to the others, as well as small time delays between the transmission times, affect the resultant beam pattern. This is usually used to form a narrower beam so that smaller areas can be insonified to give more accurate readings [29].

This narrow beam that is formed can then also be steered to "scan" over an area, which is perfect for the applications of this project. This also eliminates the costly en mechanically complex part of scanning. But in order to do beamforming, a large number of transducers is needed, which was not available during this project. An example of beamforming can be seen in Figure 2.20. In this case, isotropic sources (sources that emit waves equally in all directions) are combined into an array in such a way that it results in waves only being projected along one axis.

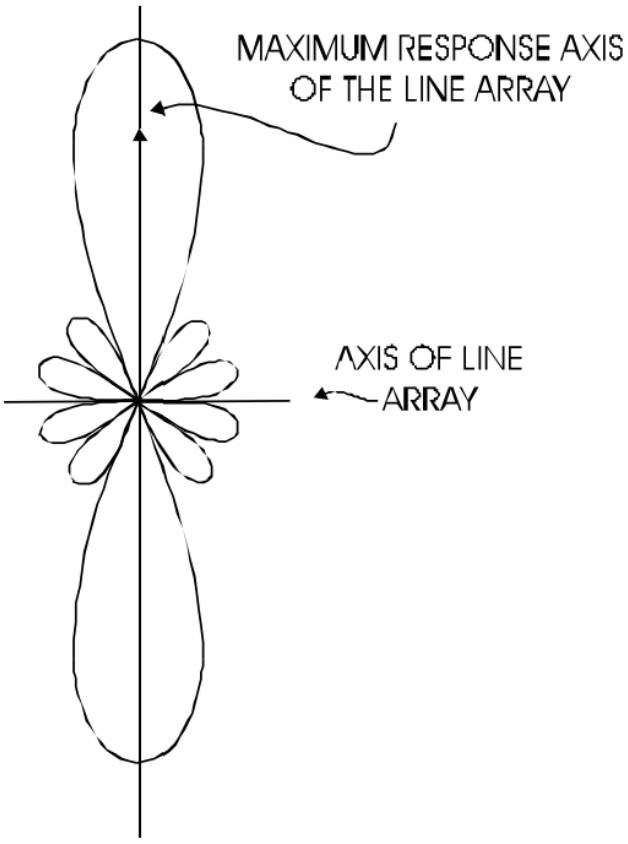

Figure 2.20 – Example of beamforming [29].

It is not necessary to use this complex concept in this project, therefore the mathematics of beamforming will not be discussed.

2.5 Using the Wavelet Transform for Peak Reflection Detection

2.5.1 Overview

Using the wavelet transform to filter processed data is a fairly new but well established concept. The wavelet transform allows more freedom than using the standard FFT (Fast Fourier Transform) and is a very effective method of getting rid of high frequency noise. It is used in this project to effectively determine the location of the peak of the reflection from a target.

This section gives a quick overview of wavelets, the wavelet transform, the uses of the wavelet transform, and its applicability to this project.

2.5.2 Definition of Wavelets

B. Vidakovic and P. Mueller, in their document, *Wavelets for Kids* [30], define wavelets as follows:

"Wavelets are functions that satisfy certain requirements. The very name wavelet comes from the requirement that they should integrate to zero, "waving" above and below the x-axis."

As stated above, a wavelet function should have a mean of 0. There are many different wavelets, and new wavelets can be developed for use in a specific application. Some examples of wavelets are shown in Figure 2.21 (Haar Wavelet), Figure 2.22 (Daubechies 4 Wavelet) and Figure 2.23 (Daubechies 20 Wavelet) below.

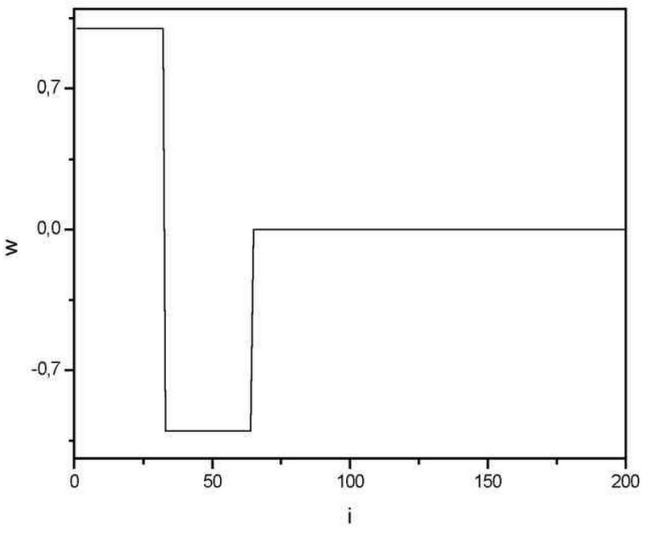

Figure 2.21 – Haar wavelet [31].

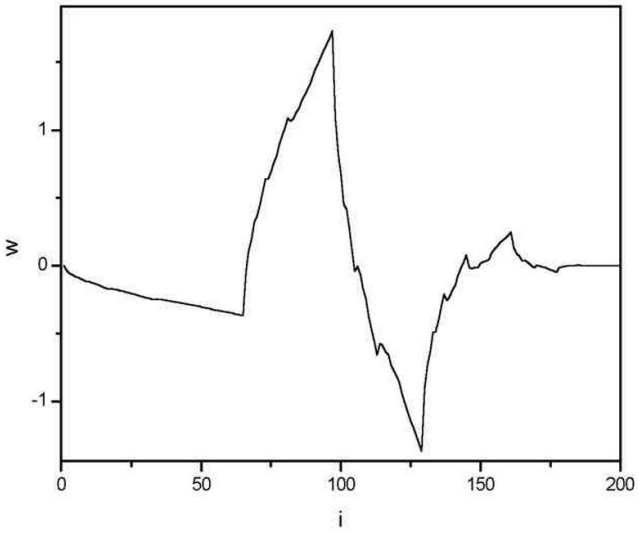

Figure 2.22 – Daubechies 4 wavelet [31].

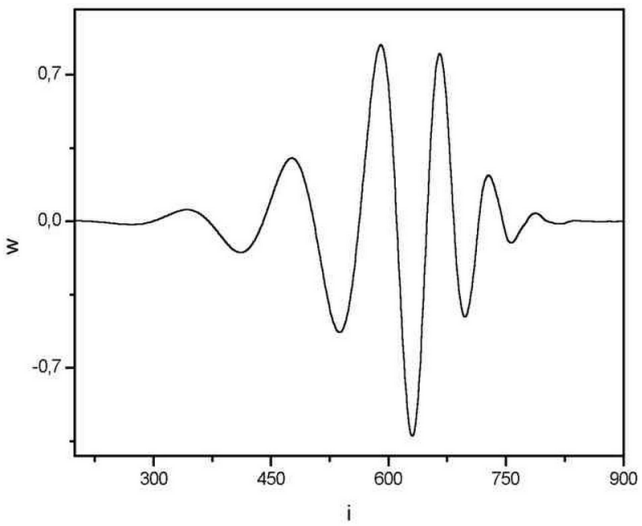

Figure 2.23 – Daubechies 20 wavelet [31].

2.5.2.1 The Wavelet Transform

The wavelet transform is a transform similar to the Fourier transform, but instead of decomposing the signal being transformed into sines and cosines, it is decomposed using the selected wavelet. If a signal is Fourier transformed, the functions used (sines and cosines) are localised in the Fourier space, whereas the wavelet transform uses functions that are localised in both the real and Fourier space [31].

The wavelet transform of an arbitrary signal, $f(t)$, can generally be written as in Equation 2.5.1.

$$\gamma(s,\tau) = \int_{-\infty}^{\infty} f(t)\psi_{(s,\tau)}(t)\mathrm{d}t, \quad [31] \tag{2.5.1}$$

where $\gamma(s,\tau)$ is the coefficient of the wavelet with scale s and time τ. $\psi_{(s,\tau)}$ is the wavelet function being used. The assumption is made that only real wavelets are used, thus the complex conjugate is ignored.

All wavelets are derived from the *mother wavelet*, as seen in Equation 2.5.2.

$$\psi_{(s,\tau)}(t) = \frac{1}{\sqrt{s}}\psi\left(\frac{t-\tau}{s}\right) \quad [32] \tag{2.5.2}$$

2.5.2.2 The Discrete Wavelet Transform

The discrete wavelet transform (DWT) is used in this project. It is an implementation of the wavelet transform using a discrete set of the wavelet scales and translations obeying some defined rules. Simply put, this transform decomposes the signal into a mutually orthogonal set of wavelets [31].

The DWT of a signal f is calculated by passing it through a series of filters. The first step involves passing the samples of the signal through a low-pass filter, g, resulting in a convolution of the two. The signal is also simultaneously filtered with a high-pass filter, h. The output of the low-pass filter is called the *approximation coefficients*, and that of the high-pass filter is called the *detail*

coefficients [33]. These two filters need to be quadrature mirror filters, meaning the magnitude response of each should be a mirror image about $\frac{\pi}{2}$ of that of the other [34].

Since half the frequencies of the signal have now been removed, Nyquist's rule states that half of the samples can be discarded (every second sample is discarded [35]), so the filter outputs are then subsampled (downsampled) by 2. This process can be summarised using the block diagram in Figure 2.24.

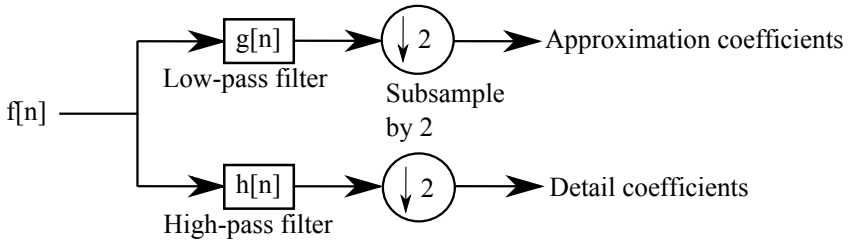

Figure 2.24 – Block Diagram of DWT filter analysis.

This decomposition process is repeated as many times as needed by continually decomposing the approximation coefficients. This results in a binary tree called a *filter bank* as seen in Figure 2.25, in which each level represents a sub-space with a different time-frequency localisation [33].

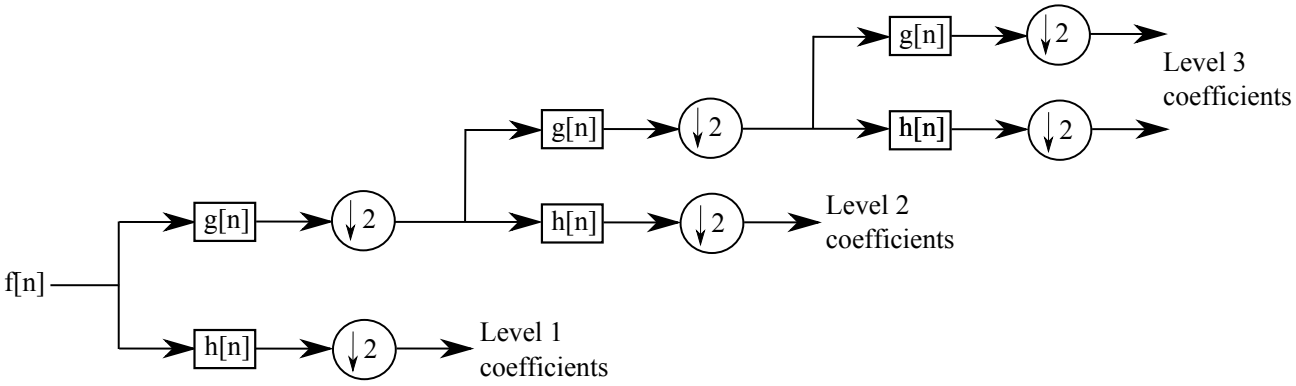

Figure 2.25 – Block diagram of DWT filter analysis.

At each level of the filter bank, the signal is decomposed into high and low frequencies. This decomposition process dictates that the number of samples in the input signal should be a multiple of 2^n, where n is the number of levels.

A simple example of this process can be done using a signal with 32 samples and a frequency range of 0 Hz to f_n Hz. It is decomposed into 3 levels as in the filter bank above, producing 4 output scales as seen in Table 2.1 as well as in Figure 2.26.

Level	Frequencies	Samples
3	0 to $f_n/8$	4
	$f_n/8$ to $f_n/4$	4
2	$f_n/4$ to $f_n/2$	8
1	$f_n/2$ to f_n	16

Table 2.1 – DWT decomposition of signal with 32 samples to 3 levels

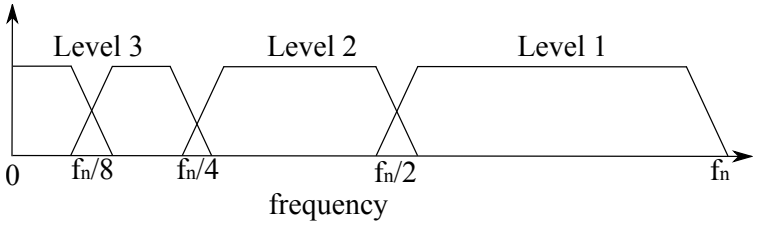

Figure 2.26 – Frequency domain representation of the DWT.

2.5.3 Application of the Discrete Wavelet Transform

As discussed above, the DWT decomposes the signal that is transformed into a set of time-domain signals that each exist in a different frequency band, as illustrated in Figure 2.26. If each of these signals are added together again, it should form a close approximation of the original signal, depending on whether the wavelet that is chosen is a good choice. An easy way to choose a wavelet is to determine how well it correlates to the original signal, or perhaps the signal that the user intends to find. The more similar the wavelet is to the signal, the better the approximation will be.

Some of the frequency bands the signal is decomposed into, contain data that is unwanted. Therefore, once the signal has been decomposed, it can be reconstructed using only the signals from frequency bands the user deems important. This makes it simple to eliminate noise of a high frequency, because those frequency bands can be ignored.

Take a simple sine wave (2001 samples) that has high frequency noise added to it, such as in Figure 2.27. The result of filtering this signal using the Daubechies 10 wavelet is seen in Figure 2.28. In this specific case, it was decomposed to 7 levels, and has been reconstructed using only the 7^{th} level of approximations and the 6^{th} and 7^{th} levels of details (approximations and details are discussed in Section 2.5.2.2).

The complete decomposition is shown in Figure 2.29. The increase in the frequency of the signals can clearly be seen has they move down in level. The higher frequencies can then simply be ignored to reconstruct a nearly noiseless version of the original signal. The DWT cannot be used to filter a signal that is completely entrenched in noise and is not at all visible. It can only result in making an already visible signal cleaner and easier to detect.

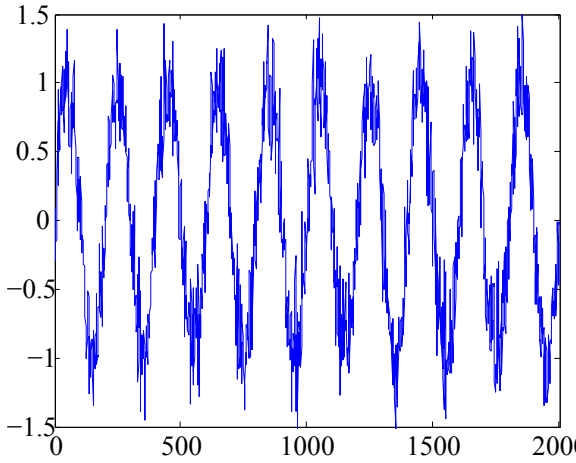

Figure 2.27 – Noisy sine wave.

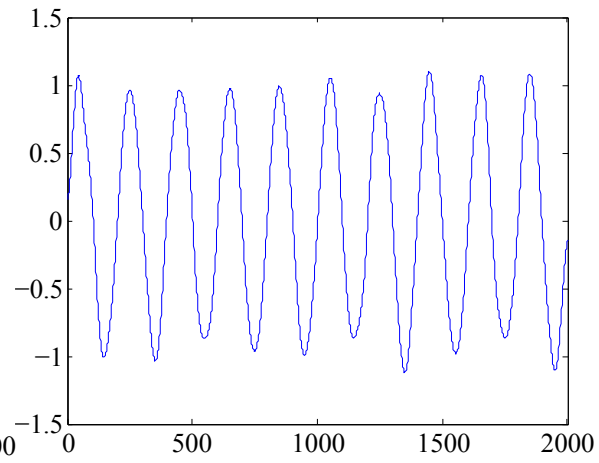

Figure 2.28 – DWT filtered sine wave.

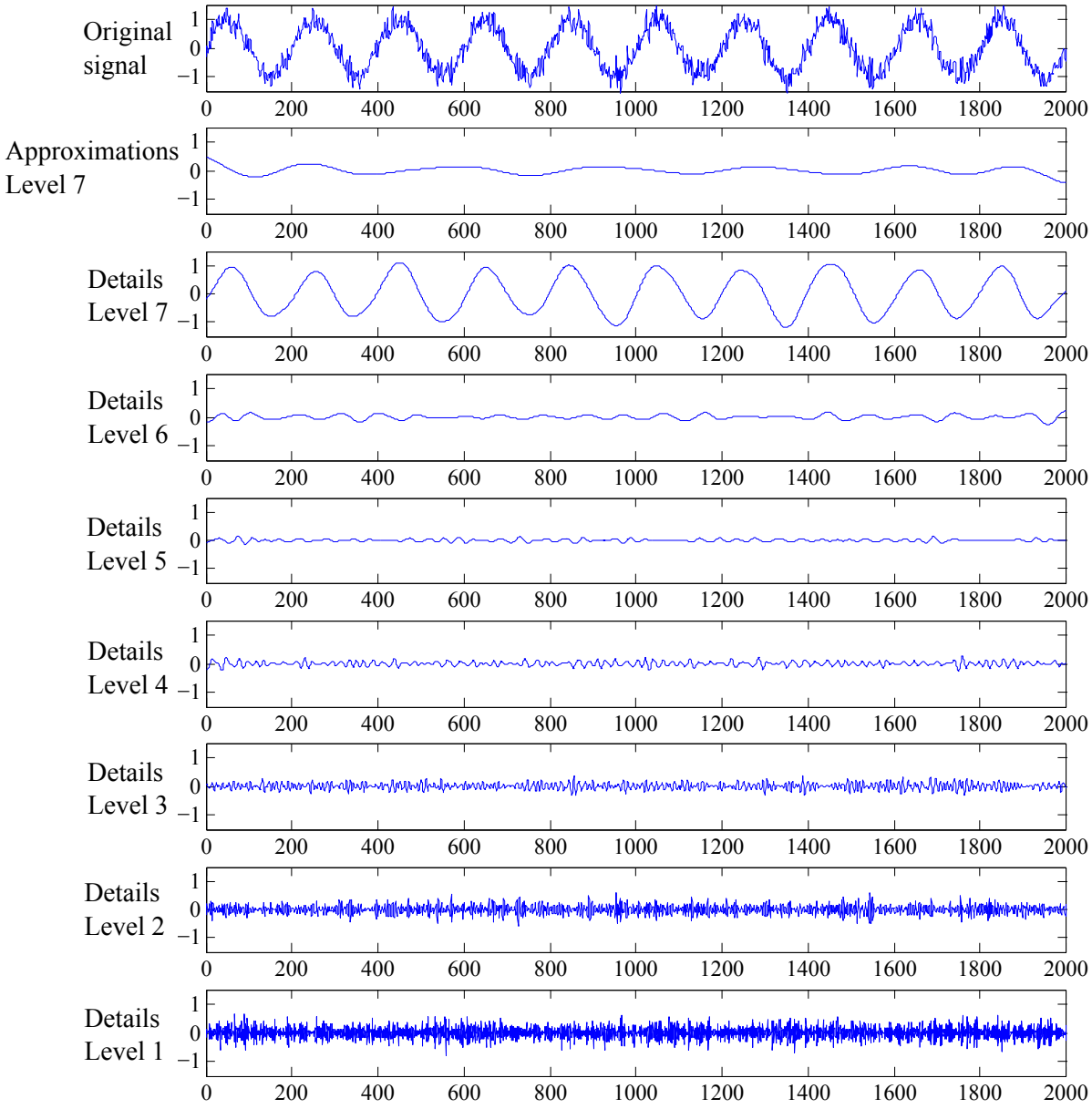

Figure 2.29 – Decomposition of a noisy sine wave.

Chapter 3

Additional Hardware Needed for the Project

3.1 Overview

As the project proceeded, extra pieces of hardware had to be added unto the existing hardware to be able to test different setups and gather more data. Most of the new hardware that was constructed during the course of this project was to enable the simulation of different SONAR transducer setups. In order to achieve the goal of this project, different configurations were designed and tested to determine what improvements could be made to the existing methods of data gathering.

3.2 Additional Hardware Discussion

The following additional pieces of hardware were designed and built during this project:

- DDS Signal Divider.
- Arduino Stepper Motor Configuration.
- Pulley System.

Each of these will now be discussed.

3.2.1 DDS Signal Divider

The DDS signal divider is a circuit board that was designed and built with the purpose of dividing the signal created by the DDS. It was deemed necessary to capture a lower amplitude version of the signal that is transmitted, to be used during the processing of the data. This means that the signal created by the DDS is sent through its normal path (amplifiers, filters, transducers), but a version of it with a reduced amplitude is sent to and captured by the ADC and FIFO to be used during data processing. The circuit design is shown below in Figure 3.1, and a photo of the final product is shown in Figure 3.2.

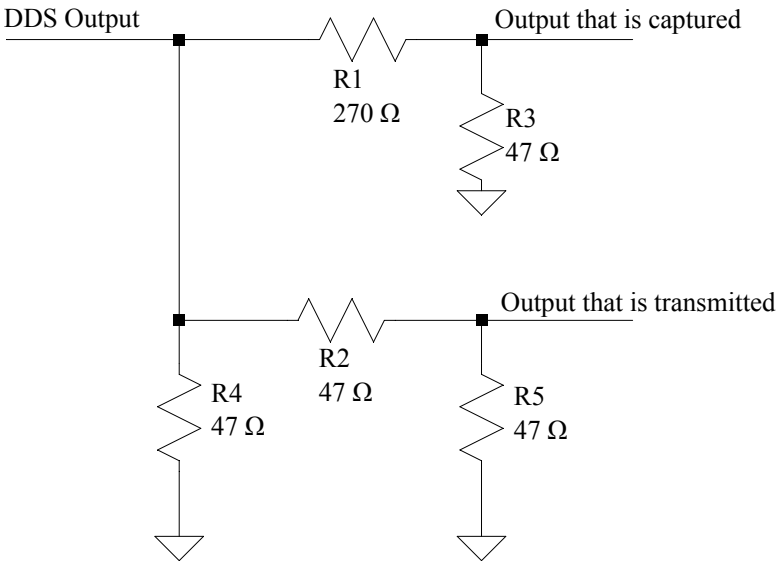

Figure 3.1 – DDS signal divider circuit diagram.

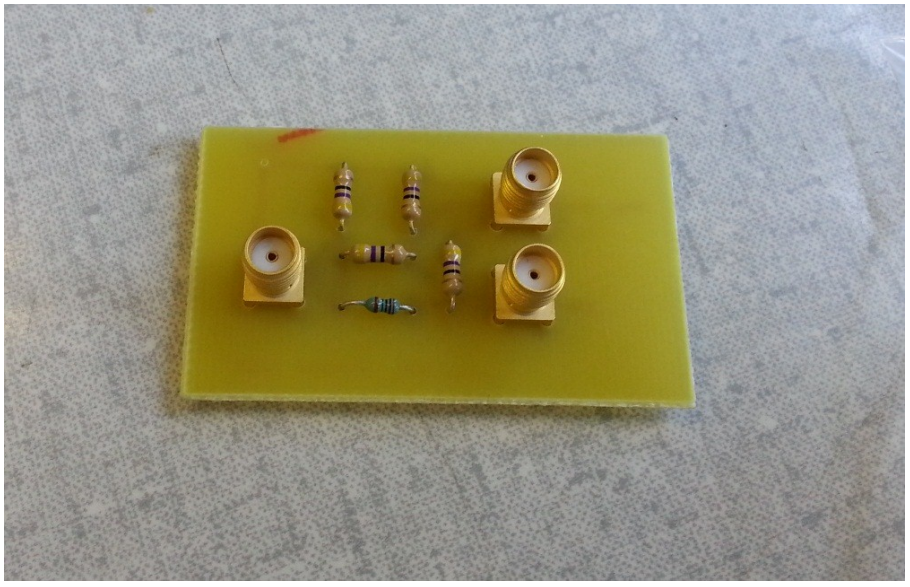

Figure 3.2 – DDS signal divider PCB.

The result of this is that the output that is transmitted is 0.5 times the amplitude of the original signal, and the output that is captured is 0.15 times the amplitude of the original signal.

3.2.2 Arduino Stepper Motor Configuration

Some of the tests that were done involved "scanning" from left to right by rotating the transducers through a certain angle. This meant that the transducers would have to stop at specific intervals so that data could be collected before rotating them to the next interval. A stepper motor seemed to be the obvious solution, and an easy way to control it would be to use Arduino [36] technology. Arduino chips are easy to buy, program and implement, and there are existing Arduino motor driver boards that can be used to power and control stepper motors as well. It is called the

Arduino Motor shield [36], and was used in conjunction with the Arduino Uno [36]. The stepper motor used is the PMG4250-01 bi-polar geared stepper motor made by Fulling Motor USA [37]. It has a gear ratio that allows for step sizes of down to $0.15°$.

The Arduino board could be programmed to step the motor through any angle that is a multiple of $0.15°$ when it is triggered by a switch that is connected to the Arduino circuit. Another switch was added to control the direction in which the motor steps. Then, a simple attachment was made to attach the stepper motor to the transducers.

The stepper motor and its connection to the PVC construction that houses the transducers is shown in Figure 3.3, and the Arduino boards as well the stepper motor are shown in Figure 3.4.

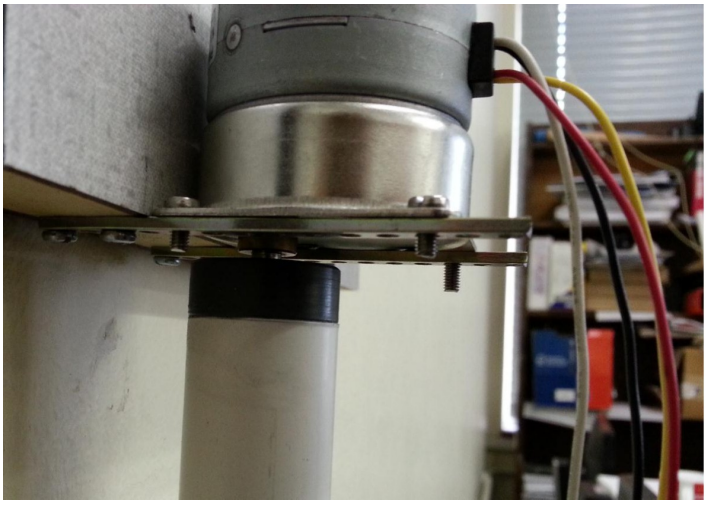

Figure 3.3 – Stepper motor.

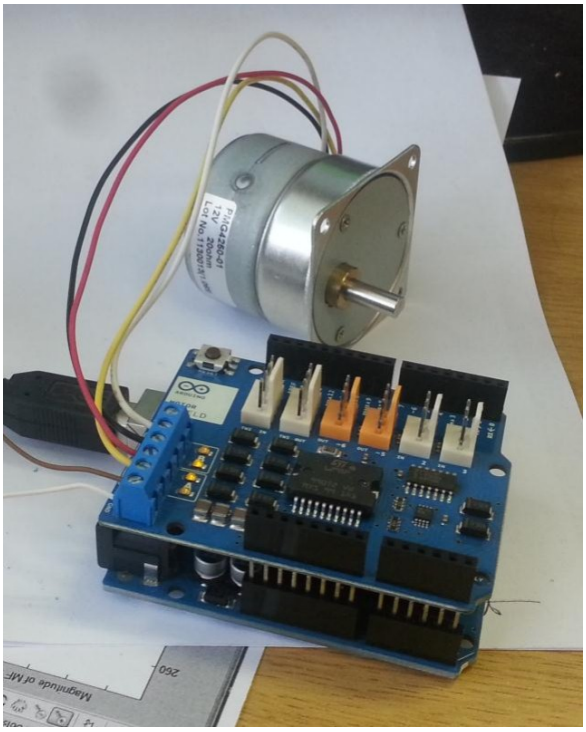

Figure 3.4 – Arduino Uno, Arduino motor shield and stepper motor.

3.2.3 Pulley System

In some of the tests that were done the transducers had to be moved laterally across the water tank (this is discussed in more detail in Chapter 4) and stopped at specific intervals for data to be gathered. Several different approaches were considered to solve this problem, but in the end a system of ropes and pulleys was deemed the most feasible.

A rope is spanned across the water and looped around pulleys on either side. The PVC construction that houses the transducers is then hung from and attached to this rope. In this way it can easily be moved laterally across the tank, and the intervals at which it is stopped are determined using a highly accurate LASER range finder. Photos of this set-up are shown in Figure 3.5 and Figure 3.6.

Figure 3.5 – The pulley system attached to the wall.

Figure 3.6 – PVC bracket for transducers hung from the rope.

Chapter 4

Object Detection, Location and Edge Location

4.1 Overview

This chapter deals with the different approaches and methods that were used in an attempt to reach the goal set for this project, which is described in Section 1.2. Tests, experiments and simulations that were done are also discussed.

It is important to geometrically define the problem at hand before diving into more detail. This is done in Figure 4.1. The AUV is assumed to be about 3m in length and 0.3m wide [5]. The area in front of the AUV that is of importance is the region between 5m and 20m in range. Targets or objects in this region need to be detected and located so as to enable collision avoidance. Any targets further than 20 m are not immediately important for collision avoidance, and it is assumed that any targets closer than 5m have already been avoided.

Figure 4.1 shows that the angle of the region that needs to be scanned is $60°$. This is just an arbitrarily chosen angle that will allow for safe navigation of the AUV.

In most SONAR systems, the error in measurement is defined by the width of the beam. Thus, the ideal SONAR system for accurately detecting the outline of an object would possess a narrow beam (less than $1°$) and operate in the ultra-high frequency (beyond a few Megahertz) spectrum. This idea is not really practical for ranges of 10m or more due to the absorption at the higher frequency [38] and other reasons discussed in Section 1.2. Thus, the aim is to develop methods and techniques that make use of transducers of a lower frequency and a wider beam-width that will enable collision avoidance.

These methods and techniques will not only be applicable to the transducers used in this project, but also to any other transducers with their own beam-width. Even a narrow beam becomes relatively wide as the range to the target increases, in which case these techniques will be applicable. Ultimately, this project will allow cheaper transducers with wider beams to be used to achieve results comparable to that of more expensive transducers with narrower beams.

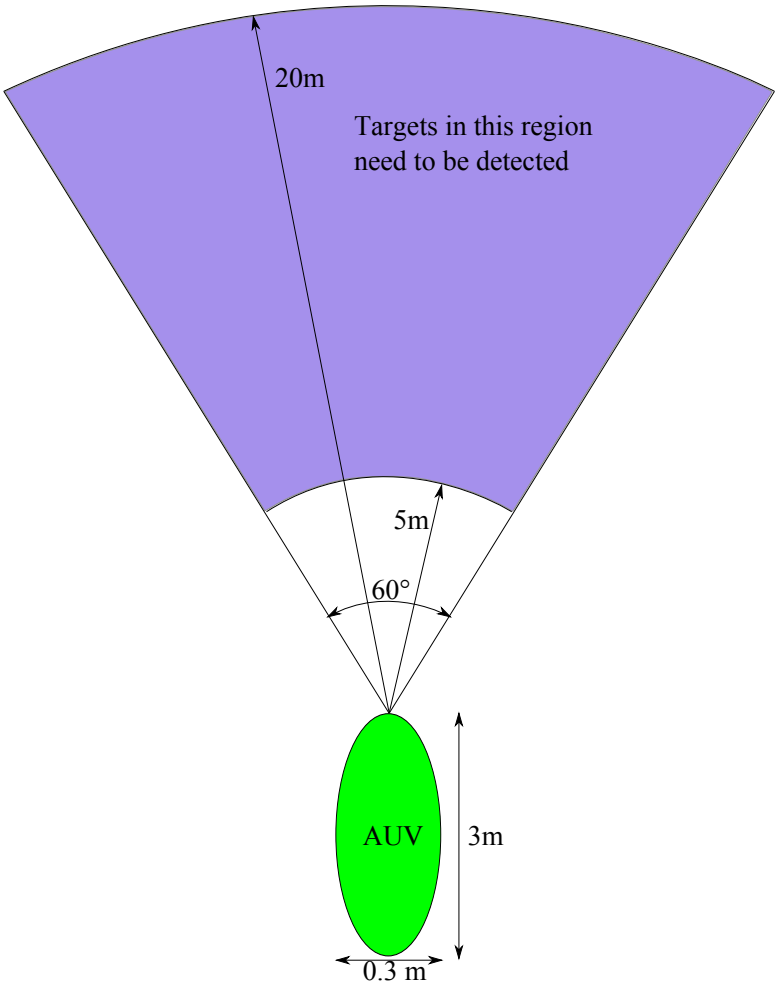

Figure 4.1 – The physical dimensions of the AUV and the region in which objects need to be detected (not to scale).

As previously discussed (see Section 2.2.6.2), the available transducers have a beam-spread of about $6°$, which is relatively wide. This means that, if they are simply used as in the previous work done [4], the data from the system, once processed, will only inform the user that there is an object at a specific distance in front of the transducers (within the insonified region), but its location in the horizontal or vertical axes and its size will be uncertain within the beam-width.

For example, at a range of 10m, a beam-width of $6°$ will result in an uncertainty of close to 1m laterally. Path planning for an AUV has to take the uncertainty in measurement into consideration. If it plans its path to pass an object by, for example, three times the uncertainty, it would mean the the AUV has to move past the object with a 3m gap between itself and the object. This places unnecessary strain on the motors and actuators of the AUV.

Thus, in order to accomplish the goal set in Section 1.2, the work done is divided into four main parts:

1. Part 1: Baseline - Recreation of previous results.
2. Part 2: Object location in the horizontal plane.
3. Part 3: Object edge location.

4. Part 4: Study of non-2D targets.

A number of different tests were done, each with a specific goal (or goals), and these goals each fall within one or more of the above-mentioned parts. The processing of the data collected during the tests was done using adapted versions of the existing *Matlab* code [4], and therefore the processing techniques are not discussed in great detail. Each of the tests and the testing environment are discussed in more detail in Appendix A.

Each of these four parts will now be discussed in detail by looking at the methods employed to reach the goal for that part and the results of employing those methods.

4.2 Part 1: Baseline - Recreation of Previous Results

4.2.1 Overview

The previous work done on this project [4] needs to be completely understood before continuing with this project, and therefore it is appropriate to attempt to recreate the previous results. Several tests are done in an attempt to do so. The tests that were done are numbered, as seen in Appendix A, and Test 1, Test 2, Test 3, Test 4 and Test 5 form part of the work done in Part 1. The results of the work done after this can then be compared to the results from this part to see if a notable improvement has been made. Therefore this part is referred to as the baseline.

The result that needs to be recreated is the ability to detect the range of objects accurately under water within the range specified in Section 4.1.

4.2.2 Approaches and Methods Employed

The basis of the previous work rests on using LFM waves to obtain accurate target ranges under water, since LFM waves give a good range resolution. The same testing environment was used as in previous work [4], such as the targets used and the range at which they were placed. Initially, the same code for the PIC processor was used, but it was eventually completely rewritten so that the user could have more options in terms of signal length and frequency.

Reproducing the previous results was more difficult than initially anticipated, and the main reason for this is the spherical targets used. A perfectly round/spherical surface has an infinite amount of infinitesimal specular reflecting surfaces that reflect sound in all directions. That means that the sound wave that reflects back to the receiving transducer can be approached as an impulse with a very small amplitude, which is very hard to detect above the environmental noise.

For example, in Test 1, a metal sphere of 10mm was not detected at a range of 25m. Figure 4.2 below shows the result of a test that was done using a 230 kHz - 330 kHz LFM wave with a length of 100ms. The data is processed using a slightly edited version of the existing *Matlab* code [4]. This specific plot is generated from data that is processed and analysed using a Matched Filter. The back wall of the water tank in which the tests were done can be seen at about 88m, but the target at 25m cannot be seen.

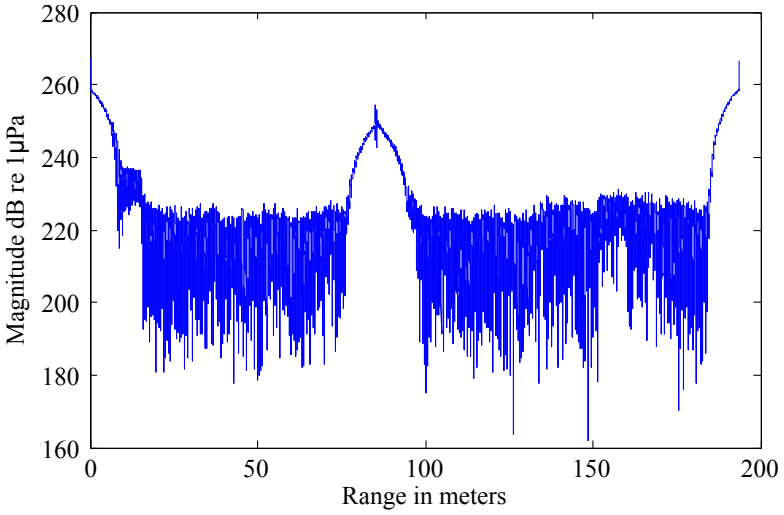

Figure 4.2 – Target at 25m not visible using 230 kHz - 330 kHz LFM sweep.

More tests were done until a positive result was achieved in Test 4. A glass sphere of 40mm in diameter was detected at a range of 10m, as well as 2 aluminium plates of different sizes (90mm x 90mm x 7mm and 140mm x 180mm x 1mm). Figure 4.3, Figure 4.4 and Figure 4.5 show each of these results, with the data processed using the Matched Filter technique. In Figure 4.3 the amplitude of the reflection is barely greater than the noise, but it can be seen, as pointed out by the red arrow. The range accuracy was very good (confirmed using a LASER range finder), as also shown in previous work [4]. It is interesting that the amplitude of the return from the smaller, yet thicker plate, is higher than the amplitude of the return from the larger, yet thinner plate. It is probable that the larger plate was not facing the transducers completely squarely, but rather at a small angle, resulting in lower amplitude reflections begin detected.

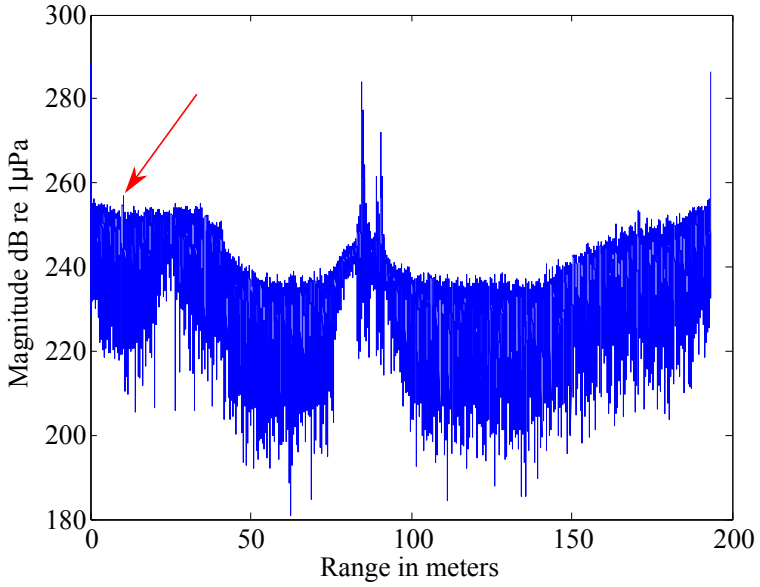

Figure 4.3 – The reflection from 40mm ball at 10m is visible.

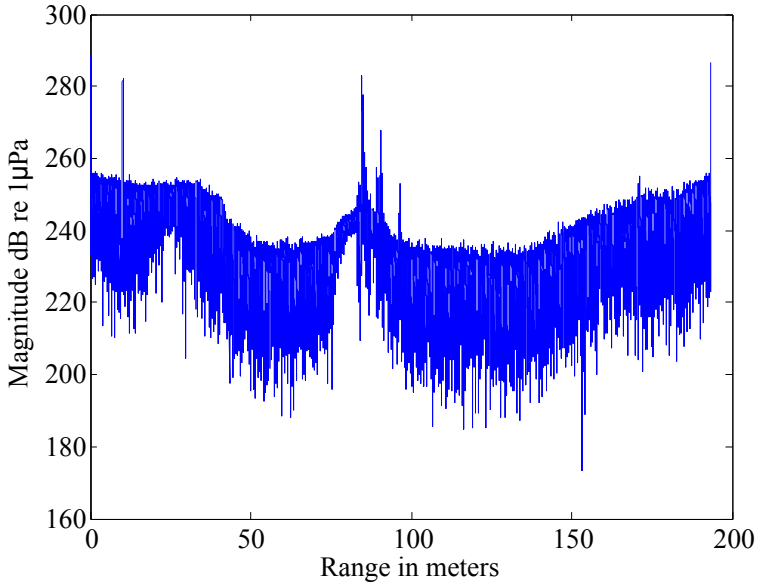

Figure 4.4 – Large reflection is seen from the small aluminium plate (90mm x 90mm x 7mm) at 10m.

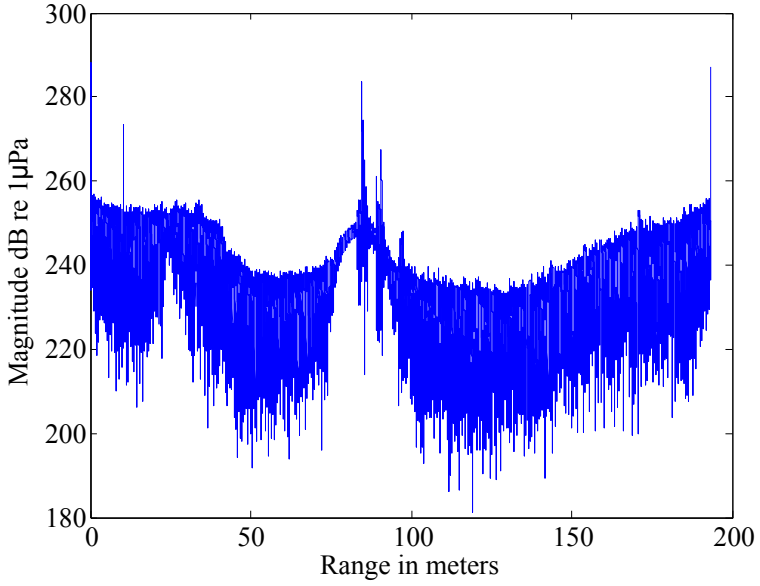

Figure 4.5 – Large reflection is seen from the larger aluminium plate (140mm x 180mm x 1mm) at 10m.

For the case of the glass sphere that has such a small reflection, it is wise to use the DWT (Discrete Wavelet Transform, as discussed in Section 2.5.2.2) so as to ensure detection of the target. Figure 4.6 and Figure 4.7 show the difference between using only the filtering techniques used in previous work [4] and using the same techniques in conjunction with the DWT respectively. The Daubechies 10 wavelet is used in this instance, decomposing the signal to 7 levels. Processing the raw data from the SONAR system using the DWT does not yield any positive results. It can only be used to improve the data that has already been processed using the existing techniques.

The reflection can be seen much more clearly once the data has been processed using the DWT, allowing the range to be more easily pinpointed. As mentioned previously, the DWT technique is only useful when the reflection has a small amplitude and is not easy to see above the noise.

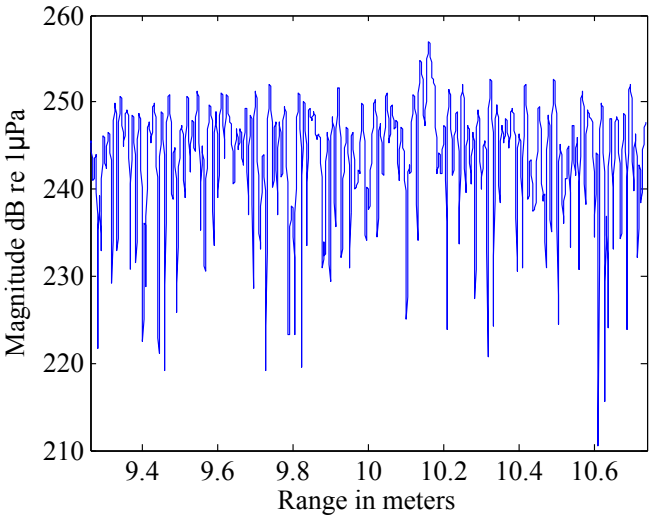

Figure 4.6 – Reflection from glass sphere, zoomed in and processed using a matched filter and windowing technique.

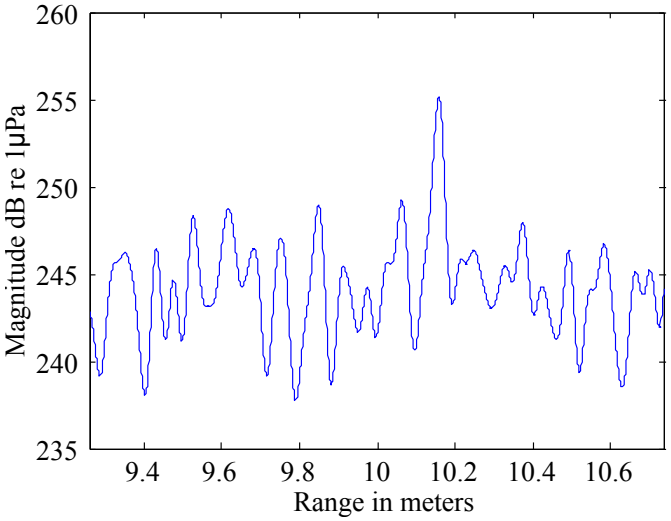

Figure 4.7 – Reflection from glass sphere, zoomed in and processed using a matched filter, windowing technique and DWT.

4.2.3 Effect of Target Size on Reflection Intensity

It is mentioned above that the intensity of the reflected wave is very small for spherical objects due to the small reflecting surface. For this reason it is much easier to detect targets with flat surfaces, such as in Figure 4.4 and Figure 4.5. This can be explained in more depth using sound intensity calculations, as is discussed in Section 2.2.1. Targets that would result in reflections with very high amplitudes, such as corner reflectors, have been avoided.

There are several factors that need to be taken into account when calculating the theoretical intensity of the sound wave that reflects back to the R_X transducer:

- Source Level,
- Propagation loss,
- Target strength,
- Directivity index,
- Noise level, and
- Reverberation level.

Each of these are discussed in Section 2.2.1. The only one of these that changes when a target of a different size is used, is the target strength (TS), which is discussed in Section 2.2.1.12. The target strength can be seen as a gain, giving an indication of the relationship between the amplitudes of the incident and reflected waves. Equation 2.2.16 and Equation 2.2.18 show how

to calculate the target strength for spherical and rectangular targets respectively, and give the following results:

10mm Metal sphere:	TS = -46.02 dB
40mm Glass sphere:	TS = -33.98 dB
140mm x 180mm x 1mm Plate:	TS = 13.62 dB
90mm x 90mm x 7mm Plate:	TS = 3.77 dB

The calculations are made assuming a centre frequency of 280 kHz. These results clearly show that the reflections from the spheres can be expected to be much smaller than that of the rectangular plates, which is the case as shown by the measurements. The target strength of the 10mm sphere is 12 dB lower than that of the 40mm sphere, and thus the reflection from the 10mm sphere should have an amplitude that is 12 dB re 1μPa lower than that of the 40mm sphere. The reflection from the 40mm sphere can just barely be seen above the noise, and therefore the 10mm sphere will not be visible. The result in Figure 4.2 shows that no reflection was seen in the test.

The target strength calculations also show that the reflection from the 140mm x 180mm x 1mm plate should be much larger than that of the 90mm x 90mm x 7mm, but as mentioned earlier, this is not the case in the results shown in Figure 4.4 and Figure 4.5. The thickness of the metal could have an influence on the intensity of the reflection, but, as mentioned above, it is more likely that the larger plate might have not been facing the transducers squarely, but rather at a slight angle. This would have reduced the intensity of the sound waves that reach the R_X transducer.

4.2.4 Conclusion of Part 1

The results seen in this section of the work reiterate that it it possible to accurately determine the range of the targets mentioned above, which is sufficient for the purposes of this project. It also shows that making use of the DWT allows the peak to be extracted more accurately when the signal to noise ratio is poor. Thus, the next part of the work could be undertaken.

4.3 Part 2: Object Location in the Horizontal Plane

4.3.1 Overview

The second part of the project involves finding the location of a target under water. In this part, the location of the centroid of the object/target is determined, as illustrated in Figure 4.8, where the angles θ_1, θ_2 and θ_3 need to be determined. The centroid can be defined as the point of maximum reflection on the target. Each of the targets in Figure 4.8 might fall within the region insonified by the transducers. This means that simply keeping the transducers stationary in one location will result in only acquiring the range of each of the targets (as done in Part 1) and not their respective angles as mentioned above. Other methods will thus have to be used in order to determine these angles. Tests 6, 7 and 9 (refer to Appendix A) deal with finding the location of targets in the horizontal plane.

It is possible that the target detected could be larger than the beam-width. The methods discussed in this part also take this into consideration.

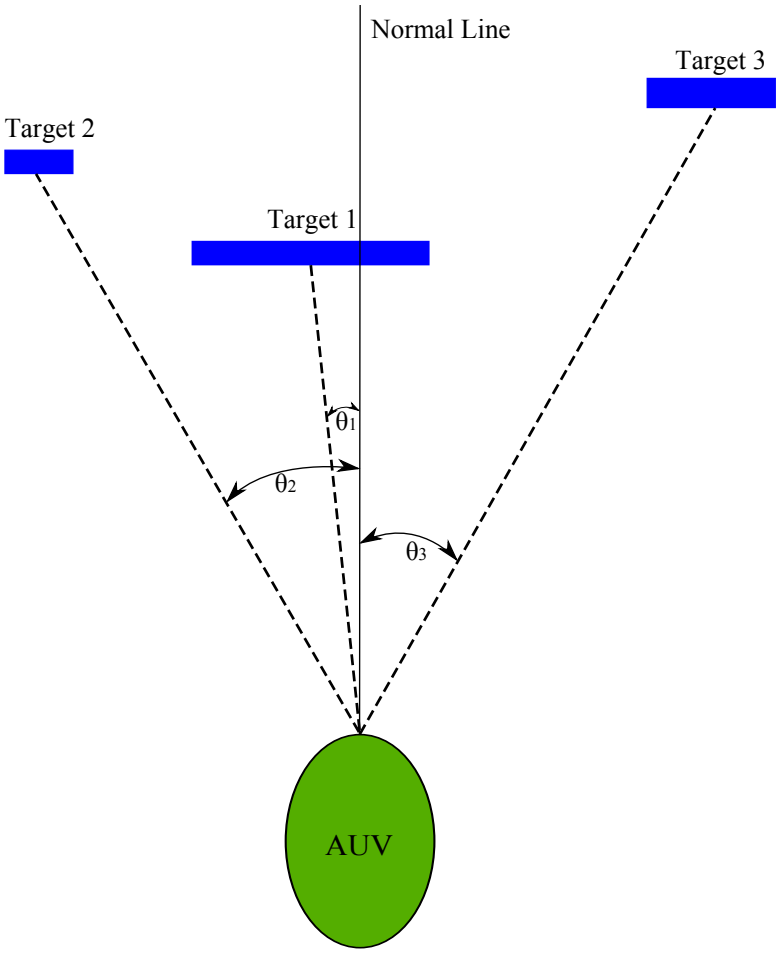

Figure 4.8 – Part 2 Goal: Finding the centroids of targets.

4.3.2 Approaches and Methods Employed

Two different methods were employed in order to determine the location of objects; **rotational scanning** and the use of **multiple receivers**. Both of these methods and the results of tests in which these methods were employed will now be discussed.

4.3.2.1 Making Use of Rotational Scanning

Rotational scanning refers to holding the T_X and R_X transducers together and rotating them in one spot, scanning across the target from one side to the other. They are rotated in small increments of a predetermined angle. The amplitude of the reflection (if there is a received reflection above the noise) from the target is then stored for each angle. Figure 4.9 shows what the setup looks like.

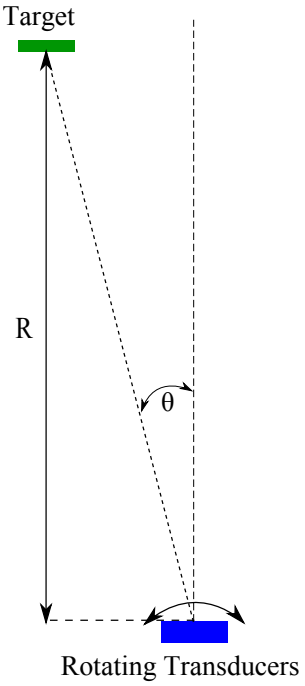

Figure 4.9 – Rotational scanning method.

This method yielded positive results in Tests 6 and 7 (refer to Appendix A for more details on these tests). In Test 6, a 90mm x 90mm x 7mm plate was placed 17m from the transducers at an angle of 3.7° to the left of centre, and the transducers were rotated in increments of 1.2°. Figure 4.10 shows the plot of the amplitude of the reflection from the target at each angle. It clearly shows that the amplitude of the reflections from the plate increases and then decreases sharply as the transducers scan over the target. The same plot is drawn in Figure 4.11, but this time each data set has been filtered using the DWT.

This result is to be expected, since as the transducers rotate towards the target, more of the target surface will be insonified, resulting in a larger reflecting surface and thus larger reflections. The inverse should happen as the transducers rotate away from the target again.

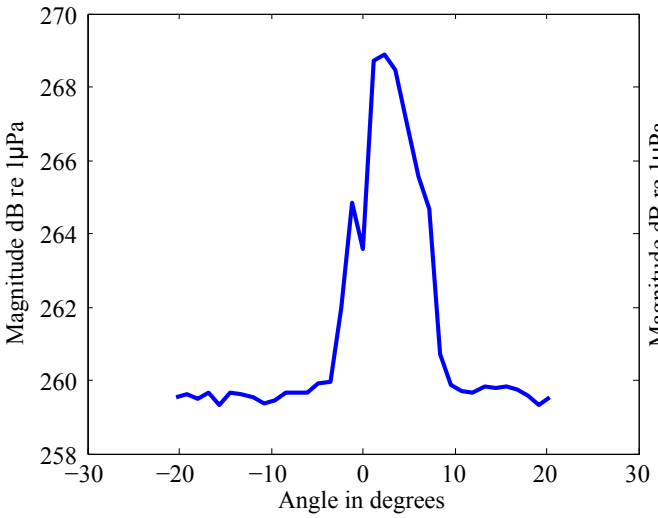

Figure 4.10 – Average amplitude of reflections from 90mm x 90mm target at 17m when scanning from right to left (Test 6).

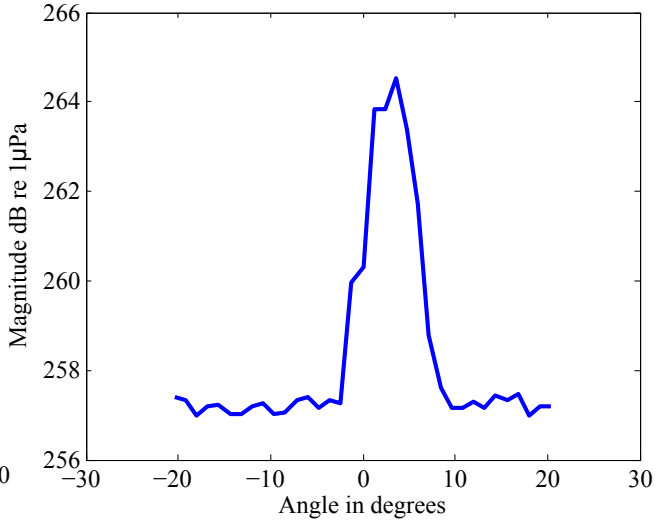

Figure 4.11 – Average amplitude of reflections from 90mm x 90mm target at 17m when scanning from right to left. DWT filtered (Test 6).

The plots in Figure 4.10 and Figure 4.11 were analysed using the **Bisecting** algorithm and the **Maximum Gradient** algorithm, as explained below.

Bisecting Algorithm

The bisecting algorithm finds the angle at which the return amplitude is 0.707 (RMS value) of the maximum value (actually the maximum value minus the average amplitude of the noise) on both the rising and falling sides of the plot. The target is then predicted to be halfway between these two angles. In this test, this algorithm predicted that the target is at $3.65°$ to the left of centre, which is very close to the actual location of $3.7°$. In the case of the data filtered with the DWT, this angle is calculated to be $3.81°$. Thus it was determined that this is a very effective way of finding an object's location in the horizontal plane. If a vertical scanning method is then employed, the same can be done in the vertical plane. Since the scanning is done from right to left, it should be noted that the negative angles on the x-axis of the plot represent the area to the right of the centre of the target.

This method is illustrated in Figure 4.12, where the final result would be in the centre of θ_1 and θ_2.

Maximum Gradient Algorithm

Another function was written to analyse the data from this test which finds the maximum gradient on either side of the curve, i.e., at which angle the amplitude of the reflection from the targets "climbs" the fastest. The initial motivation for this was that it might indicate where the object's limits are in the horizontal plane, which falls into Part 3 (as discussed in Section 4.1). The result of this was that the difference between the maximum gradient on the rising and falling sides was close to $7°$ for Figure 4.10, and exactly $6°$ for Figure 4.11. The theoretical beam-spread is calculated to be $6°$ (see Section 2.2.6.2). This confirms that the theoretical

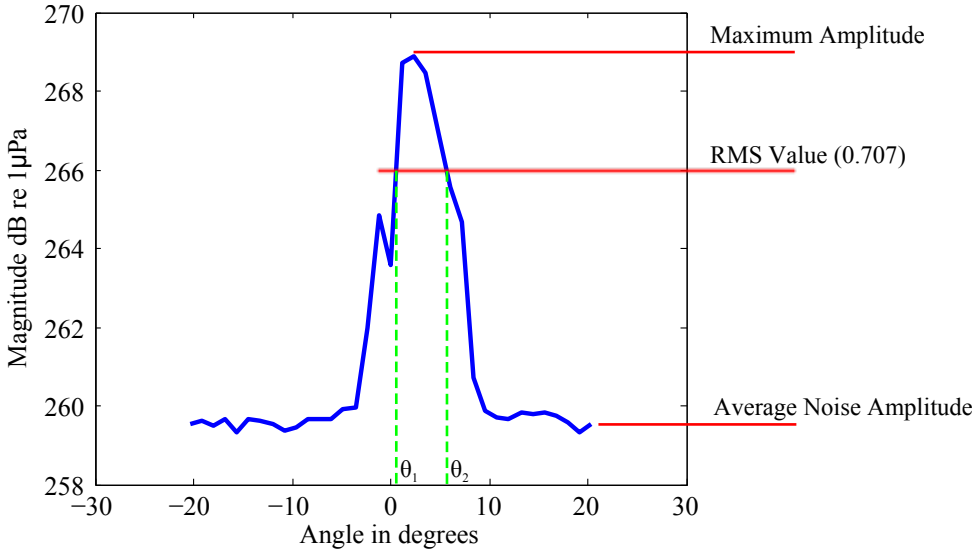

Figure 4.12 – Bisecting algorithm explained.

beam-spread is very close to the actual beam-spread. This means however, that this method of scanning is not very effective at finding where the edges of a target are, as it is limited by the beam-spread.

This also leads to other useful data such as providing a rough estimate of the size of the target. Once the user knows where the centroid of a target is and has a rough idea of the target size, further testing can be done to find the location of its edges.

In Test 7, a 750mm x 430mm x 1.5mm metal plate was placed at 10m range straight in front of the transducers, and the same test was done except that the angle increment was $0.6°$. Figure 4.13 and Figure 4.14 show the plot of the amplitude of the reflection from the target at each angle, where in Figure 4.14 the data is filtered using the DWT.

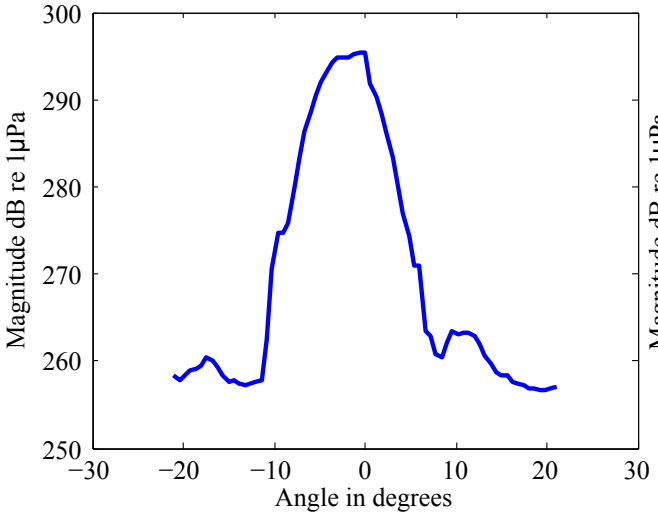

Figure 4.13 – Average amplitude of reflections from target at 10m when scanning from right to left (Test 7).

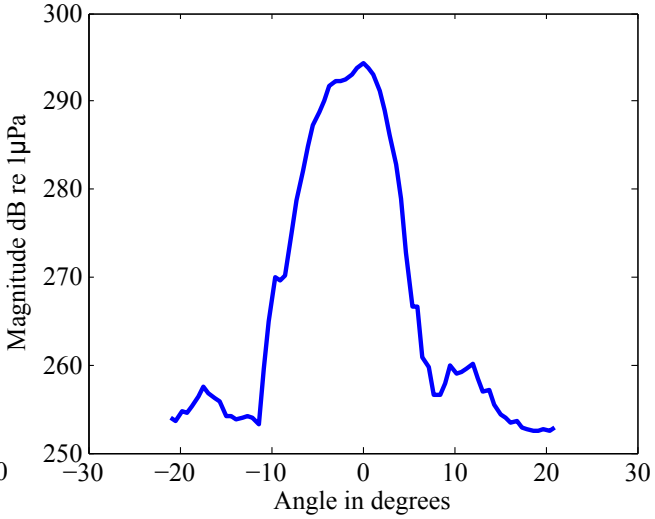

Figure 4.14 – Average amplitude of reflections from target at 10m when scanning from right to left. DWT filtered (Test 7).

The first thing that is clear from these plots, is that the plate is seen to be slightly to the right of the centre of the tank. The main cause of this would be an error in the initial angle at which the transducers were placed. This error is limited to Test 7.

If the bisecting algorithm is applied to the test data in Figure 4.13, it places the centroid of the plate at $2.1°$ to the left of centre, while the result is $1.4°$ for Figure 4.14. This result should be $0°$, but the error is caused by user error, as mentioned above. A result of $1.4°$ is an error of 23.3% of the beam-width.

If this method is to be implemented on an AUV, problems will arise due to the time taken by the mechanical scanning process. In order to reduce the time taken by the scanning process, larger steps can be taken. For example, in Test 6, the step size can be increased to $3.6°$. This results in the plot shown in Figure 4.15. Applying the bisecting algorithm to this plot gives the location of the centroid as $4.24°$, while the correct location is $3.7°$. This is an error of 14.59%, while the error is only 1.35% when the step size was $1.2°$.

If larger steps are taken, the error is greater, but the time taken by the process is much shorter. If $1.2°$ steps are taken, it will take a minimum of 1.36 seconds to scan the $60°$ area in front of the AUV (as shown in Figure 4.1). This calculation is done for a speed of sound under water of 1470 m/s. An increase in the step size to $3.6°$ will reduce the minimum scanning time to 0.45 seconds. If the scanning process is faster, the AUV can move at a higher velocity.

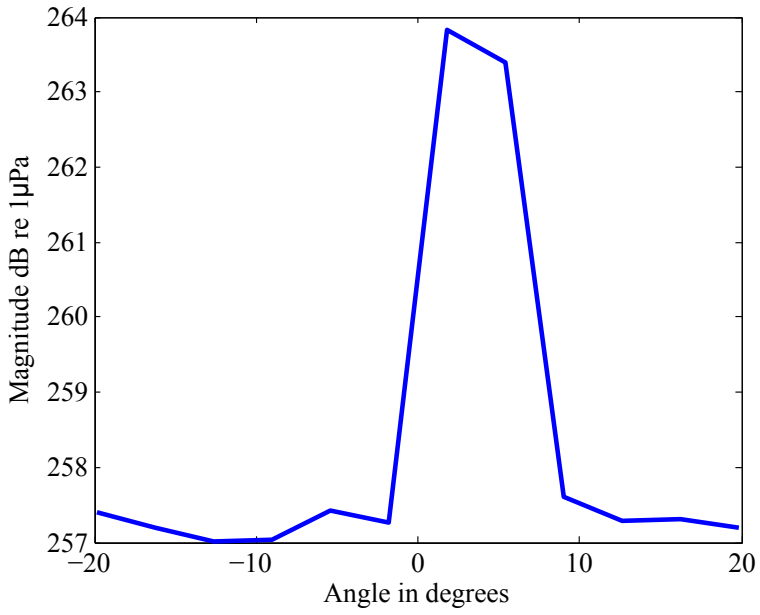

Figure 4.15 – Average amplitude of reflections from target at 17m when scanning from right to left in steps of $3.6°$.

4.3.2.2 Making use of Multiple Receivers

Using multiple receivers refers to using one T_X transducer in conjunction with two R_X transducers. The one receiver is placed as close to the transmitter as possible so as to calculate the range of the target as per usual. The other receiver is placed a known distance from the other transducers (along the same lateral line), and the distance it measures to the target is then used

together with the distance measured by the other receiver to calculate the location of the target using trigonometry. Figure 4.16 shows what this setup looks like graphically.

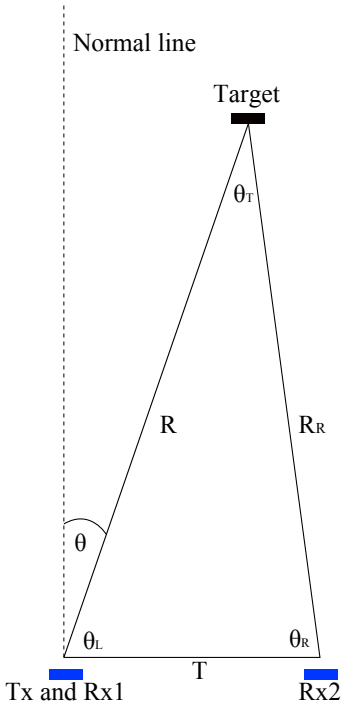

Figure 4.16 – Using multiple receivers for the purposes of object location.

In Figure 4.16, θ_L can be calculated as in Equation 4.3.1. Once θ_L has been determined, θ is known because θ and θ_L are complementary angles.

$$\theta_L(R, R_R, T) = cos^{-1}\left(\frac{R_R^2 - R^2 - T^2}{-2RT}\right) \tag{4.3.1}$$

Ideal Distance Between Transducers

It is important to determine what the distance T in Equation 4.3.1 should be. Here the beam-width of the transducers again comes into play. A certain area is insonified by the T_X transducer and only targets in that area will reflect sound back to the transducers. The receivers also have a beam-width, and sound waves that are to be detected by the receivers, have to reflect from targets in that beam-width. Note that the beam-spread of the transducers is assumed to be conical in shape with a beam-spread angle of $6°$. Thus a region is created in which the target must be located if it is to be detected by both the receivers, as illustrated in Figure 4.17. This region will hereafter be referred to as the detection region. T should be chosen such that the target is in the detection region.

The next factor to consider, is the specular nature of the reflections from a flat target. Consider placing R_X2 at two different locations, as done in Figure 4.18. If it is placed at location 1, it will detect a reflection, whereas placing it at location 2 result in the reflection not being detected. If the surface of the target is smooth, the angle of reflection will be the same as the angle of incidence. That means that, if the target is fairly small, the area insonified by specular reflections

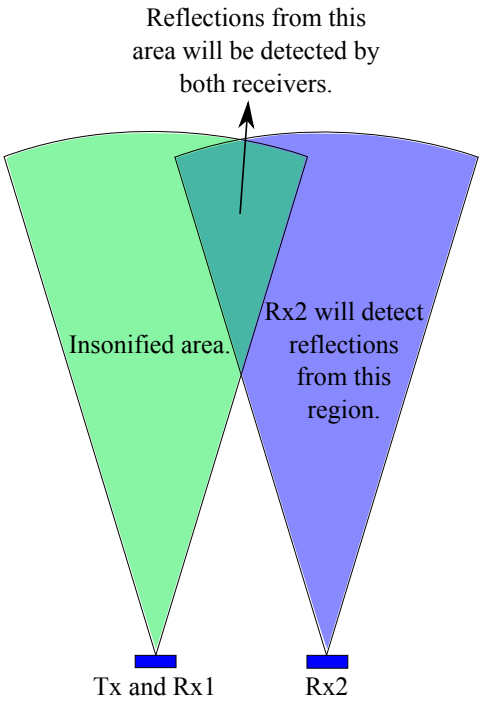

Figure 4.17 – The target has to be in the region shown if it is to be detected by both receivers.

from the target will be quite small, as illustrated by the yellow-shaded area in Figure 4.18. The length of T should be chosen so that the receiver is in that area.

Real world targets will behave differently though, as they will have rougher surfaces that reflect sound in more directions. This will allow more freedom in terms of where the second receiver can be placed, but the reflections will still have a much higher amplitude in the area of specular reflections. This is especially true of targets that have a flat reflective surface. The larger the target, the larger the area in which the second receiver can be placed.

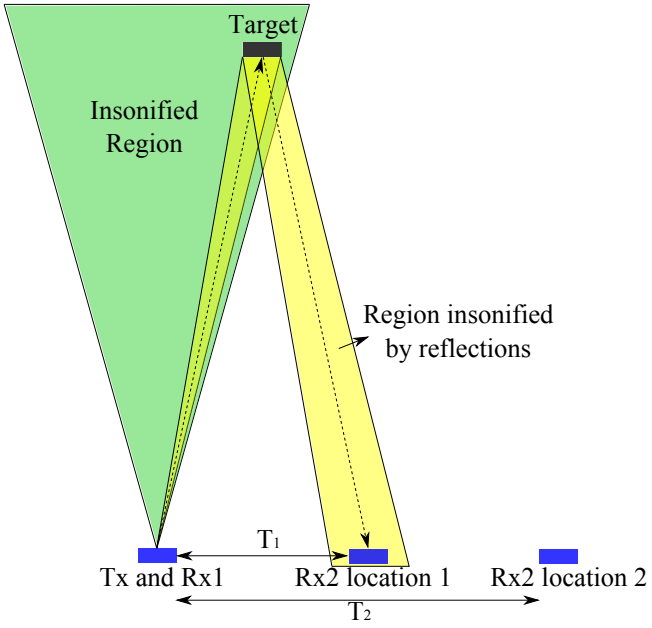

Figure 4.18 – The location of the second R_X transducer needs to be such that it will detect reflections from the target.

Now assume that the second receiver can detect the target. It is possible to calculate the value of T that minimises the error in the calculation of θ. The separation distance (T) that will minimise the error of θ_L ($\Delta\theta_L$) is a function of the range errors (ΔR and ΔR_R) and the error in the measurement of T (ΔT). Both R and R_R, as seen in Figure 4.16, will have a maximum error of $\Delta R = \Delta R_R$ = 14mm [4]. T can be measured using various methods, but its uncertainty is assumed to be ΔT = 2mm.

In Figure 4.16, R and θ_L will remain the same while R_R will vary as T is increased or decreased. Therefore, in order to calculate the amount by which θ_L can vary ($\Delta\theta_L$), Equation 4.3.1 needs to be partially differentiated in terms of R, R_R and T, as seen in Equation 4.3.2.

$$\Delta\theta_L(R, R_R, T) = \left(\frac{\delta\theta_L}{\delta R_R}\right)\Delta R_R + \left(\frac{\delta\theta_L}{\delta R}\right)\Delta R + \left(\frac{\delta\theta_L}{\delta T}\right)\Delta T \tag{4.3.2}$$

The partial derivatives are shown in Equation 4.3.3, Equation 4.3.4 and Equation 4.3.5.

$$\frac{\delta\theta_L}{\delta R_R} = \frac{R_R}{RT\sqrt{1 - \frac{(R^2 - R_R^2 + T^2)^2}{4R^2T^2}}} \tag{4.3.3}$$

$$\frac{\delta\theta_L}{\delta R} = \frac{-R^2 + R_R^2 - T^2}{2R^2T\sqrt{1 - \frac{(R^2 - R_R^2 + T^2)^2}{4R^2T^2}}} \tag{4.3.4}$$

$$\frac{\delta\theta_L}{\delta T} = \frac{-(-R^2 + R_R^2 + T^2)}{2RT^2\sqrt{1 - \frac{(R^2 - R_R^2 + T^2)^2}{4R^2T^2}}} \tag{4.3.5}$$

Using these equations and Equation 4.3.2, $\Delta\theta_L$ can be calculated for targets at different locations and different lengths of T. But, in order to calculate the ideal T, θ_L is needed. At this point θ_L is unknown, therefore a practical option is to calculate $\Delta\theta_L$ for the worst case scenario. The worst case scenario refers to the the points in the detection region that will maximise $\Delta\theta_L$. Therefore, if the target is, as assumed, detected by both receivers, and θ_L is determined, the user can calculate what the greatest error in θ_L could be. This error can then be taken into account when doing path planning and collision avoidance. Figure 4.19 shows where the expected worst case points are. The points are selected to be at the corners of the detection region. One of these points will maximise $\Delta\theta_L$. As shown in Figure 4.19, the detection region ends at a range of 20m. The reason for this is discussed in Section 4.1.

For each of the locations shown in Figure 4.19, $\Delta\theta_L$ can be determined as a function of T. Keep in mind that the transducers have a beam-spread of 6°. New formulas for R and R_R have to be determined in terms of T. To make the calculations simpler, Figure 4.19 is redrawn, as shown in Figure 4.20. This makes it much simpler to calculate the lengths of R and R_R for each of the cases using trigonometry:

Worst case 1:

$R = R_R \approx 9.55T$ m.

Worst case 2:

$R \approx \sqrt{T^2 - 2.096T + 401.1}$ m and $R_R = 20$ m.

Worst case 3:

$R = 20$ m and $R_R \approx \sqrt{T^2 - 2.096T + 401.1}$ m.

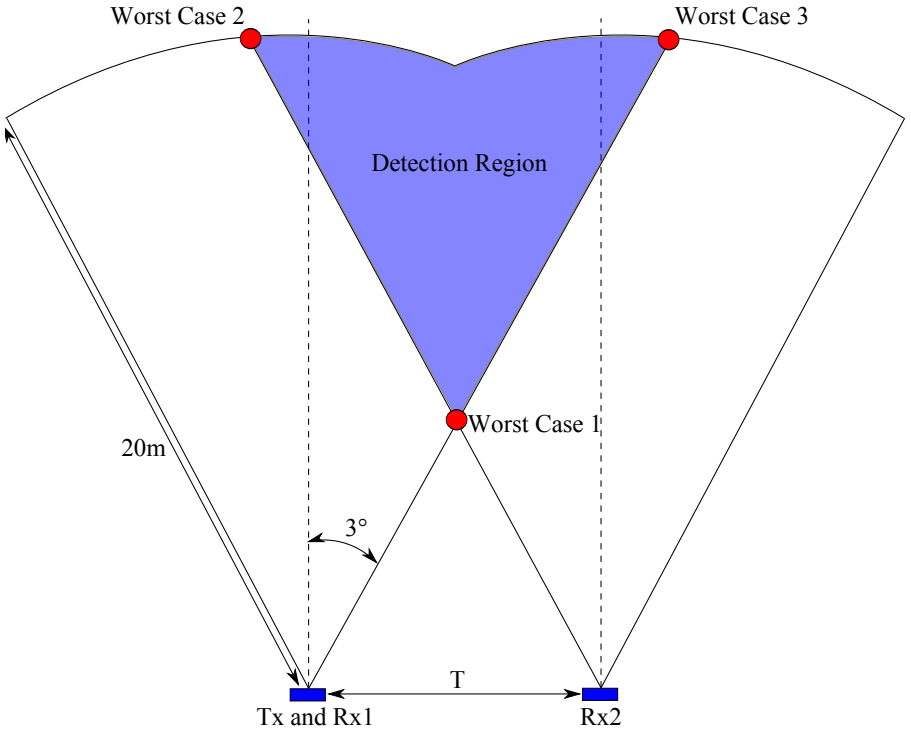

Figure 4.19 – The locations of the target (in the detection region) that could cause the largest error in the measurement of θ_L.

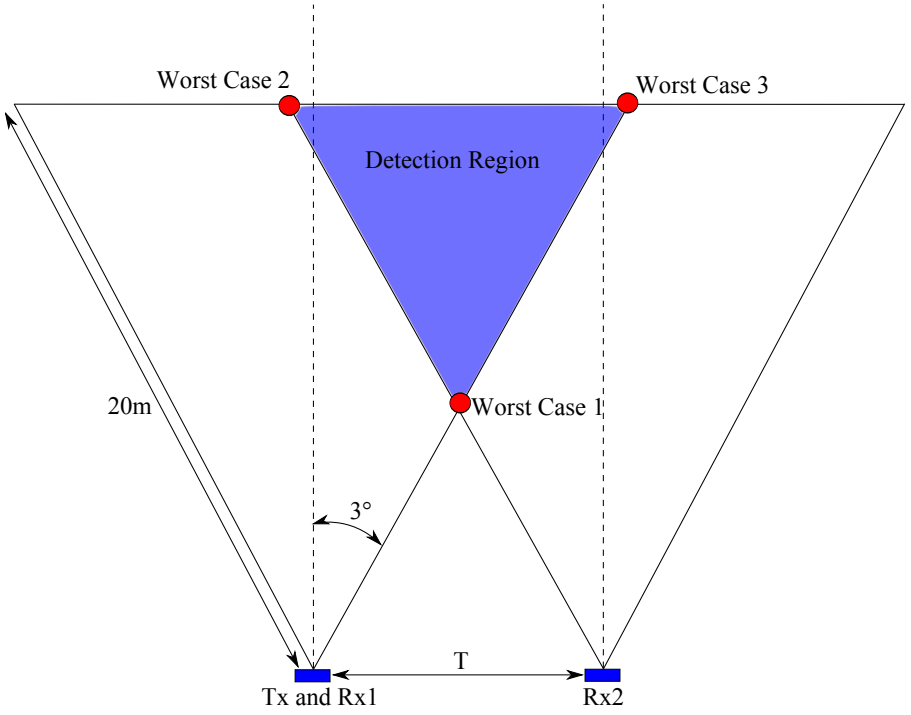

Figure 4.20 – Figure 4.19 redrawn to make the calculations of R and R_R easier for each of the worst cases.

Plots can be drawn that show the relationship of $\Delta\theta_L$ and T for each of the cases. The maximum transducer separation (T) is chosen as 5m for practical reasons. These plots are shown in Figure 4.21, Figure 4.22 and Figure 4.23 and show that the further the transducers are placed from each other (T), the smaller $\Delta\theta_L$ becomes. They also show that if T is greater than about 0.5m, increasing T no longer has a significant effect on $\Delta\theta_L$. Even though $\Delta\theta_L$ seems to increase very quickly when T becomes very small, the error still remains relatively small. For example, for worst case 1, $\Delta\theta_L = 0.00028°$ when $T = 0.1$m. An error of $0.00028°$ with a target at 20m range will result in the target being located with a lateral error of 97.74×10^{-6} m, which is negligible.

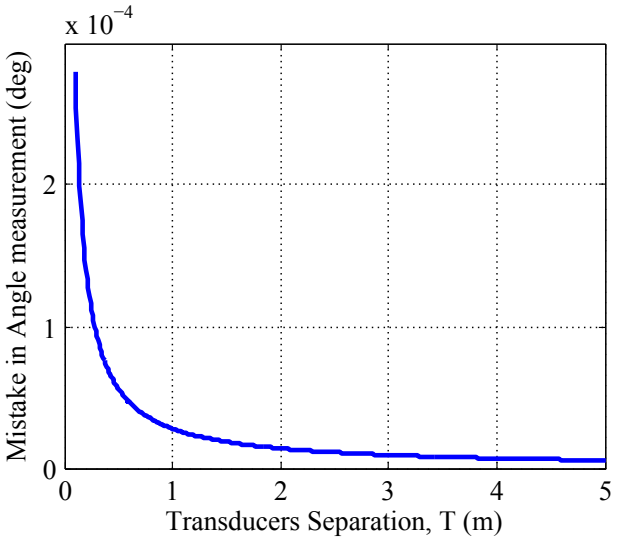

Figure 4.21 – Relationship between $\Delta\theta_L$ and T for worst case 1.

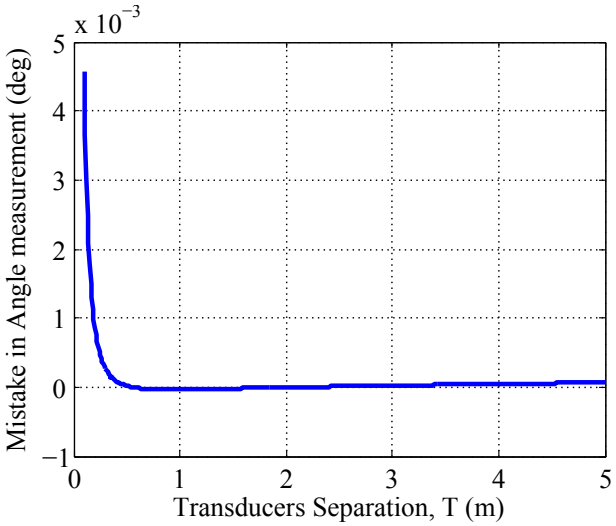

Figure 4.22 – Relationship between $\Delta\theta_L$ and T for worst case 2.

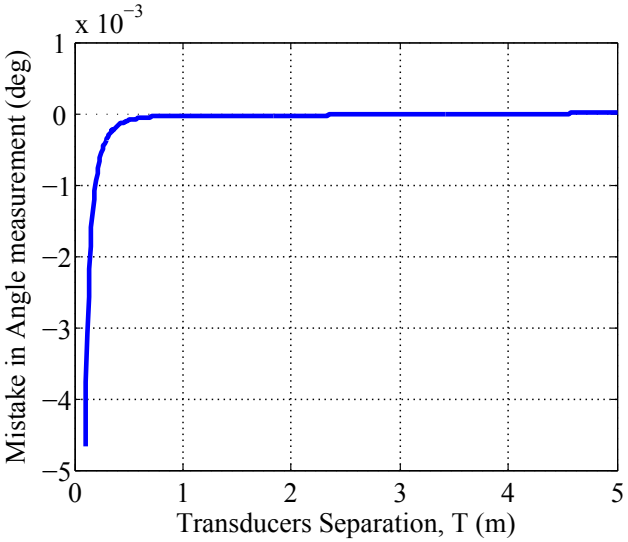

Figure 4.23 – Relationship between $\Delta\theta_L$ and T for worst case 3.

As shown in this section, $\Delta\theta_L$ is insignificant as en error source and other considerations should take presidence. Thus the location of the second R_X transducer should rather be determined by where it will detect the reflections with the highest amplitude, as discussed above. If this method

of locating a target is to be used, a generic starting point for the location of the second receiver should be used. If a reflection is detected by the second receiver, the target's location can be determined.

If a reflection is not initially detected by the second receiver at its generic location (assuming that the first receiver detected a reflection), it should be moved closer to the first receiver until a reflection is detected. To make this process easier, many R_X transducers can be used, and the range measured by the transducer that detected the strongest reflection can then be used to calculate the location of the target.

As mentioned in Section 4.1, the AUV can be assumed to have an approximate width of 0.3m. This means that the transducer separation (T) can practically not be larger than 0.3 m or 0.4 m. Even with $T = 0.3m$, $\Delta\theta_L = 0.00027°$ for the worst case, which is negligible.

Results of using Multiple Receivers

This method was used in Test 9, where a 90mm x 90mm metal plate was placed at two different locations for two different sets of tests. In both sets of tests the target was at a 10m perpendicular distance to the transducers, but at different angles to the normal line ($4.65°$ and $1.22°$).

The test yielded positive results. In the case where the target was placed at $4.65°$ to the normal line, the angle was calculated to be $4.59°$. This is quite close the the actual angle. In the other test, where the target was placed at $1.22°$, the angle was calculated to be $2.1°$, which is still close the the correct value, albeit not as accurate as in the case where the target was at $4.65°$.

4.3.3 Conclusion of Part 2

Both of the methods applied in this part proved to be relatively accurate in terms of object location. The rotational scanning method can be used for both smaller and larger targets, and can easily determine the location of the target's centroid. The method using multiple receivers is also accurate, but can not be used with larger objects. The target used for this method is 90mm x 90mm in size and can therefore be considered as quite small, especially at a range of 10m. When the target is larger, the reflections from the target that contribute to the calculation of its location do not necessarily reflect from the centre of the target, implying that the location calculated is probably not the location of the target's centroid.

Therefore, the rotational scanning method is more effective when looking for known larger targets. For smaller targets, the method using multiple receivers should rather be employed due to the fact that it is much faster. Rotating the transducers and doing tests at each increment takes much longer than simply finding the target's range using two receivers and then triangulating it's position.

If the rotational scanning process is to be implemented on an AUV, it would limit the velocity of the vehicle because it takes a fair amount of time to complete. This problem can be solved by increasing the angle between increments (step size), but this reduces the accuracy notably.

It is important to clarify what is meant by "larger" and "smaller" targets, as referred to above. What needs to be taken into consideration is the ratio of the target size to the width of the beam at the range of the target. Equation 4.3.6 [39] gives the length of a chord of a circle, c, with radius

R and the angle at the centre θ, as seen in Figure 4.24. At 10m range, the "beam" of sound waves should be 1047mm wide, if the beam-spread is taken to be 6° (as discussed in Section 2.2.1.5 and is confirmed in Section 4.3.2.1).

$$c = 2Rsin\left(\frac{\theta}{2}\right) \tag{4.3.6}$$

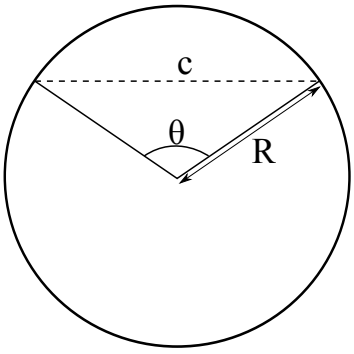

Figure 4.24 – Chord length in a circle.

The ratio of target size to beam-width for the 90mm x 90mm metal plate would be 0.086. For the purposes of this project, a target with a ratio smaller than 0.5 is defined as a small target, and a target with a ratio greater than 0.5 is a large target. Using this reasoning, the 750mm x 430mm x 1.5mm target is classified as a large target, with a ratio of 0.7.

This means that a target might be classified as a small target while the AUV is still far away from it, but as it moves closer, it might be classified as large.

It was also mentioned in this section that the method of using multiple R_X transducers can be made simpler and faster by using more than just two receivers, i.e., one primary receiver and many secondary receivers. The location of the target is then determined by using the data from the primary receiver in conjunction with the data from the secondary receiver that detected the strongest reflection.

4.4 Part 3: Object Edge Location

4.4.1 Overview

In order to navigate around an object, it is important to know not only where the object is, but where its limits/edges are. This part focuses on approximating the location of the edges of a target. For this section, only flat/2D objects are considered due to the fact that they have well defined edges which will be easier to locate. This is an acceptable approach, because AUV's are often used in a harbour environment where the walls of the harbour and even the hulls of ships have more well defined edges and appear two-dimensional. Tests 7, 8 and 10 are concerned with this part of the work (refer to Appendix A for more details on these tests).

During this section, the work done in Part 2 is considered to be accurate with regards to determining the centroid of a target. The tests done in this part rely on accurate knowledge of the location of the centroid of the target.

4.4.2 Approaches and Methods Employed

Rotational scanning (also discussed in Section 4.3.2.1) and **Lateral scanning** were employed to attempt to find the location of the edges of targets. Both of these methods and their application to this part of the work is discussed in this section.

4.4.2.1 Rotational Scanning

The rotational scanning method can also, to a certain degree, be used to determine the location of the edges of a target. Figure 4.13 and Figure 4.14 in Section 4.3.2.1 show the result of using the rotational scanning method on a 750mm x 430mm target at a range of 10m (Test 7).

The maximum gradient method, as discussed in Section 4.3.2.1, can be applied to this data. The reasoning behind this is that the sharpest increase in the amplitudes of the reflections, as the transducers scan over the target, could indicate the location of the edges. The maximum gradients on the left and right of Figure 4.13 (rotational scanning is used with a 750mm x 430mm target at a range of 10m) are calculated to be:

- Left: 10.5°
- Right: 6.3°

At a range of 10m, this means that the SONAR system sees the object to be 2.9m wide, while it is only 0.75m wide. This means that the error on either side is 1.075m. One method to improve this accuracy is to take into account that the sound waves created by a round transducer are approximated to propagate in a cone shape and that the beam-spread of the transducers is approximately 6° (as also approximated by looking at Figure 4.10 in Section 4.3.2.1). This means that, as the transducers rotate towards the target from the right, a return/reflection from the target will be detected when the centre line of the transducers is still pointing 3° (half the beam-spread) to the right of the target. So, if 3° is added to the angle at which the first reflection is detected, the location of the edge of the target can be estimated more accurately. The same can be done on the left side of the target.

Figure 4.25 gives a visual representation of the method described above.

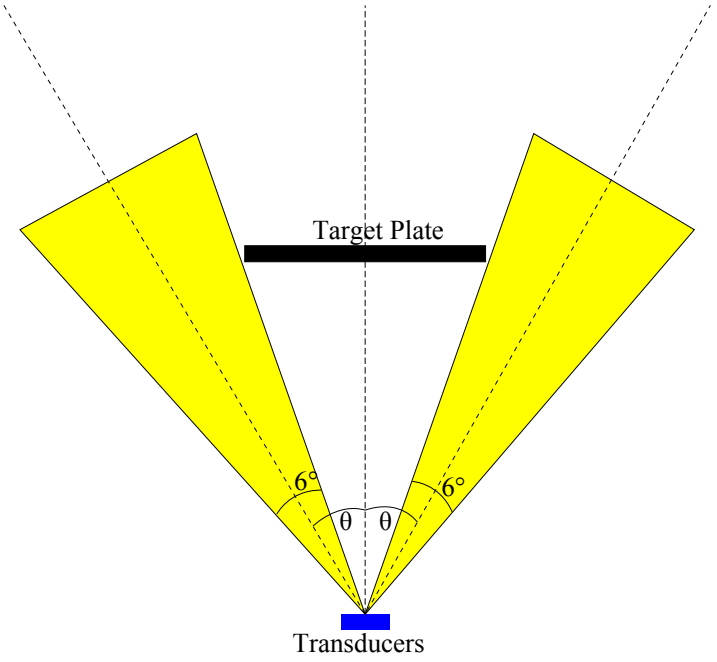

Figure 4.25 – Rotation of transducers in Test 7.

This method was applied to the data in Figure 4.13, resulting in the target being estimated as 2m in size. This means that the error is 0.625m on either side at a range of 10m. This is a definite improvement.

4.4.2.2 Lateral Scanning

The lateral scanning method of data gathering involves moving the transducers laterally across the width of the water tank in increments, and then taking measurements at each increment.

This method was applied in Test 8, where a 750mm x 430mm metal plate is used as a target at a range of 10m and two different sets of tests were done. In one set, the T_X and R_X transducers were shifted together in 30mm increments, starting 1.11m to the left of the centre of the plate and ending 0.15m to the right of the centre of the plate. The process was repeated for the second set of tests, but the R_X transducer was held stationary in line with the centre of the plate. The same process was followed in Test 10.

The data from the tests was analysed by looking at the **amplitudes** of the reflections and the **time taken** for the sound waves to return to the R_X transducer (distance travelled).

Analysis of the Amplitudes of Reflections

The amplitudes of the reflections from the target for Test 8 are shown in Figure 4.26 and Figure 4.27, where the former shows the results from the test where both transducers were moved, and the latter shows the results from the test where only the T_X transducer was moved. The vertical green line shows the location of the edge of the target plate.

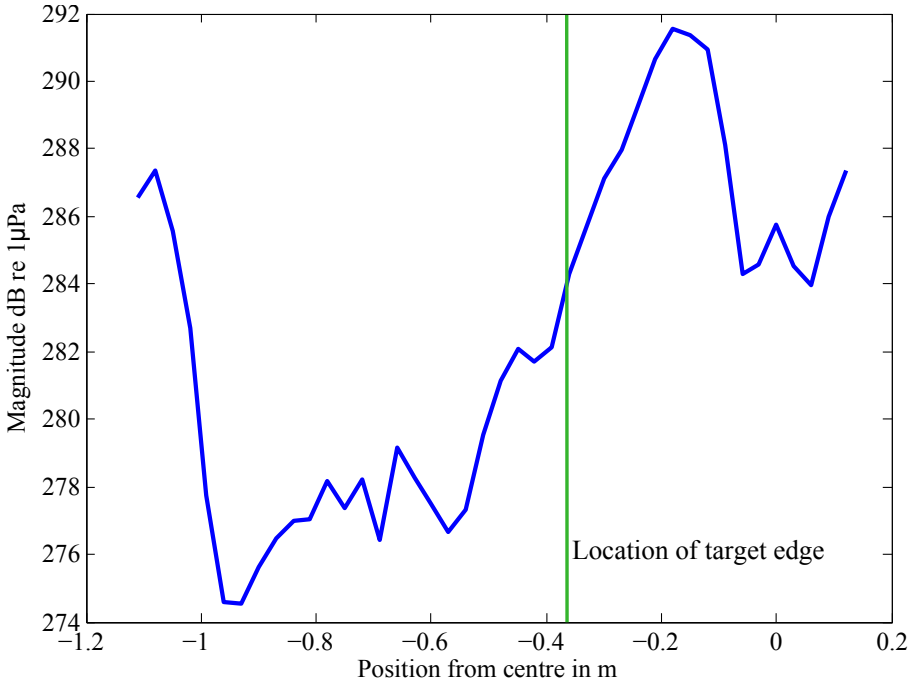

Figure 4.26 – Amplitudes of reflections from target with the T_X and R_X transducers moving together (Test 8).

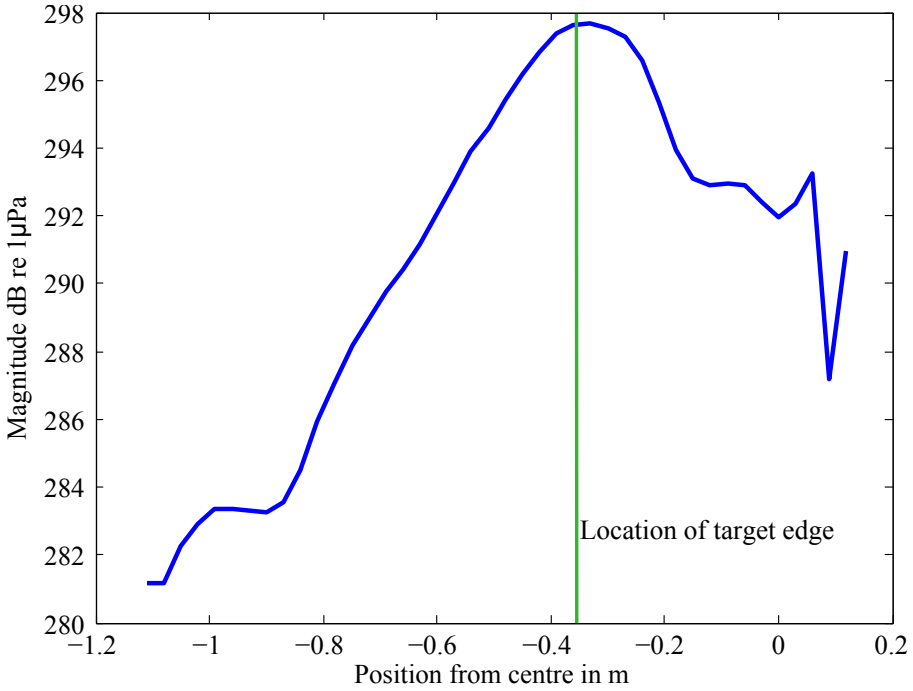

Figure 4.27 – Amplitudes of reflections from target with the R_X transducer kept stationary (Test 8).

There are several interesting things that need to be pointed out in these plots. In Figure 4.26, the first thing that stands out is the increase in the amplitude of the reflections from -99cm to -111cm. This can be written off as multi-path reflections, which is when sound waves bounce off of other objects on their way to and from a target. The same target is then detected, but it seems to be slightly further away because the sound waves travel further. Since the water tank is quite

narrow, and at this point, the transducers were placed fairly close to the left side of the tank, multi-path reflections are highly probable to occur.

Another point worth mentioning is that, in both plots, the amplitude increases as the transducers move toward the edge of the plate and then suddenly decreases, where it would be expected to increase due to an increase is the size of the reflective surface. In Section 4.4.3, the reason for this is discussed in depth. The simulations clearly show that attenuation or amplification of the received wave can occur due to constructive and destructive interference from irregularly reflected waves.

It is also worth noting that in the case of the second set of tests, where the R_X transducer was stationary, the peak of the amplitude plot occurs right on the edge of the target. If this is always the case, it can be used as an effective method of estimating the location of the edge of a target. This method could however, not be proven. Figure 4.26 shows the result of Test 10, where the same test setup was used as in Test 8, except for a higher voltage supply to the main amplifier. The green line once again shows the location of the edge of the target. The same behaviour is seen to a certain degree, where the amplitude increases as the transmitter approaches the edge, and then decreases. In this case it decreases, and then increases again. This behaviour can, again, be explained by the simulations in Section 4.4.3.

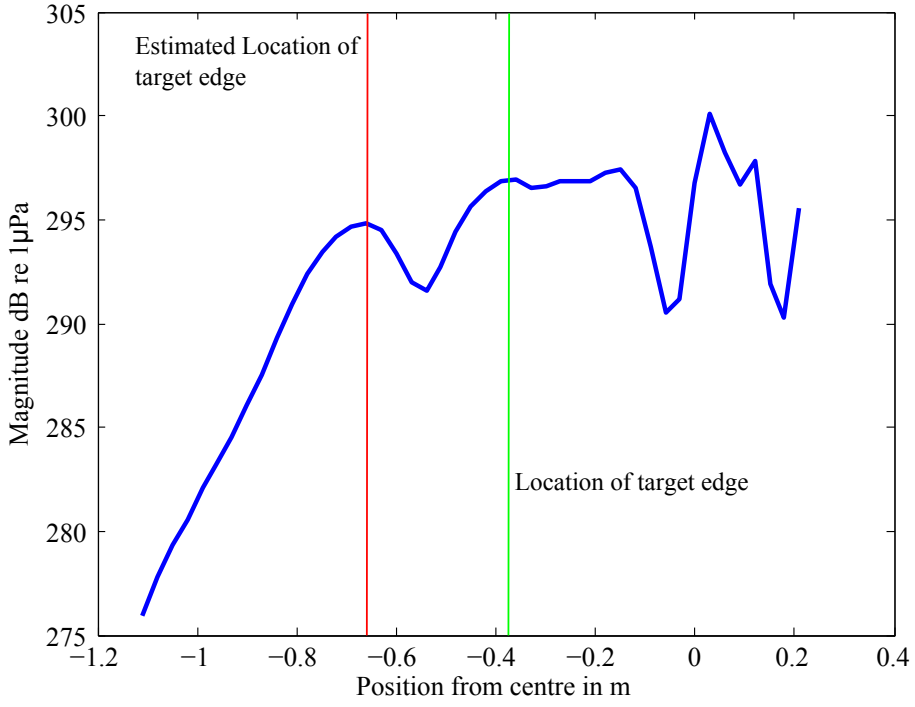

Figure 4.28 – Amplitudes of reflections from target with the R_X transducer kept stationary (Test 10).

It is clear that from the form of Figure 4.26 and Figure 4.28, that as the transducers move towards the edge of the target, the amplitude of the reflections will increase, peak, and then decrease due to the interference by irregularly reflected waves (refer to the simulations in Section 4.4.3). This peak, as shown by the red line in Figure 4.28 is quite close to the edge of the target. The edge is at 0.375m and the peak is at 0.66m. Thus, it can be assumed that, as shown by Figure 4.26 and Figure 4.28, the first peak in the amplitude, as the transducers move towards the target (in the case of a flat/2D target), is a good estimation of where the edge of the target is located.

The closer the transducers are to the centreline of the plate (as they are shifted laterally), the larger the area on the target that is insonified. This means that there are more of these irregularly reflected waves that can interfere with the reflected wave that is to be captured. Thus it can be assumed that the destructive effect of the irregular waves will also increase as the transducers move towards the plate until the effect is of such a nature that the amplitudes of the reflections stop increasing and start decreasing as the transducers move ever closer the the centre of the plate. This peak is taken to be the location of the edge of the target, as done in Figure 4.26 and Figure 4.28, and it is a relatively good estimate.

It is mentioned in Section 4.4.3 that it is not possible to estimate how many irregularly reflected waves are interfering with the wave that is to be captured, and it is also difficult to estimate the amplitudes of these waves. The reflective surface plays a large role in both these factors. For these reasons it is not possible, at this time, to mathematically prove this method for detecting the location of the edge. Studying the effects of irregularly reflected waves could be considered an avenue for future research. Therefore, the effectiveness of this method is determined by looking at test data, as has been done. For the reasons presented however, this method cannot be considered to be trustworthy.

Analysis of the Distance Travelled by Reflections (Range)

As mentioned, the data can also be analysed by looking at the range measured to the target at each location.

Figure 4.29 illustrates the case where the T_X transducer is moved while the R_X transducer is kept stationary in line with the centre of the target. Figure 4.30 shows the comparison of the measured distance to the target versus the predicted distance to the target, where the blue line is the predicted distance and the red line is the measured distance for this case. The distance measured to the plate will decrease as the T_X transducer moves towards the R_X transducer, because the sound waves travel a shorter distance. As the two transducers move closer together, $r1$ and $r2$ (as seen in Figure 4.29) decrease, which means the sound waves travel a shorter distance, resulting in the target being seen as closer. The predicted distance is calculated for the case of a target that is infinitely long.

Equation 4.3.6 gives the length of a chord of a circle, c, with radius R and the angle at the centre θ, as seen in Figure 4.24. As discussed previously, the "beam" of sound waves should be 1.047 wide at 10m range, if the beam-spread is taken to be 6°.

This means that, in theory, as the T_X transducer moves towards the plate (750mm x 430mm), the first direct reflection from the plate should occur when it is 0.9m from the centre of the plate. Before it reaches this point, the reflections that are received should be multi-path reflections, which means the target will appear further away. This seems to be the case, as shown by Figure 4.29, where the measured distance plot matches the predicted distance plot, but then increases drastically as the transducer moves past 0.8m away from the centre of the plate.

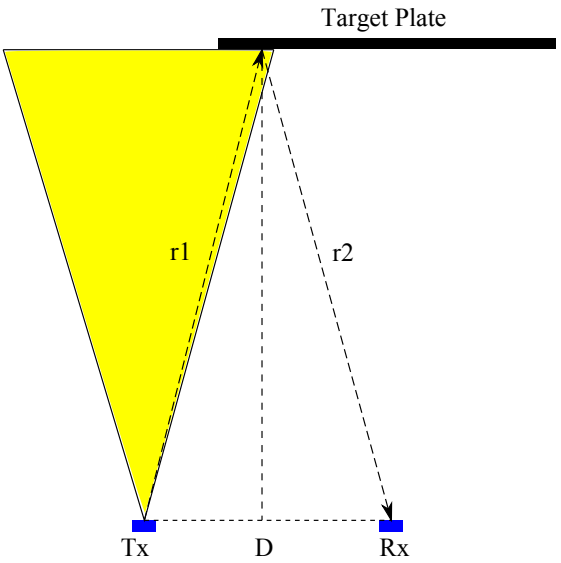

Figure 4.29 – Visual representation of the second set of tests, where the R_X transducer is stationary.

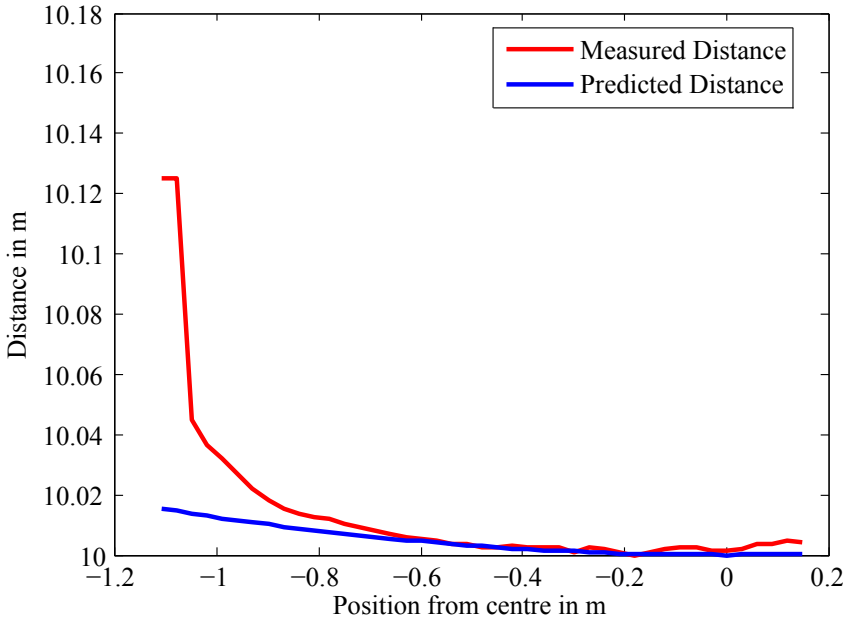

Figure 4.30 – Measured distance vs. predicted distance to target when R_X transducer is stationary (Test 8).

The distance to the target for the case where both transducers are moved, is also plotted, as seen in Figure 4.31. The time delay of the reflection from the target at each step is used to calculate this distance. Since the transducers are moved together, the same argument used to discuss Figure 4.30 cannot be used again. In this case, the distance from both the transmitter and receiver are assumed to be the same since they are close together.

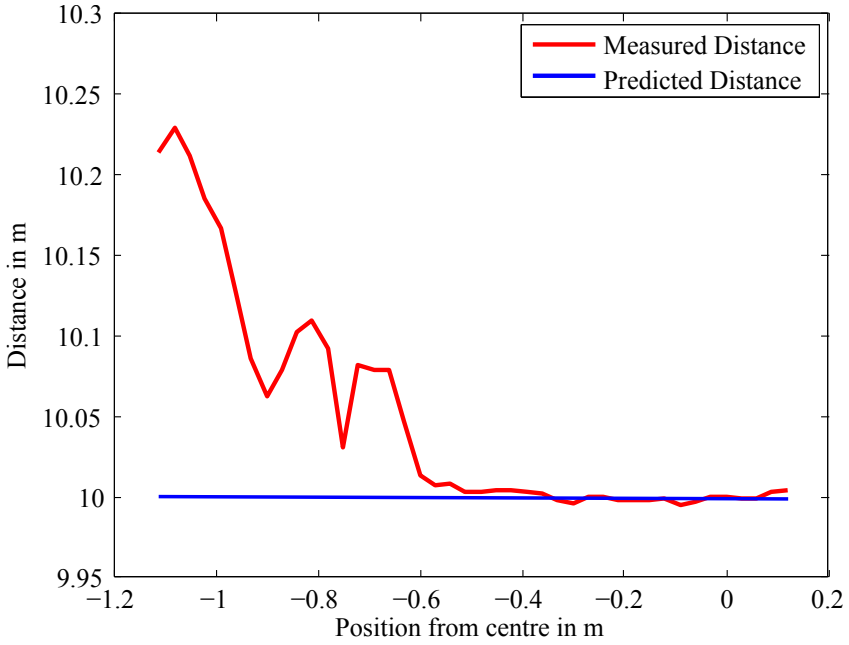

Figure 4.31 – Measured distance vs. predicted distance to target when both transducers are moved (Test 8).

The amplitude data shown in Figure 4.26 and the range data shown in Figure 4.31 can be combined to generate a 3D plot, as shown in Figure 4.32. The data seems to be very "choppy", as expected from the underwater environment. The plot can be improved by using the DWT, as shown in Figure 4.33. Here, the ridge formed by the reflections from the target can be seen more clearly.

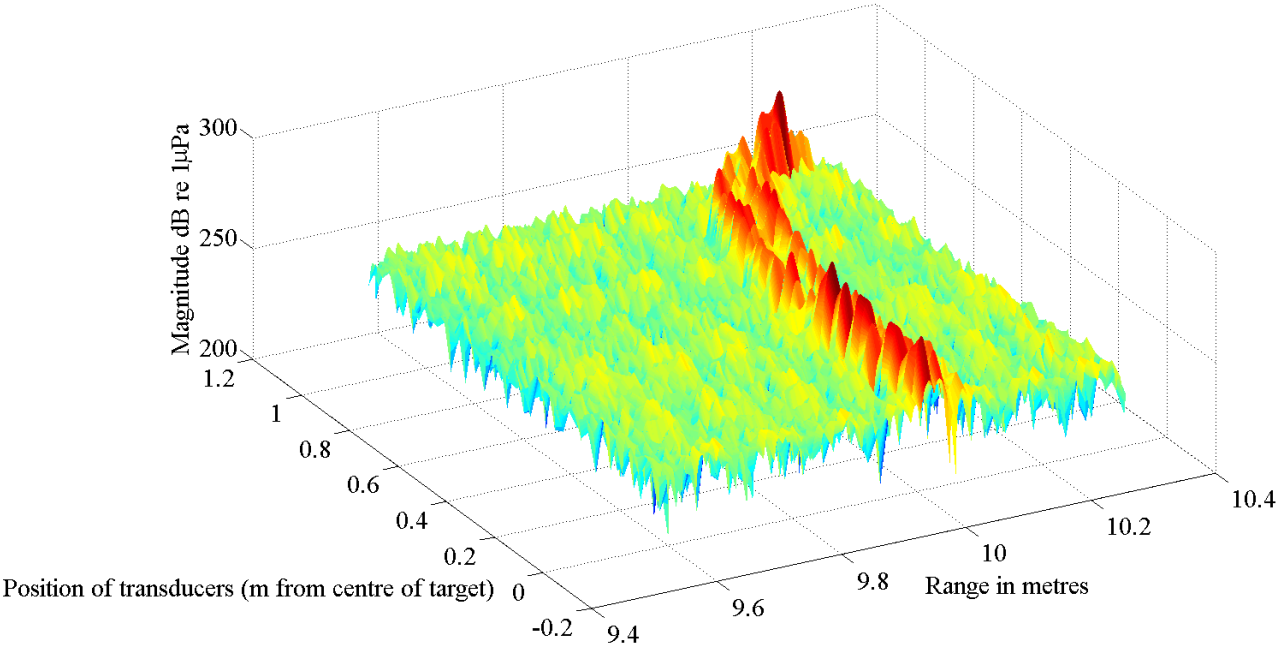

Figure 4.32 – 3D plot of the data from Test 8 (amplitude and distance data).

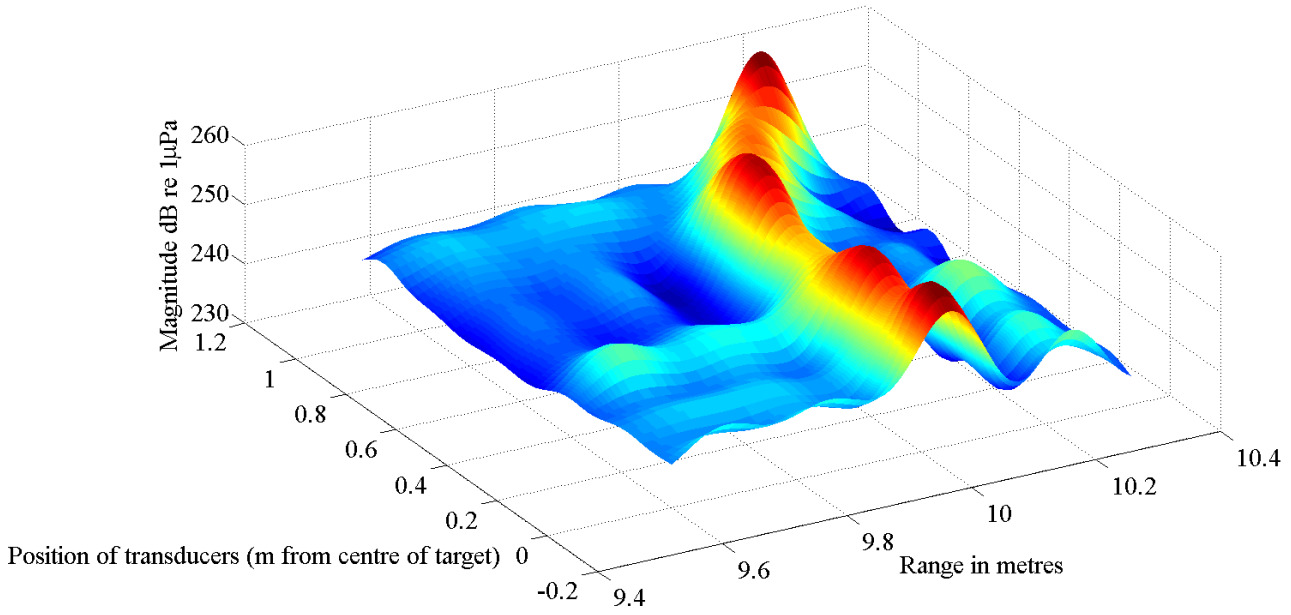

Figure 4.33 – 3D plot of the data from Test 8, filtered with the DWT (amplitude and distance data).

In the ideal case, where the sound propagates in an exact cone, the first reflection from the plate should occur when the edge of the cone at 10m range is in line with the edge of the target. From this point onwards, as the transducers move towards the centre of the target, the reflection from the edge of the plate should be the first one detected by the receiver. Then, once the transducers are in line with the edge of the plate, the measured distance should remain equal as they move to the centre of the plate. The predicted distance in Figure 4.31 is plotted, as in Figure 4.30, for an infinitely long target at a 10m range. Since the transducers are moved together, this distance will remain 10m while they they are in line with the target.

The plot shows that the measured plot follows the predicted plot quite closely, until about 0.55m from the centre (as the transducers move away from the centre). It can be assumed that the reflection from the target that is detected, is from the point on the target that is closest to the transducers. That means that as the transducers move from the centre to the edge of the target, the range should remain 10m, which is the case as shown by Figure 4.31. Theoretically, once the transducers move past that point, the distance to the target will increase as they move. This can be seen in Figure 4.31 at 0.55m from the centre. That means that the edge can be estimated to be 0.55m from the centre of the target, which is relatively close to the actual value of 0.375m, making the error only 0.175m. This method is only valid if the target is flat and has a well defined edge.

As discussed for Figure 4.30, the first direct reflections from the target (if the beam-spread is assumed to be 6° and the sound propagates in a cone shape) should occur when the transducers are 0.9m away from the centre of the plate. This is not quite the case according to the measurements. It would seem the multi-path reflections play a role here because at this point, the transducers are not far from the left-hand side of the water tank. These multi-path reflections can already be seen at close to 0.6m. Since the transducers are moved together, the receiver is also closer to the side wall of the tank, making the system more susceptible to the effects of multi-path reflections.

4.4.3 Simulation of Irregularly Reflected Sound Waves

Section 4.4.2.2 mentions unexpected changes in the amplitude of reflections from a flat/2D target (refer to Figure 4.26, Figure 4.27 and Figure 4.28). This section attempts to explain why this happens.

It is generally assumed that sound waves will reflect evenly off of a smooth, hard surface, as discussed in Section 2.3. This means that the angle of incidence will equal the angle of reflection. The material the surface consists of, has an absorption coefficient that determines how the reflected wave's amplitude will relate to the incident wave's amplitude due to sound absorption.

Surfaces are generally not completely smooth, and contain small bumps and irregularities. This results in small amounts of the sound waves reflecting in irregular directions. In SONAR applications, these small reflections can have very small, almost negligible interference effects on waves that are used to detect targets. The effect of one of these waves might be negligible, but the possibility exists that a large amount of these waves could interfere with the wave that reflects back to the receiving transducer, adversely affecting the signal that is processed.

The primary signal at the receiving transducer can be defined as in Equation 4.4.1.

$$y(x,t) = Asin(kx - \omega t) \tag{4.4.1}$$

The wavenumber, k, is defined in Equation 2.3.2. Let one of the small, irregularly reflected signals be defined as in Equation 4.4.2.

$$z(x,t) = Bsin(kx - \omega t + \phi), \tag{4.4.2}$$

where B is an amplitude much smaller than A, and ϕ is the phase shift of signal $z(x,t)$ in relation to the phase of $y(x,t)$. This phase shift is due to the extra distance the irregularly reflected waves have to travel. This phase shift can be calculated as done in Equation 4.4.3.

$$\phi = \left(\frac{2t_d}{T}\right)(2\pi), \tag{4.4.3}$$

where ϕ is the phase shift, t_d is the time delay and T is the period of the wave. The time delay is multiplied by 2 because the wave has to travel to the target surface and back, and is calculated by using simple trigonometry, as can be seen in Figure 4.34.

The distance l is the distance from the point perpendicular to the surface and the transducer, and the point of reflection of the irregular wave. The distance d is the perpendicular distance from the transducer to the surface. Thus the distance travelled by the irregular wave can easily be calculated, and the time it takes can be calculated by dividing the distance travelled by the sound propagation speed (see Section 2.2.1.1).

Now, the final signal that reaches the transducer can be calculated adding n amount of the irregular signals, each with their their phase shift, ϕ_i and amplitude B_i to the signal $y(x,t)$, to get $y_f(x,t)$:

$$y_f(x,t) = Asin(kx - \omega t) + \sum_{i=0}^{n} B_i sin(kx - \omega t + \phi_i) \tag{4.4.4}$$

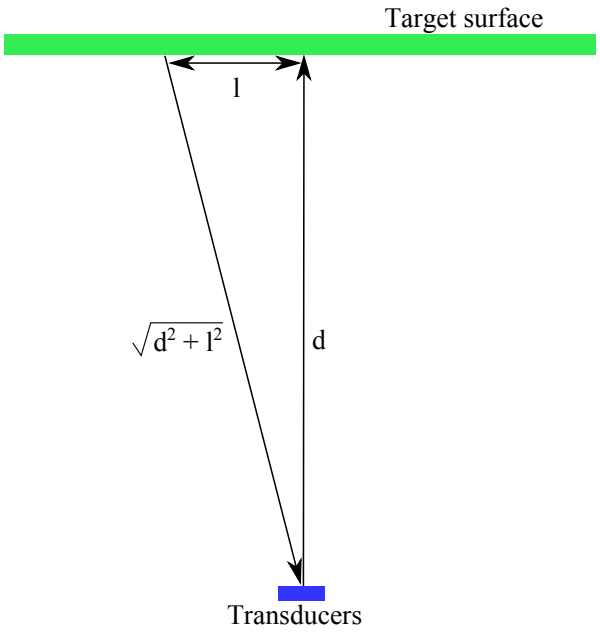

Figure 4.34 – Irregular reflections of sound waves from target surface.

To see if this could have a significant effect on the received wave, simulations were done using *Matlab*. Simulating this posed a few questions:

- What is the amplitude of the additive waves (B) in relation to the original wave?
- How many additive waves need to be simulated?

Wave Amplitude

It is very difficult to predict what the amplitude could be. There are several factors that contribute to the amplitude of the reflections. These include the propagation losses (PL), the reflection coefficient (σ) and the gains of the transducers. In this simulation, the transducers' gains are ignored, as the path that is considered is from where the signal is transmitted by the T_X transducer up to right before it is received by the R_X transducer.

The propagation loss is defined in Equation 2.2.12 as $\frac{PL}{dB} = 10log(r)$, where r is the distance travelled under water by the wave. This is, of course, in decibels. A voltage gain is converted to decibels using Equation 4.4.5.

$$G_{dB} = 20log(G_V) \tag{4.4.5}$$

where G_V is the voltage gain and G_{dB} is the gain in decibels. In the case of a propagation loss G_V would be less than 1, and G_{dB} would be equal to the propagation loss in Equation 2.2.12, $\frac{PL}{dB}$. Thus in order to convert the gain in decibels to a voltage gain, Equation 4.4.6 can be used.

$$G_V = 10^{\frac{PL}{20}} \tag{4.4.6}$$

It is important to note that the propagation loss needs to be calculated for the distance $2r$, because the wave has to travel to the target and back.

The reflection coefficient (σ) gives the percentage of a wave's energy that will reflect back off of the reflecting surface. In the case of waves that do not have the same angle of reflection and angle of incidence, such as the waves in question, the reflection coefficient can be taken to be much smaller due to the fact that most of the wave energy will reflect with the same angle as the angle of incidence. Let the reflection coefficient for these waves be called σ_i.

Thus if the amplitude of the wave, as it is transmitted, is denoted as A_0, the amplitudes A and B can be defined as in Equation 4.4.7 and Equation 4.4.8.

$$A = A_0 G_V \sigma \tag{4.4.7}$$

$$B = A_0 G_V \sigma_i \tag{4.4.8}$$

Number of Irregular Waves

The number of these additive waves that should be considered is also not possible to estimate. It depends on not only the area of the reflective surface that is insonified, but also on the texture of the surface. A rougher surface will cause more wave scattering and thus more additive waves that can cause interference.

Simulations

Since the reflection coefficient and the number of additive waves, as discussed above, is quite uncertain, the simulation covered a large variation of amplitudes and numbers of waves. Figure 4.35 to Figure 4.42 show the amplitude of the final wave, each time using additive waves of a different amplitude. They also show the effect the number of additive waves has on the final wave's amplitude. The target surface is taken to be 0.75m long and at a range of 10m from the transducers (as in Test 8), and the transmitted wave's amplitude is normalised.

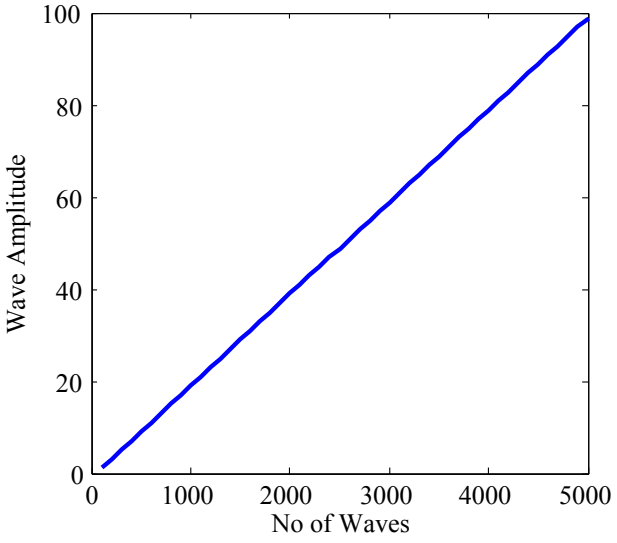

Figure 4.35 – Amplitude of final wave. Interfering waves' amplitude = 0.01.

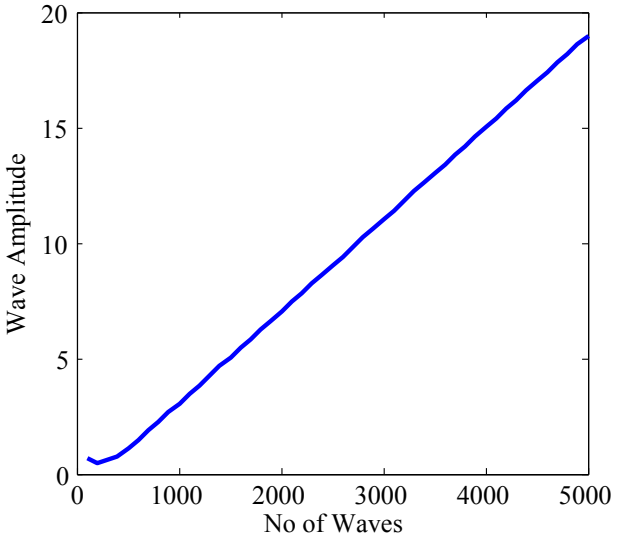

Figure 4.36 – Amplitude of final wave. Interfering waves' amplitude = 0.002.

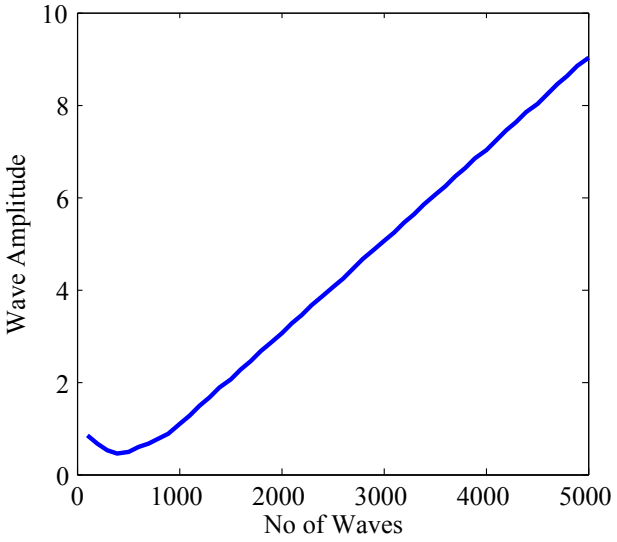

Figure 4.37 – Amplitude of final wave. Interfering waves' amplitude = 0.001.

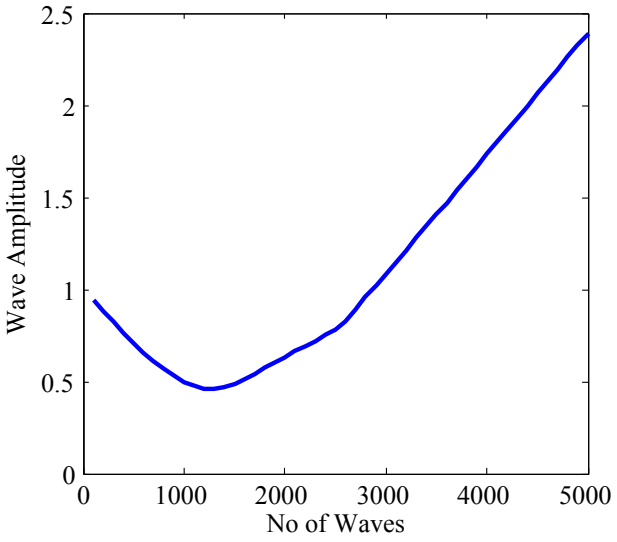

Figure 4.38 – Amplitude of final wave. Interfering waves' amplitude = 0.00033.

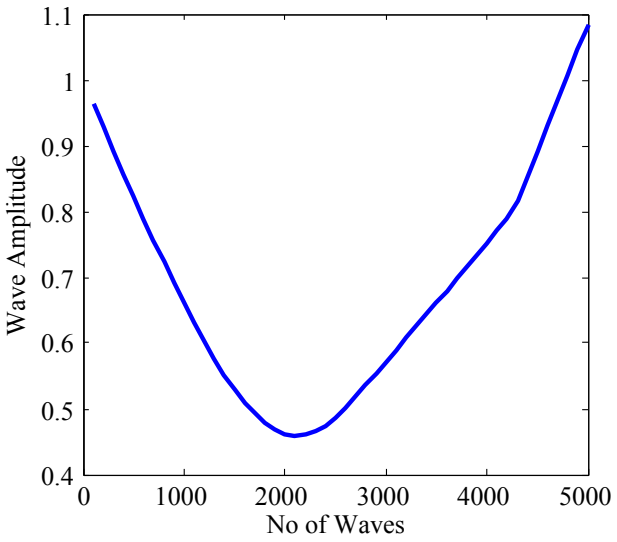

Figure 4.39 – Amplitude of final wave. Interfering waves' amplitude = 0.0002.

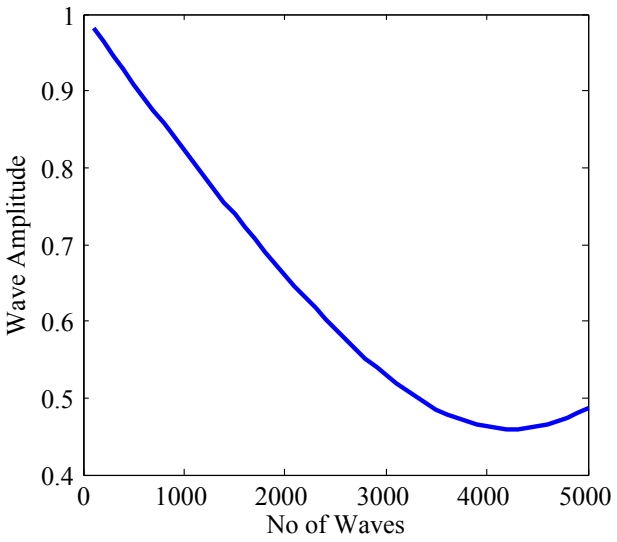

Figure 4.40 – Amplitude of final wave. Interfering waves' amplitude = 0.0001.

The simulations were done using the basic premise discussed above, but also included the fact that the transmitted wave does not have a constant frequency, but rather sweeps through 100 kHz in 100 ms.

The results of this simulation show that the greatest attenuation that can occur due to waves that reflect irregularly and interfere with the received wave results in a wave of amplitude = 0.46. This occurred when the interfering wave amplitude and number of waves were as follows:

- Amplitude = 0.0001 and number of waves = 4200.
- Amplitude = 0.0002 and number of waves = 2100.
- Amplitude = 0.000333 and number of waves = 1300.

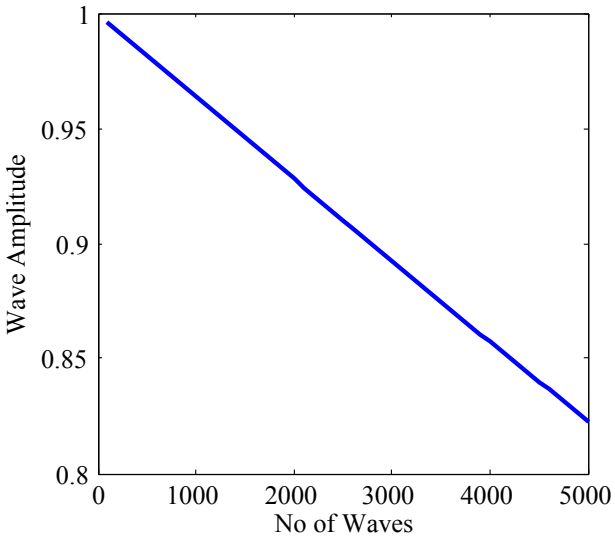

Figure 4.41 – Amplitude of final wave. Interfering waves' amplitude = 0.00002.

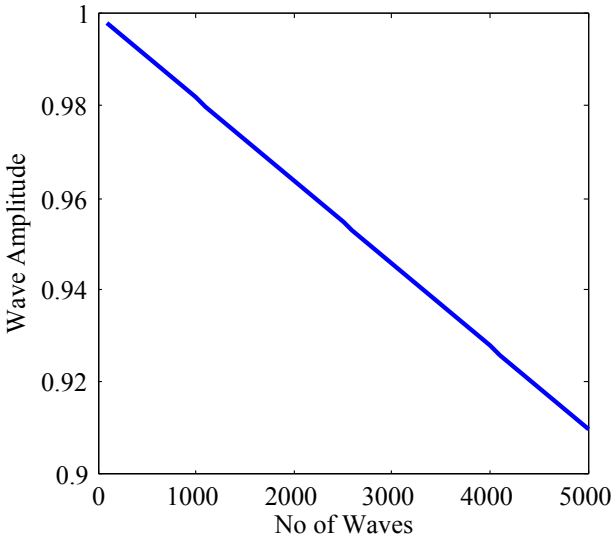

Figure 4.42 – Amplitude of final wave. Interfering waves' amplitude = 0.00001.

The simulations also prove that amplification is quite possible.

4.4.4 Conclusion of Part 3

Interesting results were obtained from the tests towards determining the edge of the target. Using the rotational scanning method achieved positive results, as can be seen in Figure 4.43. The edges of the target are located with an uncertainty of 0.625m. The lateral scanning method achieved even greater success, detecting the edge to within 0.285m when analysing the amplitudes of the reflections, and 0.175m when analysing the range information of the reflections. If this system was implemented on an AUV, it would allow for improved edge estimation that may be used for navigation and collision avoidance.

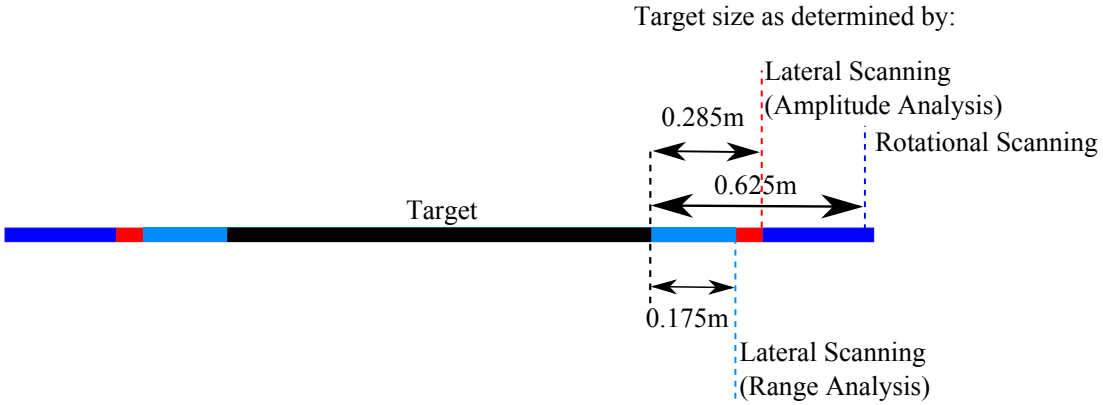

Figure 4.43 – Effectiveness of the rotational and lateral scanning methods for edge location.

Practical implementation of the lateral scanning method might be problematic. A solution for this would be to have several sets of transducers placed at intervals along the same lateral line. These transducers can then be used to emulate the lateral scanning method. Another solution would be to physically move the transducers from side to side, as done in the tests, but using a stepper motor.

The real problem with implementing this method though is the limits placed on the system by the physical size of an AUV. Figure 4.1 shows that the AUV can be expected to have a width of about 0.3m. This means that a smaller scale version of the method could be implemented, but it will be less accurate.

The methods discussed in this part are effective ways of estimating the location of the edges of a flat target. Once the centre of the target is located using rotational scanning as in Part 2, the edges of the target can be estimated with an acceptable error for the purposes of this project.

4.5 Part 4: Study of non-2D targets

4.5.1 Overview

Up to this point, only flat/2D targets have been used that have well defined edges. The fact that they are flat results in reflections with high amplitudes, making them easy to detect and locate. As discussed in Section 4.4.1, the use of flat targets is a good approximation of a harbour environment. Unfortunately, there are other objects to be found under water, and this part of the project is aimed at studying the effects of using these objects as SONAR targets.

All of the methods of edge location that are discussed in previous sections, rely on the fact that the object is flat and thus it is important to be able to differentiate, using SONAR data, between objects that are flat with well defined edges and objects that have depth. This section will try to show that this is possible.

This section of the work also attempts to obtain a rough estimate of the profile of the rounded edge of a target. All of the work done in this part still makes use the wide-beam SONAR transducers used in previous sections.

The test object that was chosen has a profile (as seen from the top) as seen in Figure 4.44. It has a flat surface, but with rounded edges to give it depth.

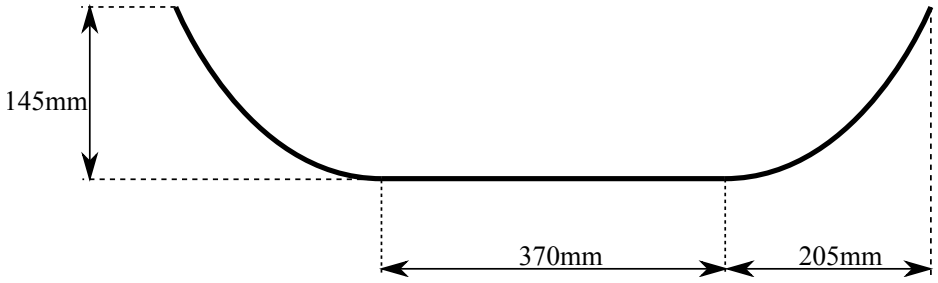

Figure 4.44 – Target with rounded edges.

It is immediately apparent that problems will arise with the reflections from the rounded edges. The flat area will reflect sound back to the transducers, but the rounded regions will scatter sound waves that fall on it leading to multi-path reflections. Sound waves that do reflect from the rounded areas back to the transducers will have a significantly lower amplitude and might not be distinct above the ambient noise.

4.5.2 Approaches and Methods Employed

4.5.2.1 Differentiation Between Flat and Rounded Targets

As mentioned, it is important to be able to differentiate between an object that is flat and has a well defined edge, and one that does not. The **Lateral Scanning** method was employed with the rounded plate shown in Figure 4.44 placed at a range of 10m in Test 10 (refer to Appendix A). The results of this were not very promising, but there were some positives to be drawn from the data.

As mentioned in Section 4.5.1, the rounded regions of the target could cause multi-path reflections. Figure 4.45 shows what these multi-path reflections look like in the processed data. The

plot shows the result of processing the SONAR data using a matched filter and "zooming in" at 10m range. At this point, the transducers were placed 870mm to the left of the centre of the target. There is a clear reflection at 10.22m, and another at 10.43m. The reflection at 10.22m would be from the section of the target facing towards the transducers, while the reflection at 10.43m is a multi-path reflection. This concept is illustrated in Figure 4.47. The DWT is used to filter this data set, resulting in the plot in Figure 4.46, in which the two reflections are more clearly visible.

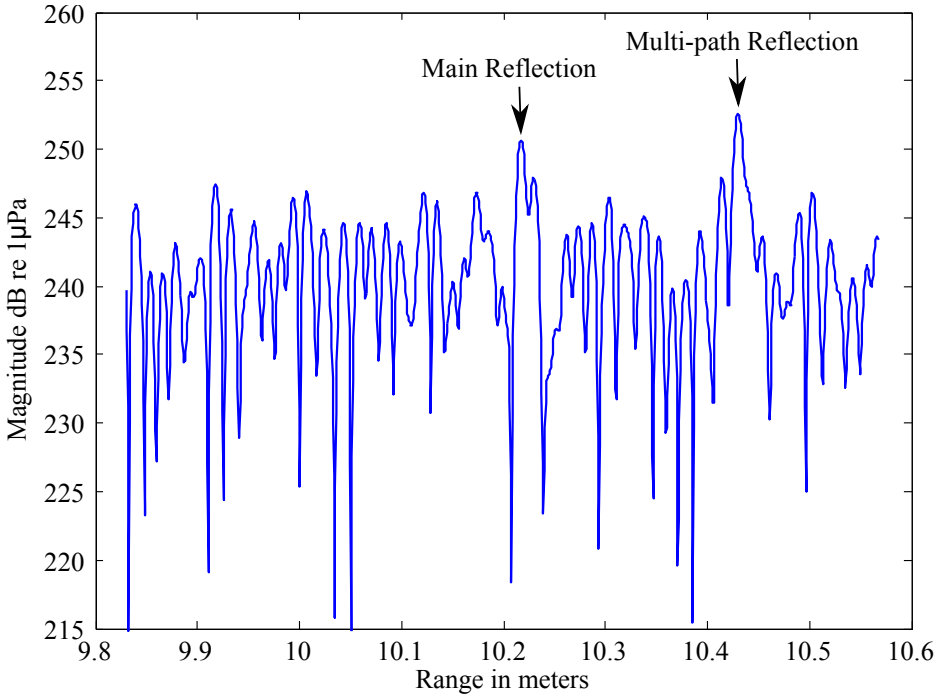

Figure 4.45 – Result of SONAR data from rounded target at 10m processed using a matched filter. Transducers are placed 870mm to the left of the centre of the target (Test 10).

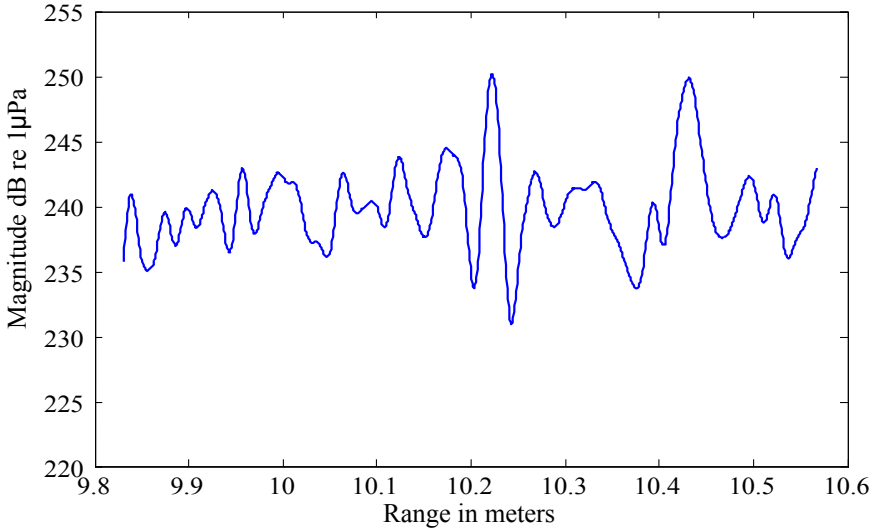

Figure 4.46 – Result of SONAR data from rounded target at 10m processed using a matched filter. Transducers are placed 870mm to the left of the centre of the target and the data is filtered using the DWT (Test 10).

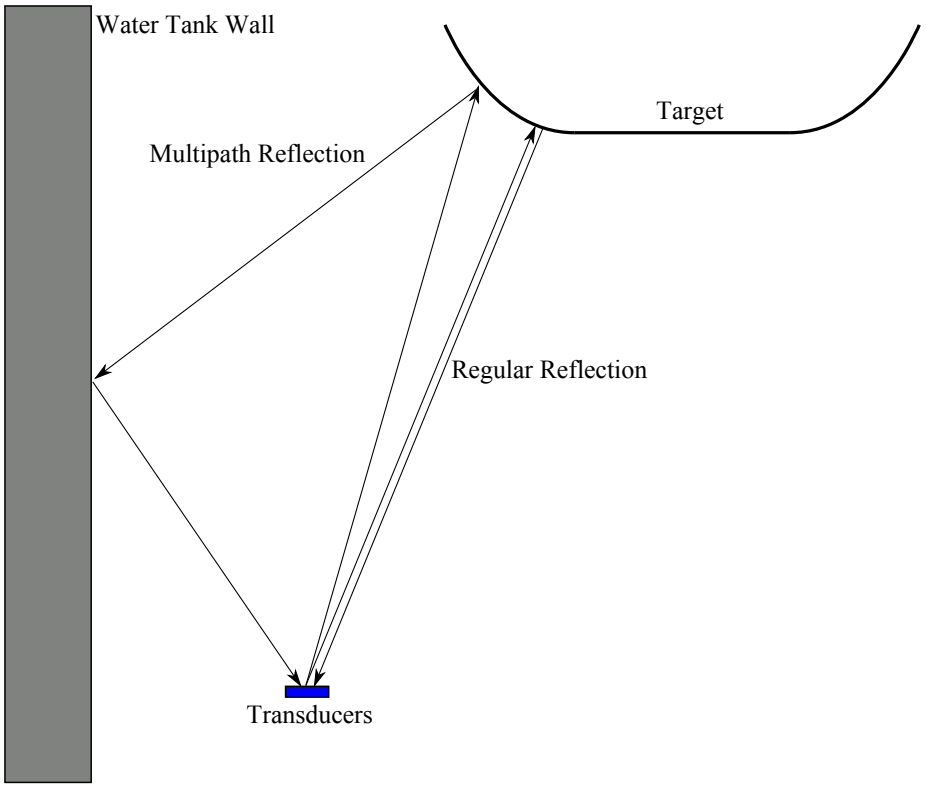

Figure 4.47 – Multi-path reflections (Test 10).

In Test 11, better results were achieved using the same target, but the surface was covered with sand to make it rough, which will lead to more sound wave scattering. This can be assumed to be a good replication of real world underwater targets, as they will be covered with rust or plant-growth and concrete surfaces are rough to begin with. The main reason for doing this is the fact that the smooth, rounded edges of the plate reflected the sound waves away from the receiver causing strong multi-path reflections. The rough, sand-covered surface will reflect sound in more directions, which means that some sound waves might reflect off of the rounded edges towards the R_X transducer.

This method proved to be quite effective, resulting in less multi-path reflections. The amplitude plot shown in Figure 4.48 again shows the same behaviour as in previous results, where the amplitude increases as the transducers approach the plate and then decreases as they move towards the centre of the plate. Once again, the simulations in Section 4.4.3 provide a possible explanation for why this happens. In fact, the amplitude decreases even more than in any of the previous results. This supports the idea that irregular waves are causing destructive interference, because the sand coating causes even more irregularly reflected waves, resulting in more interference.

In the ideal case, the reflection that is detected should be from the point on the target that is closest to the transducers, as it would be the first point that is insonified with the wide beam. Using this reasoning and an approximation of the dimensions of the target, a plot can be generated that shows the predicted distance to the target as the transducers are moved. The predicted distance is calculated by finding the shortest distance to the target at each interval. This plot is shown in Figure 4.49, where the red line represents the profile of target, the green line is the predicted distance and the blue line is the distance measured to the target at each interval. The

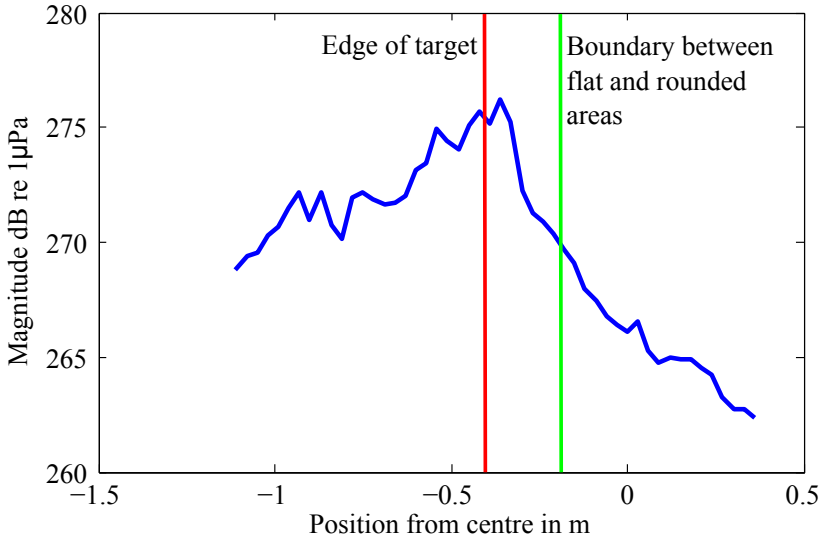

Figure 4.48 – Amplitudes of reflections from target when both transducers are moved together (Test 11).

predicted distance is generated using the premise that the beam-width is infinite, which is not the case. This explains why the measured distance does not match the predicted distance further than 0.6m from the centre, because the point on the target that the reflection is predicted to come from is no longer within the insonified region.

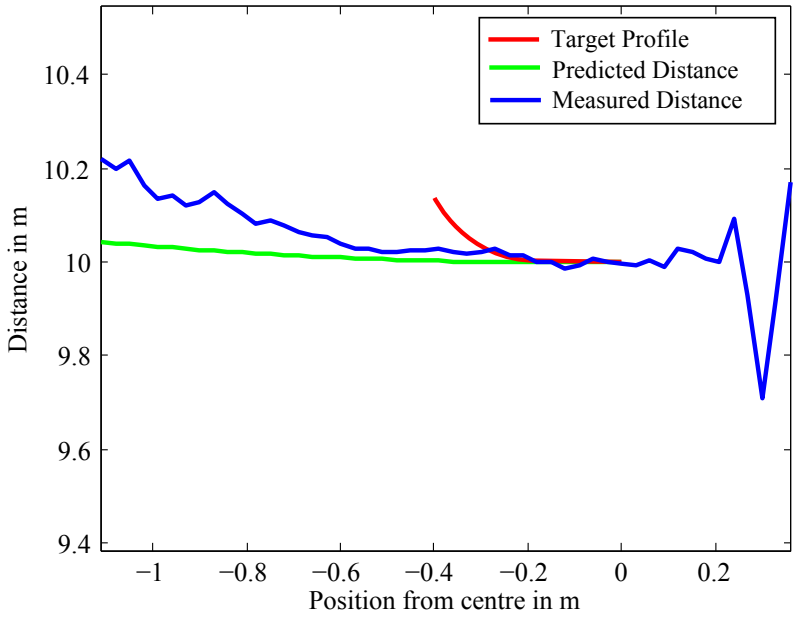

Figure 4.49 – Predicted nearest distance vs. physical profile vs. measured distance.

The concept of the closest point to the transducers is illustrated in Figure 4.50, where the shortest distances (R1 to Rn) for the different locations of the transducers (L1 to Ln) are shown. If the transducers are to the left of the boundary point, the shortest distance to the target will be the boundary point, as long as that point is in the insonified region. The boundary point is the point on the boundary between the flat and rounded areas of the target.

The insonified region for each transducer location is portrayed in Figure 4.50 by the coloured areas. This is a portrayal of the ideal case, where the sound "beam" is a perfect cone. In the case where the boundary point falls outside the insonified region, another point will be closer to the transducers. While the transducers are in line with the flat part of the target, the closest distance will simply be the perpendicular line between the target and the transducers.

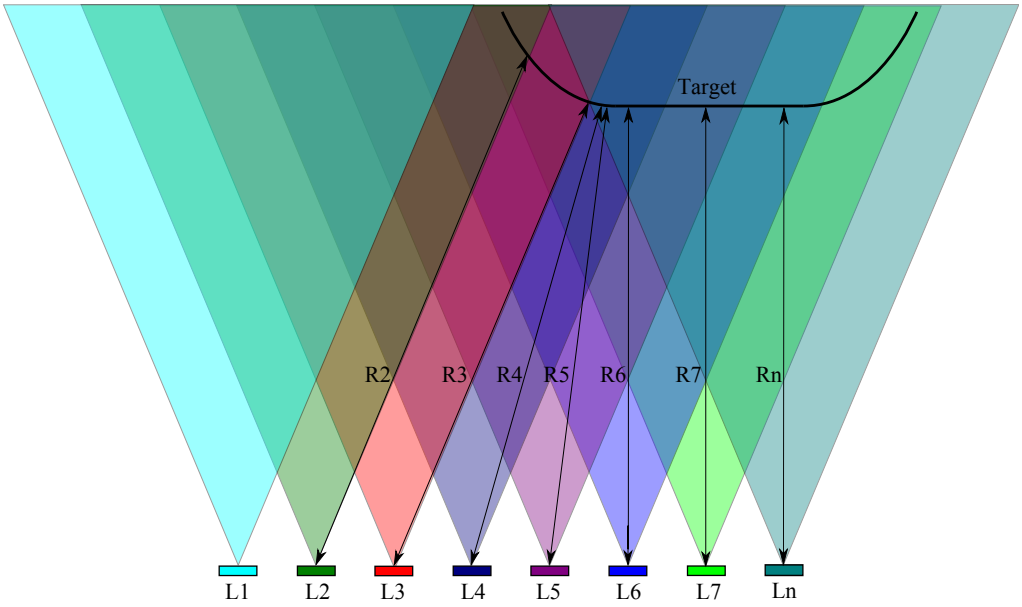

Figure 4.50 – The insonified region changes as transducers are moved. The shortest distance to the target (R1 to Rn) is shown at different locations of the transducers (L1 to Ln).

Figure 4.51 shows the comparison between the distances measured to a flat target (as used previously: 750mm x 430mm) and the rounded target. They are nearly the same size horizontally (750mm and 780mm), but this plot shows that it is possible to see they are different in shape. The distance measured to the rounded target stays more or less the same (as the transducers move away from the centre) until the transducers are in line with the edge of the plate at 0.18m to the left of the centre. This point is the boundary point between the flat and rounded areas of the target, as seen in Figure 4.44. Once the transducers move to the left of this point, all the reflections will come from that point (as discussed previously). At this point the distance measured starts increasing (as predicted), while it stays constant for the case of the flat target. The distance measured to the flat target only starts increasing once the transducers move past its edge.

The reflections from the target when the transducers are 60mm and further to the right of the centre of the rounded plate are not trustworthy. They are of such a small amplitude that they cannot be distinguished above the noise, as can also be seen in Figure 4.48, where the amplitudes become very small to the right of about 60mm from centre.

The distance measured to the rounded target varies more than expected between intervals and can appear “choppy”. This is due to the rough surface of the target. Figure 4.52 shows what the reflections from the rounded target look like (using a matched filter) when the transducers are 810mm from the centre of the target. There are several reflections that can be seen above the noise, and this is due to the sound wave scattering caused by the rough surface. If the surface is

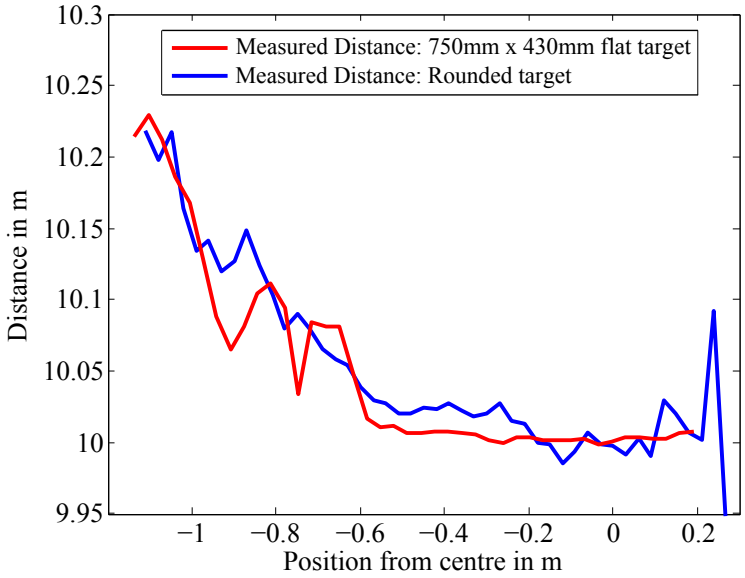

Figure 4.51 – Comparison of distances measured to both targets: 750mm x 740mm flat target and rounded target.

uniform, there is only one clear reflection and perhaps one or more multi-path reflections, such as in Figure 4.45. In the case of Figure 4.52 the reflections are closely spaced, which means they are from different areas on the target.

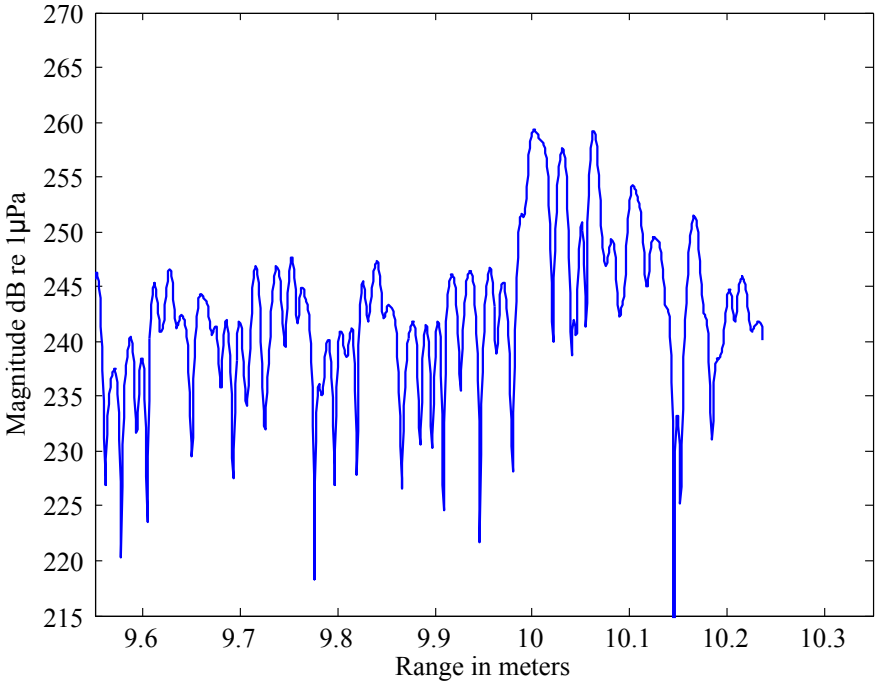

Figure 4.52 – Result of SONAR data from rounded target at 10m processed using a matched filter. Transducers placed 810mm to the left of the centre of the target (Test 11).

The measured distance in Figure 4.49 is generated by taking the range of the reflection with the largest amplitude at each interval, such as in Figure 4.52. The rough surface causes many reflections, which means that the largest reflection at each interval might come from a different area of the plate causing the range to differ slightly. This explains why the data varies between intervals as it does in Figure 4.51.

These results show that, if it is possible to first determine the estimated size of object in the horizontal plane, it will be possible to determine whether the object is flat or rounded. The problem lies with estimating the object's size. The methods for estimating the size of a target, discussed in Part 3 of this thesis, are only applicable to flat targets, with the exception of perhaps the rotational scanning method, which is not very accurate.

If the sizes of the objects were unknown for the case of Figure 4.51, it will not be possible to say which is the flat target and which is the rounded target. The distance plot of the rounded target could be representative of a flat target that is as wide as the flat section of the rounded target.

4.5.2.2 Target Profile Estimation

This section discusses whether it is possible to estimate the profile of the target in Figure 4.44 if it is already known that it is not a flat target. In order to determine the profile, points along the profile need to be collected, and then a line can be interpolated between these points. The easiest way to do this is to gather the locations of two points; the boundary between the rounded edge and the flat surface, and the edge of the target. If the locations of these points are known, a straight line connecting them will give a rough estimate of the profile. This idea is illustrated in Figure 4.53.

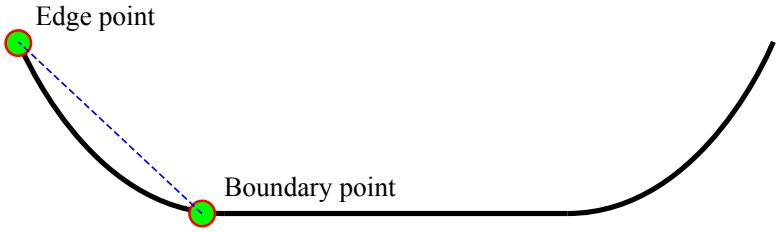

Figure 4.53 – Interpolation between two points to describe target profile.

The location of the boundary point has already been determined previously to be at 0.18m to the left of the centre, which is very accurate. Figure 4.54 shows the location of the boundary point, where the distance measured starts increasing as the transducers move away from the centre of the target.

The edge of the target needs to be located as well. There is however, no real way of determining this edge with reliable accuracy. Due to the width of the SONAR "beam" and its side lobes, there is no way to tell whether a reflection received is from the edge. The argument used previously that states that the reflection received should be from the point on the target closest to the transducers, is not applicable, because the edge is never the point closest to the transducers. The curved nature of the target means that there is always another point closer to the transducers.

Figure 4.55 shows a 3D plot of the SONAR data from Test 11 (see Appendix A), where the rounded target is used. It is the same data that is used to generate Figure 4.49. The plot shows that the data is very "choppy", which is to be expected from SONAR data because of the treacherous underwater environment. It can also be expected because of the rough surface of the target that causes multiple reflections (as mentioned previously). The "ridge" formed by the reflections from the sand-covered target can clearly be seen. As expected, there are many different peaks at each interval, as also shown by Figure 4.52.

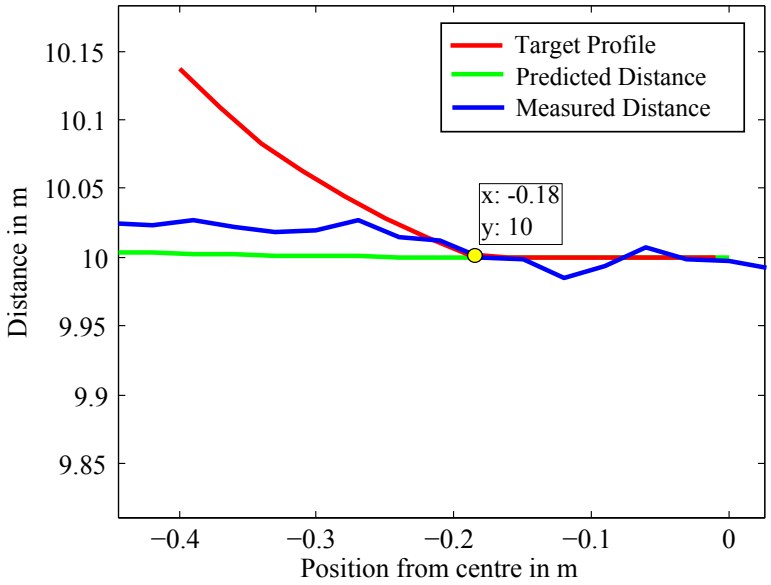

Figure 4.54 – Predicted nearest distance vs. physical profile vs. measured distance.

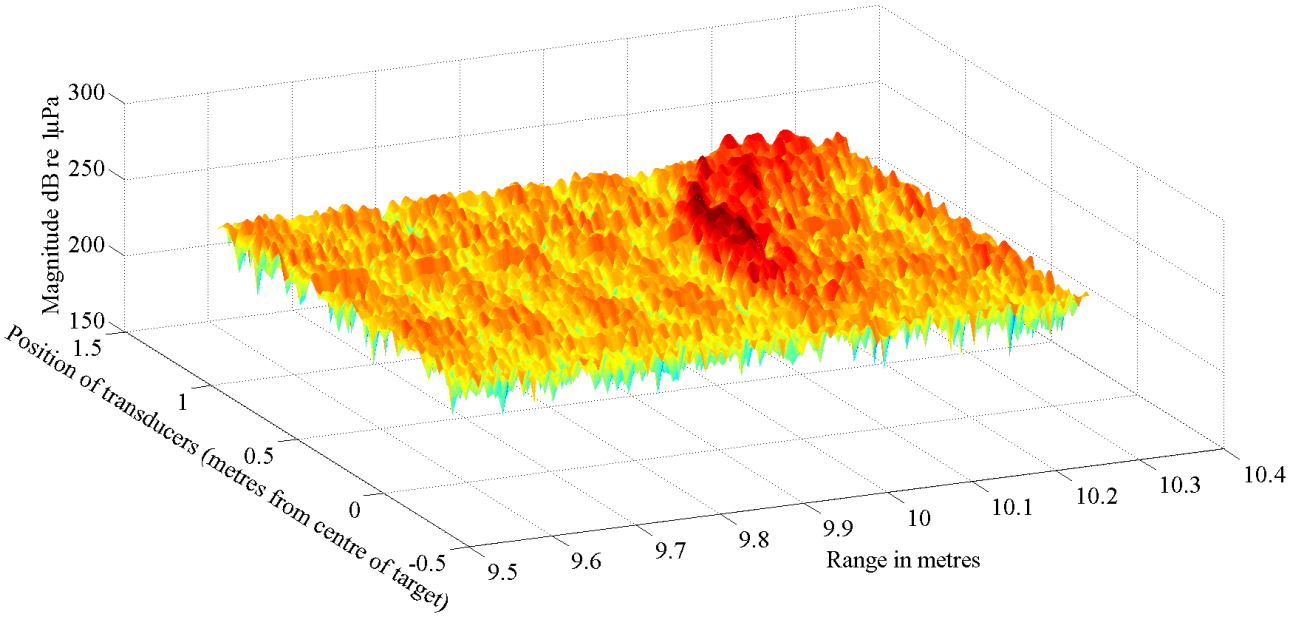

Figure 4.55 – 3D plot of SONAR data from rounded target (Test 11).

The same plot, when filtered using DWT techniques, is shown in Figure 4.56. Here the ridge can be seen much more clearly. When compared to the plot of the distance of the reflections (Figure 4.49), it can be seen that the measured distance follows the crest of the ridge in Figure 4.56. It should be noted that this ridge does not look like the actual target. Rather, it only represents the distance measured to the target at each interval. The reflection received does not necessarily come from straight in front of the transducers due to the wide beam-width, but rather from the point on the target closest to the transducers.

Again, this data does not allow for the estimation of the profile of the target. The beam-spread of the transducers is too wide.

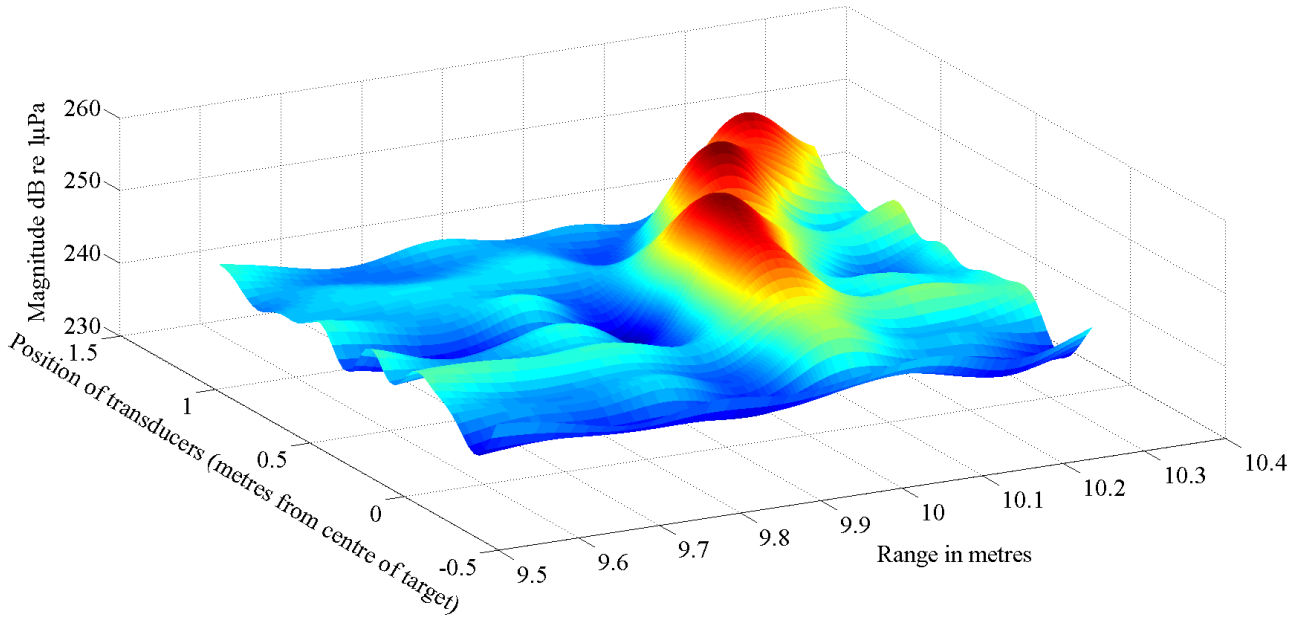

Figure 4.56 – 3D plot of filtered (DWT) SONAR data from rounded target (Test 11).

4.5.3 Conclusion of Part 4

This part of the work shows that it is only possible to differentiate between flat objects under water and objects that have depth and rounded edges if the horizontal size of the target is known. Determining the profile of a target with a rounded edge was not possible, but could be a viable avenue for future work.

4.6 Summary of Work Done and Results Achieved

The work done for Chapter 4 was broken down into four parts, and the results of each of the parts are discussed here. This section also attempts to link the tests and measurements done in this chapter to the real world, to see how feasible the methods and techniques are for use on an actual AUV.

4.6.1 Part 1

In Part 1, the goal was to recreate the results achieved in the previous work done on this project [4]. The results of Part 1 can be summarised as follows:

- Spherical target located at 10m range, and
- Rectangular plates of various sizes located at 10m range.

The work done in Part 1 shows that the SONAR platform can detect targets and accurately determine the range to the targets. It also shows that spherical targets are very hard to detect due to the small amplitude of the reflections from a sphere. Flat targets are much easier to detect, and thus their range can be determined accurately. If this SONAR system is placed on an AUV, it would allow for accurate target detection and ranging.

4.6.2 Part 2

The goal of Part 2 of this project was to determine the location of the centroid of an object under water in the horizontal plane. Two main methods were used, namely **rotational scanning** and the use of **multiple receivers**. The positive results for both of these methods can be summarised as follows:

Rotational Scanning:

- Target at 3.5° to the normal line detected to be at 3.65°.

Multiple Receivers:

- Target at 4.65° to the normal line was detected to be at 4.59°, and
- Target at 1.22° to the normal line was detected to be at 2.1°.

These results are relatively accurate, and show that the techniques used allow for the location of targets with an error much smaller than the beam-width. For the case of rotational scanning, the error is only 0.147°, which is 2.45% of the beam-width. When using multiple receivers, the error was 1% of the beam-width in one test, and 14.66% in another test. These errors are small relative to the beam-width, and show that an error much smaller than the beam-width can be achieved.

It is also mentioned that the rotational scanning method should be used for larger targets where the centroid needs to be determined, while the method using multiple receivers should be used for smaller targets. The difference between large and small targets as used in this context is

thoroughly discussed in Section 4.3.3. To summarise, any target larger than 0.5 times the beam-width at the range the target is found is considered to be a large target, while any target smaller than 0.5 times the beam-width is considered a small target.

It is also noted that the method of using multiple receivers could be improved by using more than just two receiving transducers. The data from the receiver that detects the strongest reflection should then be used to calculate the location of the target.

Implementing the rotational scanning method on an AUV poses a problem. The AUV needs to be moving, and thus the scanning process needs to happen very quickly. For example, scanning the $60°$ area in front of the AUV in $1.2°$ increments (as done in Part 2) with a maximum range of 20m (as shown by Figure 4.1, will take a minimum of 1.36 seconds. This is calculated using a sound velocity of $c = 1470$ m/s. If the AUV is moving at a speed of 1 m/s [5], it will move 1.36m while it scans the area once. This scanning time does not even take into consideration the time it takes for the sound waves to dissipate between increments.

Therefore, the scanning process needs to be fast relative to the velocity of the craft if this SONAR system is to be implemented on an AUV, especially if the target is relatively close. The time taken by the process can be reduced by increasing the step size, as discussed in Section 4.3.2.1. Increasing the step size from $1.2°$ to $3.6°$ allows for the process to occur three times faster, but it reduces the accuracy of the location of the centroid. The error in the determination of the centroid increases from 1.35% to 14.59%. Another option is to keep the AUV stationary during the scanning process, but this unrealistic.

The results from Part 2 show that it is possible to locate the centroid of a target with an error much smaller than the beam-width.

4.6.3 Part 3

Part 3 was concerned with developing techniques that can be used to find the edge of a flat target. The techniques that were used and the success achieved for each is as follows:

Rotational Scanning:

- Edge detected 0.625m from the actual location.

Lateral Scanning:

- Edge detected 0.175m from the actual location.

Both of these methods involved different methods of data analysis, as has been discussed in Section 4.4.

At a range of 10m, the rotational scanning method achieved an error of 60% of the beam-width. For the lateral scanning method, the error is 16.7% of the beam-width, which is much more accurate. These results show that an error smaller than the beam-width is achievable.

Section 4.4.3 discusses simulations that were done in order to understand unexpected behaviour encountered during the analysis of the data from using the lateral scanning method. It has been proven that small, irregularly reflected sound waves can and do interfere with the wave that is

to be received, causing the amplitude of the wave to be much lower than expected. In fact, this lead to the development of a method used to estimate the location of the edge of the target.

As mentioned before, the rotational scanning method will place a limitation on the velocity of the craft. Lateral scanning will have the same effect. Another problem is that this method, as used during the course of this project, cannot realistically be implemented on an AUV with the dimensions shown in Figure 4.1. A smaller scale version of the method can be used, but it can be assumed to be less accurate when it comes to edge location.

The methods developed for Part 3 allow for relatively accurate edge location, but it will be difficult to implement these methods on an AUV.

4.6.4 Part 4

The goal of Part 4 was to enable the user to differentiate between a flat object with the well defined edge and an object that has depth, or a rounded edge. The results of the work done for Part 4 showed that it is only possible to differentiate between a flat target and a rounded target if the horizontal sizes of both the targets are known. The wide beam-spread of the transducers does not allow for the estimation of the profile of a rounded target either.

In order to achieve the goal for Part 4, transducers with a narrower beam will be needed. This can be considered an avenue for future research.

Chapter 5

Conclusion

5.1 Final Conclusion

During the course of this project new data gathering and data analysis techniques have been developed that can be used to detect, locate and find the dimensions/limits of objects under water using wide-beam (wide-angle) SONAR transducers.

The long-term plan for this project is to develop a system that can be implemented on an actual AUV. Such a system will probably make use of different hardware and better transducers, but the techniques developed in this project can then be applied to improve the results of better hardware even further.

To summarise, the goal for this project is to develop methods and techniques that make use of the existing SONAR laboratory platform and existing wide-beam SONAR transducers to **detect** and **locate** objects, their **edges** and the **range** to the objects in water in the horizontal plane.

The goal also makes mention of using wide-beam SONAR transducers. The transducers used in this project have a relatively wide beam of $\pm 6^{\circ}$, and all of the tests done during this project were done using these transducers. The methods developed can then also be applied to transducers with a narrower beam to achieve even better results.

The success achieved for each of the key points mentioned above will now be discussed.

Target Detection and Ranging

Part 1 was concerned with the detection of targets and determining their range, and this was done to verify that the previous work done on this project [4] can be recreated. Different targets were detected at different ranges with a good range accuracy.

Target Location

Part 2 was focussed on locating and object or an object's centroid in the horizontal plane. The results show that it is possible to determine the location of the centroid of a target with an error much smaller than the beam-width of the transducers. Two methods were applied; rotational scanning and using multiple receivers. When using the rotational scanning method, the maximum error that can be expected is 2.45% of the beam-width (if there is no user error

in the setup of the equipment). When using multiple receivers, the maximum expected error is 14.66% of the beam-width.

Target Edge Location

The last part of the goal was to determine the location of the edge of a target. Two methods were used to do so; rotational scanning and lateral scanning. The results show that the use of rotational scanning does not deliver results with an acceptable error. When using lateral scanning however, the edge of a flat target can be located with an error of 16.7% of the beam-width at a range of 10m.

All of the work mentioned above made use of flat targets with well-defined edges, which is a good approximation for a harbour environment where the walls of the harbour and even the hulls of ships can be seen as flat. There are however, targets under water that are not flat, but rather have depth and rounded edges. The last part of the work done was focussed on finding the bounds/limits of a target with rounded edges, as well as attempting to determine the profile of the target. The results show that is not possible to do so with the available transducers. Transducers with a much narrower beam-width will have to be used.

The techniques and methods that have been developed and tested allow for wide-beam SONAR transducers to be used for target detection, target ranging, target location and target edge location with an error that is much smaller than the width of the SONAR beam.

5.2 Strategy for Future Work

The results from the four different parts need be combined to form a strategy that can be used to locate objects and their edges. A possible strategy to follow can be summarised as follows:

1. A target and the range to the target is detected using the work done in Part 1. A general idea of the location of the target is known because the beam-width of the transducers is known.
2. Multiple receivers can be used to quickly get a more accurate location of the target.
3. The rotational scanning approach may be used to determine a rough estimate of the size of the target as well as the location of its centroid.
4. If the target is small, further data gathering is unnecessary, because its location is already known.
5. If the target is large, determine the location of its edges using lateral scanning.

If this system is to be implemented on an AUV, the craft will have to be stationary (or moving very slowly) if the lateral scanning or rotational scanning methods are to be used. What also can be done is to increase the step size of rotational scanning method. This will reduce the time taken by the scanning process, but also reduces the accuracy.

Another issue with the strategy discussed above, is that the lateral scanning method, as used during the course of this project, cannot realistically be implemented on an AUV with the dimensions shown in Figure 4.1. A smaller scale version of the method could be used, but it can be assumed to be less accurate when it comes to edge location.

The work done also shows that the underwater environment is treacherous and that it can produce results that are unexpected. The raw data that is received and stored must be processed using a range of techniques before any useful information can be extracted from it. The effects of multi-path reflections can also affect results immensely. All of these factors need to be taken into account when making use of SONAR for underwater object detection and location.

If the profile of a target that has depth and rounded edges needs to be determined, transducers with a narrower beam will need to be used. It is not possible to do so with the existing SONAR system.

Appendix A

Tests

A.1 Overview

The tests that were done during the course of this project as well as their results are referred to frequently in Section 4. This section discusses the testing environment that was used and each of the tests that were done.

A.2 Testing Environment

All of the tests and experiments discussed in this section were done at the towing tank of the Mechanical and Mechatronic Engineering Department of Stellenbosch University. This concrete water tank is 88m in length, 4.5m in width and 3.5m deep.

The sonar equipment is always set up on the wave-generator end of the towing tank, and the transducers are placed in the water using different methods to suit the requirements of each test, as will be discussed separately for each test. Targets are hung in the water using a sturdy PVC pipe that is placed across the tank, and distances are measured using a LASER range finder that is accurate to within 1mm. The range finder is also used to find angles using trigonometric approaches.

A laptop is used to control the SONAR equipment, as well as to retrieve and store captured data from the FIFO. This data is then later analysed using *Matlab* techniques. Power supplies are used to power the equipment. This includes the 12V DC, 15V DC and 60V DC needed for the development boards, amps and filters, as discussed in Section 2.2.6.

Figure A.1, Figure A.2 and Figure A.3 below illustrate some of the concepts discussed above. Figure A.4 shows the bracket that houses the transducers.

Figure A.1 – The laptop, power supplies and SONAR equipment set up at the towing tank.

Figure A.2 – Transducers hanging in the water.

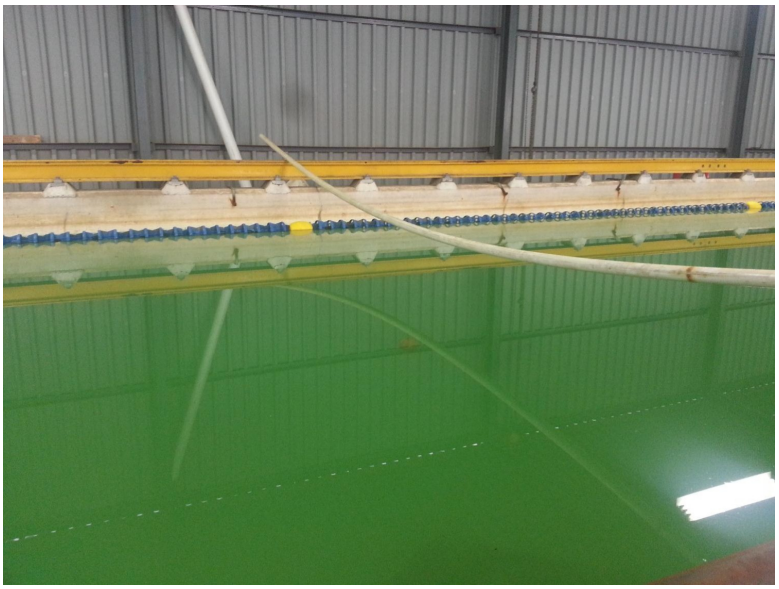

Figure A.3 – The PCV pipe used to hang targets in the water.

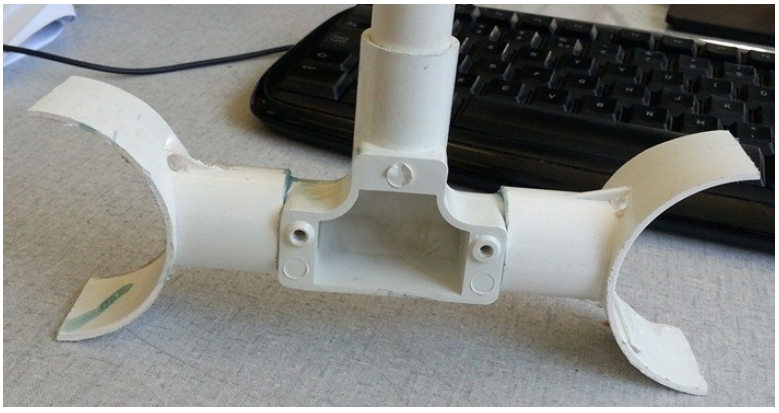

Figure A.4 – The bracket used to house the transducers.

A.3 Discussion of Tests

Each if the tests will be broken down and discussed in the following criteria:

- Goals of the Test
- Test Setup
- Tests Done

The results of the tests are not discussed here, since they are discussed in detail in Chapter 4.

A.3.1 Test 1

Goals of the Test

The main goal of Test 1 is to check whether the SONAR system worked well after all the code on the PIC had been rewritten. It allowed for more frequencies and pulse lengths, and these options has to be tested. Thus the system is tested to see whether results comparable to those in the previous work done [4] could be achieved using the same signal types and frequencies, and pulses of different frequencies and lengths are also tested to see whether the system would cope.

Test Setup

In this test, the transducers are hung from a beam across the water tank using PVC piping, and kept stationary at a depth of 1m, facing toward the other end of the tank. The targets are hung in the middle of the width of the tank, at different distances from the transducers. The target used is a spherical lead sinker, 10mm in diameter. The voltage supply of the main amp is set to 40V.

Tests Done

The following tests are done three separate times, with the target placed at 25m, 50m and 70m from the transducers:

1. Original PIC code: CF wave, 330 kHz (100 ms length),
2. Original PIC code: LFM chirp up, 230 kHz - 330 kHz (100 ms length),
3. Original PIC code: LFM chirp up and down, 230 kHz - 330 kHz (100 ms length),
4. New PIC code: CF wave, 230kHz (100 ms length),
5. New PIC code: CF wave, 280kHz (100 ms length),
6. New PIC code: CF wave, 330kHz (100 ms length),
7. New PIC code: CF wave, 350kHz (100 ms length),
8. New PIC code: CF wave, 380kHz (100 ms length),
9. New PIC code: CF wave, 280kHz (150 ms length),
10. New PIC code: CF wave, 330kHz (150 ms length),
11. New PIC code: CF wave, 350kHz (150 ms length),
12. New PIC code: CF wave, 380kHz (150 ms length),
13. New PIC code: LFM wave, 230 kHz - 330 kHz (100 ms length),
14. New PIC code: LFM wave, 280 kHz - 380 kHz (100 ms length),
15. New PIC code: LFM wave, 230 kHz - 330 kHz (150 ms length), and
16. New PIC code: LFM wave, 280 kHz - 380 kHz (150 ms length).

A.3.2 Test 2

Goals of the Test

The goal of this test is to see whether powering the main amp with a higher voltage would enable the detection of a spherical target 40mm in diameter.

Test Setup

This test is done using the exact same setup as in test 1, but the main amp is powered using 50V instead of 40V, and the target is 40mm in diameter. The ball is hung in the water using a net.

Tests Done

The following tests are each done six separate times, with the target placed at 5m, 10m, 15m, 20m, 30m and 40m from the transducers:

1. Original PIC code: CF wave, 330 kHz (100 ms length),
2. Original PIC code: LFM chirp up, 230 kHz - 330 kHz (100 ms length,
3. New PIC code: CF wave, 230kHz (100 ms length),
4. New PIC code: CF wave, 280kHz (100 ms length),
5. New PIC code: CF wave, 330kHz (100 ms length),
6. New PIC code: LFM wave, 230 kHz - 330 kHz (100 ms length), and
7. New PIC code: LFM wave, 280 kHz - 380 kHz (100 ms length).

A.3.3 Test 3

Goals of the Test

In this test, the goal is to see whether the net used to hang the 40mm target sphere in the previous test affected the results negatively.

Test Setup

The setup is exactly the same as in Test 2, but the target is hung by gluing a thin piece of rope to the target. The main amp voltage is set to 50V.

Tests Done

The following tests are done five separate times, with the target placed at 5m, 10m, 20m, 30m and 40m from the transducers:

1. Original PIC code: LFM chirp up, 230 kHz - 330 kHz (100 ms length),
2. New PIC code: LFM wave, 230 kHz - 330 kHz (100 ms length), and
3. New PIC code: LFM wave, 280 kHz - 380 kHz (100 ms length).

A.3.4 Test 4

Goals of the Test

The goal of this test is simply to detect a target. Thus a wide range of targets are used and placed at several different distances.

Test Setup

The general setup in Test 4 is the same as before, but as mentioned, more targets are used. Two different aluminium plates are used as well as the 40mm sphere used in previous tests. The plates have sizes of 90mm x 90mm x 7mm and 140mm x 180mm x 1mm. Each of these are tested individually, i.e., only one target was in the water at a time.

The voltage supply of the main amp is set to 60V, which is the maximum that can be supplied by the power supply available. The amp is designed for up to 80V.

Tests Done

The following tests are done using each of the targets mentioned above at 5m, 10m, 20m, 30m and 40m distances:

1. New PIC code: LFM wave, 230 kHz - 330 kHz (100 ms length).
2. New PIC code: LFM wave, 280 kHz - 380 kHz (100 ms length).

A.3.5 Test 5

Goals of the Test

In this test the goal is to detect a toilet float ball. The purpose of this is to see whether a spherical object could be detected, as attempted in previous tests with smaller spheres.

Test Setup

The basic setup is the same as in previous tests, but the target used is a toilet float ball with a 110mm diameter, filled with sand so that it would sink.

Tests Done

A 230 kHz - 330 kHz LFM chirp test is done with the target at 5m, 10m, 15m, 20m, 30m and 40m.

A.3.6 Test 6

Goals of the Test

This is the first test in which the transducers were moved. One of the goals is to see whether the location of an object, and perhaps where its limits are in the horizontal plane, could be determined. Another goal is to check whether the stepper motor configuration works acceptably. The stepper motor setup is discussed in Section 3.2.2.

Test Setup

The target used in this test is the 90mm x 90mm x 7mm aluminium plate that was used in previous tests. It is placed in the water, 17m from the transducers, at at an angle of $3.5°$ to the left of the normal line. The transducers are connected to the stepper motor (as discussed above) and are rotated through $40.8°$. Figure A.5 below is a simple diagrammatic representation of what the setup looks like.

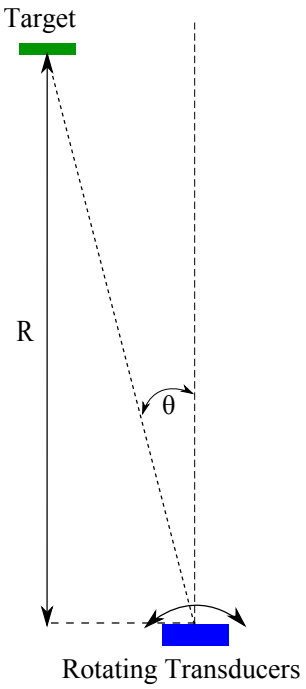

Figure A.5 – Test Setup for Test 6.

Tests Done

The transducers are rotated through $40.8°$ in steps of $1.2°$, starting from $20.4°$ to the right of centre. At each step the 230 kHz - 330 kHz LFM chirp test is done 10 times to ensure that the possibility of an incorrect result is eliminated. The target is left in the same location for the entire duration of the test.

A.3.7 Test 7

Goals of the Test

In this test, the goal is to see whether the accuracy of the detection of a target's edges, as found in Test 6, could be improved on if the target is much larger and smaller angular steps are taken.

Test Setup

The same stepper motor setup is used as in Test 6, but the Arduino board is programmed such that the stepper motor would rotate only $0.6°$ with each step. The target used is an Aluminium plate of dimensions 750mm x 430mm x 1.5mm, and was placed 10m from the transducers, exactly in the centre of the width of the water tank.

Tests Done

The 230 kHz - 330 kHz LFM chirp is used once again, and the transducers are scanned from 21° right of centre to 21° left of centre. At each step, the same test is done 10 times.

A.3.8 Test 8

Goals of the Test

This is the first test in which the pulley system discussed in Section 3.2.3 is used, and the goals are to test whether the pulley system works and to determine whether the edge detection results from test 7 could be improved upon by using a new method of scanning.

Test Setup

The same Aluminium plate (750mm x 430mm x 1.5mm) is used at a range of 10m, but the transducers are attached to the pulley system that allows them to be moved laterally across the width of the tank. The distance they are shifted by is monitored using a LASER range finder.

Tests Done

Two different sets of tests are done with the target placed at 10m from the transducers. In one set of tests, both the R_X and T_X transducers are shifted together, starting 1.11m to the left of the centre of the plate and ending 0.15m to the right of the centre of the plate. The transducers are shifted by increments of 30mm at a time, and the 230 kHz - 330 kHz LFM chirp test is done 10 times at each increment.

In the other set of tests the exact same process is followed, but the R_X transducer is stationary in line with the centre of the plate.

In both these cases, only the one side of the target is scanned, since the same results are to be expected on the other side.

A.3.9 Test 9

Goals of the Test

The goal of this test is to ascertain whether a target's location can successfully be determined by using two separate R_X transducers and one T_X transducer.

Test Setup

The test setup is the same as the default setup, where the T_X and R_X transducers are placed closely together at a depth 1.5m, and an extra R_X transducer is placed at a distance T from the other transducers. In this test, the transducers were placed 1.4m apart. The target used is the small aluminium plate, as used in previous tests, and it is placed at a range of 10m from the transducers at different angles (θ) from the normal line. Figure A.6 shows a visual representation of this setup. Once again, the distances and angles are determined using a highly accurate LASER range finder.

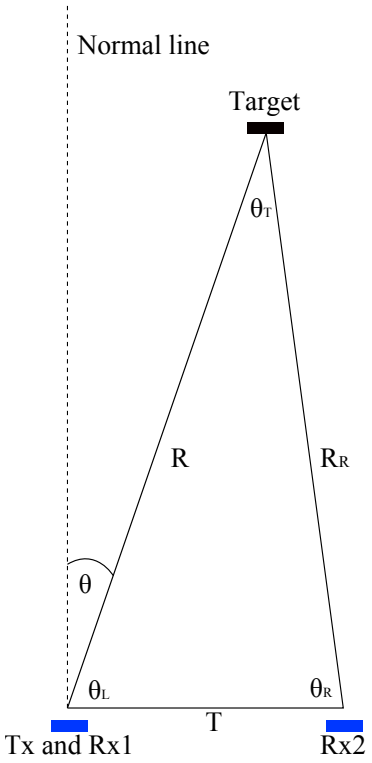

Figure A.6 – Setup of Test 9 using an extra receiving transducer.

Tests Done

The target is placed at two different angles to the normal line ($4.65°$ and $1.22°$), and in each case the 230 kHz - 330 kHz LFM chirp test is done 10 times. The data from both receivers is captured and stored.

A.3.10 Test 10

Goals of the Test

The goal of this test is twofold. The first goal is to determine whether the results from Test 8 with the 750mm x 430mm x 1.5mm metal plate could be reproduced. The second goal is to see whether wide-beam transducers could be used to find the outline of non-2D objects.

Test Setup

In the first part of this test, the test setup is the same as in Test 8, where the R_X transducer is kept in line with the centre of the target, and the T_X transducer is moved using the pulley system. The target is placed at a range of 10m from the transducers, and the transducer is moved in 30mm increments. The only difference between Test 8 and Test 10 is that the voltage supply of the main amplifier is set to 60V in this test, whereas in Test 8 it was set to 50V.

The second part of the test is the same as the first part, but involves using the lateral scanning method with the rounded plate (depicted in Figure 4.44) as a target. Both transducers were moved together.

Tests Done

At each increment, the 230 kHz - 330 kHz LFM chirp test is done 10 times, starting at 1.11m to the left of centre and finishing at 0.21m to the right of the centre of the plate. This is done for both sets of tests.

A.3.11 Test 11

Goals of the Test

The goal of this test is to check whether better data could be gathered using the rounded plate that is used in Test 10. The plate is covered in glue and sand to make the surface of the plate rough, which will reflect sound in more directions. The reasoning behind this is that, due to the fact that the surface of the plate is smooth and uniform, the rounded areas of the plate reflect sound away from the transducers and cause large amounts of multi-path reflections. If the surface of the plate rather scattered sound in more directions, it is possible that waves could reflect from the rounded areas back to the transducers.

Thus the goal is to determine whether better data could be gathered from the round plate so as to enable the user to differentiate between a flat target and one that has rounded edges and some depth to it.

Test Setup

The plate that has been covered in sand is placed at a range of 10m from the transducers, and the lateral scanning method is used with the transducers moved together.

Tests Done

At each increment, the 230 kHz - 330 kHz LFM chirp test is done 10 times, starting at 1.11m to the left of centre and finishing at 0.36m to the right of the centre of the plate.

Appendix B

User Manual

B.1 Overview

The hardware that was built by Konrad Friedrich has been left mostly unchanged, thus only the use of the new pieces of hardware, as discussed in Section 3, will be explained. The user manual for the hardware that was built by Konrad Friedrich can be found in Appendix B of his thesis [4].

The software has changed, since new code was written for the PIC and new *Matlab* scripts were written to process the data. The use of each of these will be discussed.

B.2 Hardware Setup

As stated above, only the use of new hardware that was constructed will be discussed. These are the DDS signal splitter and the stepper motor setup. The pulley system will not be discussed, as it is quite easy to use.

B.2.1 DDS Signal Splitter

The output from the DDS is attached to the connector labelled "DDS", and the two output connectors are also labelled appropriately. The one output needs to be connected to the pre-amplifier, and the other to the ADC. Unfortunately there is an issue with setting up the ADC and FIFO to store two separate sets of data concurrently. Due to time limitations this was not investigated in great detail, and only one of the channels of the ADC was used in this project.

B.2.2 Arduino Stepper Motor Setup

In order to use the stepper motor setup, the Aduino board and the Arduino motor shield need to be connected, the switches need to be connected to the motor shield, and the motor should be connected to the motor shield. The motor shield also needs to be connected to a 12V supply.

One of the switches is a toggle switch. It is connected to pin 4 on the motor shield, and switches between 0V and 5V. The Arduino chip has been programmed such that pin 4 determines the direction in which the motor turns. The other switch is a variant of a push-button switch and is connected to pin 2 on the motor shield. The program is written such that the stepper motor will step through a user determined angle each time this button is triggered. The angle through

which the motor steps is specified in the Arduino code. The two switches are pictured in Figure B.1.

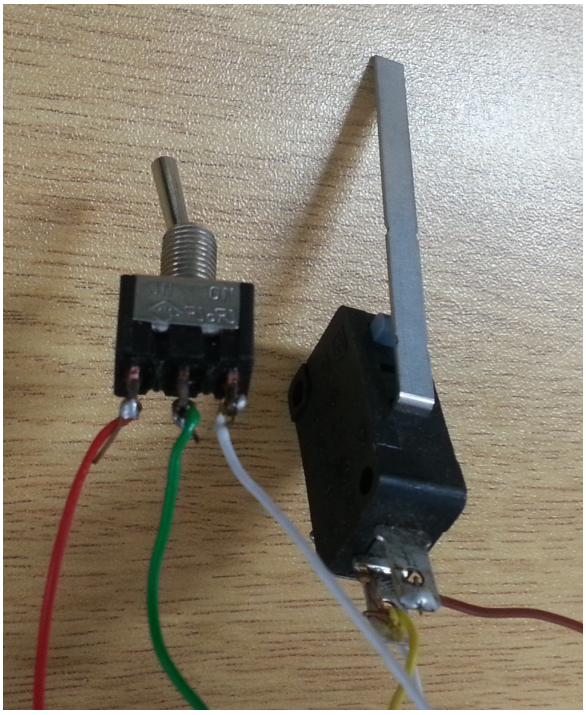

Figure B.1 – Toggle switch (left) and push button switch (right) used for the stepper motor.

A connector was made that connects the stepper motor's shaft to a PVC pipe. It fastens onto the shaft using a grub screw. The transducers can then be attached to the PVC pipe. The stepper motor connects to the motor shield using a 4-wire ribbon cable as shown in Figure B.2.

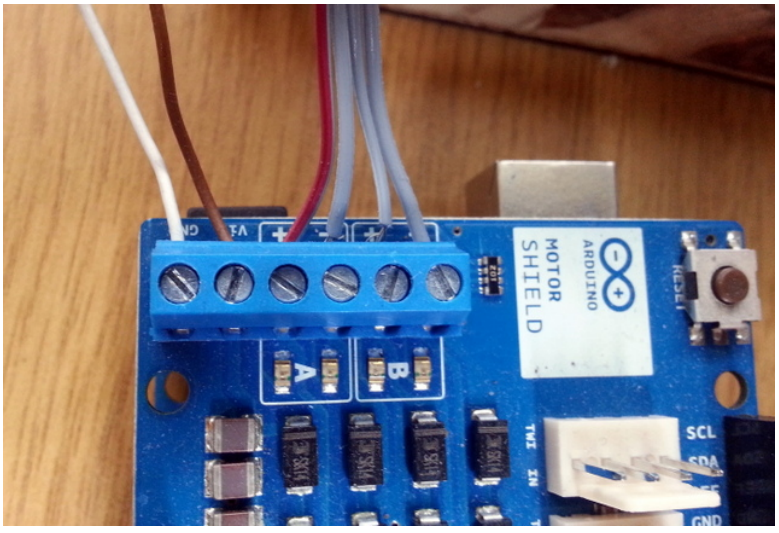

Figure B.2 – Motor connection to Arduino motor shield.

B.3 Software Setup

The following software needs to be installed on a PC in order to use the SONAR system:

- *Terminal v1.9b*.
- *ADC Analyzer* from Analog Devices.
- *Matlab*.

Terminal v1.9b is used to communicate with the PIC, *ADC Analyzer* is used to begin the data capturing process and get the data from the FIFO, and Matlab is used to process the data. The use of each of these will now be discussed.

B.3.1 Terminal

Terminal is used to give commands to the PIC which in turn programs the DDS to create the signal the user specifies. Once the PIC is powered and connected to the PC using a serial to USB converter, *Terminal* can connect to communicate with the PIC. The PIC code has been rewritten to make it a more user-friendly experience and to give the user more options in terms of signal frequency and length.

A good way to check whether the PIC is connected and the correct COM port is selected, is to reset the DDS by sending an 'r' character. The following will be received if the command is received by the pic: *! DDS has been reset!*

If the DDS has been reset, it can be set up to generate one of the following types of signals by sending the applicable character:

- Constant Frequency Pulse: Send "C".
- LFM up-chirp: Send "L".
- LFM up-chirp and down-chirp: Send "L".

Once one of these characters is sent, the PIC will reply with further instructions that are easy to follow. It is important to note that when the user is asked for the signal frequency or signal length, a length or frequency of 3 characters must always be sent, even if it is less than 100. For example, if the user wants a signal with a length of 80ms, the following should be sent: "080".

If an unknown character is sent, a "u" will be received.

B.3.2 ADC Analyser

The use of ADC analyser has not changed during the course of this project. Therefore the instructions found in Section A.3.1 in Konrad Friedrich's thesis [4] are still applicable. The only thing that changes is the centre frequency that the user enters in the Windowing settings. The centre frequency of the wave the user selected in *Terminal* should be entered (in MHz) instead of the 0.28 specified.

So, to summarise, these are the steps to follow with ADC Analyser:

1. Start ADC Analyser.
2. Click "OK" in the "About ADC Analyzer" window.
3. Click on "Configuration".
4. Select the "AD9248.cfg" file.
5. Select "FFT" under the "Config" menu.
   a) Set the number of samples to 262144.
   b) Set the Encode Frequency to 1 MSPS.
   c) Do this for Channel A and Channel B if needed. The rest of the options can be left as default. (Channel A represents Analog Input B on the ADC).
   d) Select "OK".
6. Select "Windowing" under the "Config" menu.
   a) Select "None" and click "OK".
   b) Select "Analog Input Frequency (MHz)".
   c) Enter the centre frequency of the signal chosen in MHz.
   d) Click "Calculate" and the click "OK".
7. To generate the signal, transmit it and capture it, click the "Time Data" button.
8. The data will be displayed. Right-click on the data window and choose the "Export Data" option.
9. Save the data to a file (.csv).

B.3.3 Matlab

Matlab is used to process the data that has been stored by the FIFO. If the raw data is plotted it does not give the user much indication as to where and how far targets are under water. Therefore the data has to be processed using the methods described in Section 2.2.3.

The basic processing method to find the distance to targets has stayed the same, but since new methods of data gathering are used, the data needs to be processed slightly differently. Therefore, the steps to process the data changed with each test.

If a data set is to be processed in order to find the range of underwater targets, the process is simple:

1. Place the .csv file from ADC Analyzer in same the directory as the *Matlab* files.
2. Open the "`Target_Processing_Code`" *Matlab* script.
3. Set the type of the pulse used (for range processing, this should be LFM).
4. Import the replica pulse and the data stored from ADC Analyzer (the "`get_data`" script can be used to do so).

5. Set "`v_tx`" as the imported replica pulse and "`data`" as the received pulse.

6. Run the code.

This should result in different graphs being plotted with the data processed using a few different processing and windowing techniques. The code can be edited to make use of different processing techniques and windowing methods.

Bibliography

[1] Wise, J.: How Air France 447's Missing Wreckage Was Found - and Why It Took So Long. Internet: http://www.popularmechanics.com/technology/engineering/robots/how-air-france-447s-missing-wreckage-was-found-5583302, April 2011. [July 6, 2012].

[2] Jay, F.: *IEEE standard dictonary of electrical and electronic terms*. New York: Institute of Electrical and Electronic Engineers, 1984.

[3] Urban, H.G.: *Handbook of Underwater Acoustic Engineering*. STN Atlas Electronic, 2002.

[4] Friedrich, K.J.: *Development of an active SONAR platform for AUV applications in a closed environment*. Master's thesis, Department of Electrical and Electronic Engineering ,University of Stellenbosch, 2011.

[5] Naval auv product range: The hugin & remus family. Booklet.
Available at: http://www.km.kongsberg.com/ks/web/nokbg0397.nsf/AllWeb/E6A084C5FC13CBA2C125754A0048D4B8/$file/TheHUGINandREMUSFamily_Jan09_lowres.pdf?OpenElement

[6] P450 series. Website.
Available at: http://www.blueview.com/products/2d-imaging-sonar/p450-series/

[7] How does sonar work?
Available at: http://www.exploratorium.edu/theworld/sonar/sonar.html

[8] Unknown: Piezoelectric transducers. Website, .
Available at: http://www.ndt-ed.org/EducationResources/CommunityCollege/Ultrasonics/EquipmentTrans/piezotransducers.htm

[9] Kinsler, L. and Frey, A.: *Fundamentals of acoustics*. Wiley, 1950.
Available at: http://books.google.co.za/books?id=EANRAAAAMAAJ

[10] Unknown: Starfish chirp signal processing. Website: http://www.starfishsonar.com/technology/chirp.htm, July 2012.

[11] Selecting a transducer. Website, 2013.
Available at: http://www.raymarine.com/

[12] Unknown: Accoustics unpacked. Website, .
Available at: http://www.acousticsunpacked.org/acoustics/AcousticBackground/AcousticTransducers.asp

[13] Unknown: Transducer beam spread. Website: http://www.ndt-ed.org/EducationResources/CommunityCollege/Ultrasonics/EquipmentTrans/beamspread.htm, . [July 12, 2012].

[14] Waite, A.: *Sonar for practising engineers*. Wiley, 2002. ISBN 9780471497509.
Available at: http://books.google.co.za/books?id=GXgZAQAAIAAJ

[15] Nave, R.: Sound intensity. Website.
Available at: http://hyperphysics.phy-astr.gsu.edu/hbase/sound/intens.html

[16] Urick, R.: *Principles of underwater sound for engineers*. McGraw-Hill, 1967.
Available at: http://books.google.co.za/books?id=DqERAQAAIAAJ

[17] USNA: Target strength.
Available at: http://usna.edu/Users/physics/ejtuchol/documents/SP411/Chapter17.pdf

[18] V. Pjachev, V.V.: Sonar signal waveform impact on interference resistance. In: *European Signal Processing Conference*. 2008.

[19] Mahafza, B.: *Radar Signal Analysis and Processing Using Matlab*. CRC Press, 2009. ISBN 9781420066432.
Available at: http://books.google.co.uk/books?id=cke5dMO-r_AC

[20] Wilkinson, A.: Signals and systems ii: Matched filter. University Lecture, University of Cape Town.

[21] Sharma, N.: Trading detection for resolution in active sonar receivers: A thesis in electrical engineering. 2010.
Available at: http://books.google.co.za/books?id=wwrqSAAACAAJ

[22] Website, 2012.
Available at: http://www.eaglenav.com/Support/Tips-and-Tutorials/Sonar-Tutorial/

[23] Truax, B.: Handbook for acoustic ecology. Website, 1999.
Available at: http://www.sfu.ca/sonic-studio/handbook/Sound_Propagation.html

[24] Halliday, D. and Resnick, R.: *Fundamentals of Physics*. John Wiley and Sons, Inc, 1970.

[25] Russel, D.: Superposition of waves.
Available at: http://www.acs.psu.edu/drussell/demos/superposition/superposition.html

[26] NOAA: Noaa office of coast survey. Website.
Available at: http://www.nauticalcharts.noaa.gov/csdl/AUV.html

[27] Y. Petillot, I. Ruiz, D.L.: Underwater vehicle obstacle avoidance and path planning using a multi-beam forward looking sonar. *IEEE Journal of Oceanic Engineering*, 2001.

[28] Throner, J.E.: Approaches to sonar beamforming. 1990.

[29] Unknown: Multibeam sonar theory of operation. Tech. Rep., SeaBeam Instruments, 2000.

[30] Vidakovic, B. and Mueller, P.: Wavelets for kids: A tutorial introduction. Duke University.

[31] Klapetek, P.: Wavelet transform. Website, February 2002.
Available at: `http://klapetek.cz/index.html`

[32] Menke, W.: Lecture 19 - the wavelet transform. January 2009.
Available at: `http://www.ldeo.columbia.edu/users/menke/QMDA/`

[33] Akansu, A., Serdijn, W. and Selesnick, I.: Emerging applications of wavelets: A review. *Physical Communication*, 2010.

[34] Vaidyanathan, P.: Quadrature mirror filter banks, m-band extensions and perfect-reconstruction techniques. *IEEE ASSP Magazine*, 1987.

[35] Fugal, D.: *Conceptual Wavelets*. Space & Signals Technical Publishing, 2009.

[36] Arduino. Website.
Available at: `http://www.arduino.cc/`

[37] Fulling motor usa.
Available at: `http://www.fullingmotorusa.com/Pages/default.aspx`

[38] Unknown: Underwater sound propagation. Website, .
Available at: `http://www.arc.id.au/UWAcoustics.html`

[39] Unknown: Website, 2009.
Available at: `http://www.mathopenref.com/chord.html`